The Role of the Basal Forebrain in Cognitive Inhibition

by
Jeffrey Mayse

A dissertation submitted to Johns Hopkins University in conformity with the requirements for the degree of Doctor of Philosophy

Baltimore, MD
February 20th, 2015

Abstract

Cognitive inhibition is an integral component of normal cognitive functioning. This thesis represents a significant step towards a greater understanding of the neural circuits underlying cognitive inhibition. In Chapter 1, we established a novel rodent version of the stop signal task (SST), linking a powerful behavioral paradigm for studying a form of cognitive inhibition to the advantages of rodent models. We utilized this novel rodent SST in Chapters 2 and 3 to examine a novel node in the neuronal circuits underlying stopping, the basal forebrain (BF). In Chapter 2, we examined whether age-related slowing of processing speed and SSRT were independent in a naturally-occurring rodent model of normal cognitive aging, and whether these changes related to altered BF integrity. We find that aging is associated with substantial nonoverlapping impairment in stopping, spatial navigation, and processing speed, and that altered sustained attention in aged animals is accompanied by changes in the integrity of the BF cholinergic population. In Chapter 3 we utilized this rodent SST and in vivo electrophysiological recording to study the role of putative non-cholinergic bursting neurons in the BF in stopping. We find substantial causal evidence that this population of BF neurons is capable of controlling the latency of cognitive inhibition, stop signal reaction time (SSRT). Together, these studies make several critical advances towards the study of cognitive inhibition and broaden the scope of existing proposed neuronal circuits underlying stopping to include the cortically-projecting basal forebrain.

Table of Contents

Table of Figures

General Introduction

The History of Inhibition

Neuroscientists have long sought to understand how different brain regions and networks cooperate and compete to select and implement an output. However, the notion that inhibition, generally defined as a force that suppresses or reduces excitation, was involved in this selection was not widely accepted during the post-Enlightenment revolution in neuroscience. Instead, early anatomists and physiologists were concerned chiefly with observable, measurable phenomena. While methodological limitations influenced this viewpoint, for much of the post-Enlightenment study of neuroscience, the notion of inhibition in the nervous system was met with active, philosophical resistance. In his writings at the end of the 19th century, a critical period for the development of the philosophical idea of inhibition, Samuel James Meltzer wrote about scientific resistance to inhibition that:

> The active manifestations of life aroused our curiosity; the phenomena of contraction, secretion, sensation presented problems and were studied. The absence of these phenomena was no problem. A muscle is at rest, it was implicitly assumed, when there is no cause for its contraction. Thus all the laws and conceptions which were formulated upon this one-sided basis are obstacles to the progress of the conception of inhibition. (Meltzer, 1899; Macmillan, 1992)[1].

[1] Much of the summary of the history of inhibition is derived from a combination of my general knowledge, Roger Smith's *Inhibition: History and Meaning in the Sciences of Mind and Brain* (1992) and Malcom Macmillan's *Inhibition and the Control of Behavior* (1992). While citing and reading the primary sources and certainly integrating Smith and Macmillan's works into my own knowledge, it is only fair to give them both credit for ideas learned from their histories.

Throughout the history of cognitive science, the study of inhibition has suffered because of its very nature: the effect of an inhibitory process is the cessation of an excitatory one and the inhibitory process itself is not easily observable. Early physiologists found no reason to look for a mechanism for muscle relaxation when cessation of muscle stimulation was perfectly sufficient (Macmillan, 1992; Smith, 1992). Later, theories of sensory-motor integration and localization of function in the central and peripheral nervous system found no need for an inhibitory process to resolve how different functional regions competed to produce a behavior; the stronger region provided more excitation and won out over the weaker ones. In this way, production of a behavior or response was viewed as a product of a balance of excitatory forces with no room for inhibition (Macmillan, 1992; Smith, 1992).

Since the end of the Enlightenment, understanding the localization of functions has been a central goal of anatomists, physiologists, and psychologists. One early and influential attempt at understanding localization by Franz Joseph Gall hypothesized that discrete organs within the cortex subserved discrete psychological and social functions. It is now well-known that in Gall's phrenology it was believed that one could directly ascertain the size (and therefore relative strength) of each region by measuring the skull above it. Surprisingly, Gall never directly stated how these different regions interacted to produce a behavior, only implying that behavior was a balance of excitatory forces (Macmillan, 1992). He was so convinced that the balance of excitatory forces controlled behavior that he would occasionally publically examine the heads of prisoners whose crimes he

was not aware of and declare, based only on the relative size of their cortical organs, what crimes they had committed (apparently with some success, Gall 1835, pp. 293-303). Gall did not believe these faculties were static. He believed that education, religion, laws, etc. could shrink or grow (and therefore weaken or strengthen) different regions and faculties, altering the balance of excitation (Macmillan, 1992). Nonetheless, nowhere in Gall's theorizing was the idea that the action of one region or faculty was to inhibit or suppress others.

The first recorded evidence of cognitive inhibition in the nervous system arose from experiments by Volkmann and later the Weber brothers into the effect of vagus nerve stimulation on the heart. Volkmann first reported that whereas stimulation of the heart muscle caused it to contract, stimulation of the vagus nerve occasionally caused the heart to relax. The viewpoint that the body was controlled solely by a balance of excitatory forces was so strong that even Volkmann rejected this finding, attributing it to an error in his technique (Macmillan, 1992). Only after the Weber brothers found similar results from the same experiment nearly a decade later did these results get taken as anything more than technical error, providing the first real evidence that a force separate from excitation existed in the nervous system (Macmillan, 1992).

This notion was codified in a set of very simple experiments by Ivan Sechenov seventeen years later. Sechenov observed, as had others, that separating the cerebrum from the spinal cord sped how quickly a frog would withdraw his leg from an acid bath, a spinally-mediated reflex. Sechenov's contribution was in the finding that this effect must be localized to a specific portion

of the brain. In potentially the earliest experiments using changes in reaction time (RT) as a measure for the effect of an underlying hidden neural process, Sechenov set about sectioning the frog brain at different levels, quantifying the speeding of the frog's leg withdrawal, and then attempting to replicate this effect by chemically or electrically stimulating the same portion of the brain in an intact frog (Macmillan, 1992). He found that sectioning a portion of the thalamus caused the greatest reflex speeding, whereas stimulating this same region caused slowing of the reflex. Sechenov concluded that exciting this region activated a "special [mechanism]" that was "absolutely different from the sensory and motor apparatuses of the organism." (Sechenov c. 1863). In other words, Sechenov was the first to localize a specific inhibitory process separate from excitation in the brain itself (Macmillan, 1992). Again, however, the prevailing scientific theories of excitation meant that Sechenov's findings were ignored for decades; nonetheless, Sechenov's experiments were the first of several to provide indisputable evidence that inhibition was a common force in the nervous system.

Selective Stopping as a Case Study of Cognitive inhibition

While this brief history of the origins of inhibition as a concept may seem tangential, it serves to highlight the intrinsic difficulties of studying inhibition. Whereas excitation is often obvious in its effects, inhibition is far more subtle and generally viewed only in the context of excitation. In his seminal Nobel lecture, Charles Scott Sherrington noted that even for simple spinal reflex arcs, the effects of inhibition are only interpretable in the context of excitation: "the only index available at present for inhibition is its effect on excitation; thus, a standard twitch-

reflex, representing a standard-sized volley of centrifugal discharge, can serve as a quantitative test for reflex inhibition." The same is true behaviorally: for most of its history cognitive inhibition has only been assessed in the context of its effects on response generation. The overwhelming majority of tasks assessing cognitive inhibition require subjects to suppress irrelevant information (often information that was previously relevant), and infer the effect of inhibition by the RT cost for making a response. For example, inhibition in the Stroop task, in which participants must report the typeface color of a word while suppressing the innate tendency to read the word itself, is often assessed by quantifying changes in RT as a function of the degree of conflict between the color of the typeface and the word itself. Similarly, when subjects are required to find a target that was a distractor in previous trials in an array, RT is considerably longer than when the target had not been previously ignored. This RT cost is attributed to a phenomenon called negative priming (Hasher et al., 1991). In rodents, inhibition is often assessed by comparing the number and characteristics of go responses made on no go trials in a go/no go contingency reversal in which a stimulus that previously instructed animals to make a response now instructs them to withhold one (Dufort et al., 1954; North, 1950; Rapp, 1990; Schoenbaum et al., 2002a). This deficit improves with subsequent training, demonstrating that reversal learning is to some degree a skill (Bourke, 1954; Schoenbaum et al., 2002b). Even tasks requiring cognitive flexibility, or the ability to switch between varying task demands, rules, or sets of relevant information (e.g., the Wisconsin card sorting task), do so by requiring subjects to suppress irrelevant information in addition to utilizing newly relevant information. It

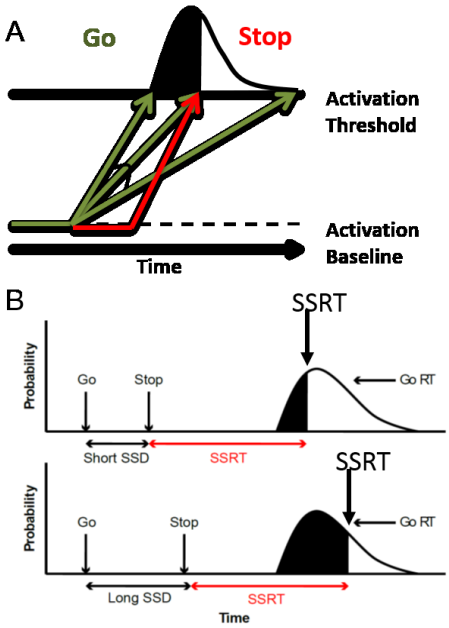

Figure 1 - Race Model Schematic and Hypothetical Reaction Time Distributions

A. Race model schematic. Go process indicated with green arrows, stop process with red arrows. The accumulation rate for the go process is variable between trials but constant on a given trial such that, for a given stop signal delay (go-stop onset asynchrony), some trials will escape inhibition (shaded black region) and others will be captured by the stop process and canceled (white region). **B.** Hypothetical RT distributions when stopping is required for a short (top) and long (bottom) stop signal delay with a constant SSRT. SSRT is estimated as the latest point in time in the go RT sampling distribution (black region).

is clear that cognitive inhibition is a critical component of the general (and poorly defined) suite of cognitive features we call executive function. However, while changes in RT are powerful indicators of the presence of cognitive inhibition, they provide relatively little information about the features of a specific mechanism for suppressing irrelevant information or behaviors.

The development of the stop signal task (SST) was a major turning point in the study of cognitive inhibition because it allows for the estimation of a characteristic of the inhibitory process itself (Lappin and Eriksen, 1966; Logan and Cowan, 1984; Logan et al., 1984). In the SST, subjects are required to make a rapid behavioral response following a go signal and cancel the preparation of this response following an infrequent stop signal (Lappin and Eriksen, 1966; Logan et al., 1984). The ability of subjects to stop on a given trial is a function of the delay between the go and stop signals (stop signal delay, SSD), with stopping being more difficult at longer delays. Additionally, accuracy also depends on the speed

of response preparation, with stopping being more difficult when subjects are faster (Logan and Cowan, 1984).

The empirical relationship between selective stopping (i.e., canceling only the action being prepared), SSD, and the speed of response preparation led to the development of a simple model to describe inhibition in the context of the SST. In this model, called the Horse Race model, two hypothetical processes race to control behavior, each initiated following presentation of its accompanying stimulus: a generative go process and an antagonistic stop process (Logan and Cowan, 1984, Figure 1A). These processes accumulate arbitrary activity from a baseline to an activation threshold, at which point the winning process controls behavior. If the go process reaches threshold first, the response is made, whereas if the stop process reaches threshold first, preparation of the response is arrested (Logan and Cowan, 1984). Because this model assumes both that the rate of accumulation for each process is constant on a given trial and that the duration of the stop process is constant and invariant (or has such low variability as to be functionally constant within measurement error, Band et al., 2003), the only factors that determine whether stopping will be successful is the delay between when the stop and go processes are initiated, set by the SSD, and stochastic variability in the rate of accumulation of the go process, measured via the variability in the empirical go RT distribution (Figure 1A).

Importantly, in this model, any response generated on a trial in which the stop signal was presented happens because *the go process won the race.* Therefore, any response observed on a stop trial is a response drawn from the go

trial RT distribution and is *unaffected by the presence of the stop process,* unlike responses in the Stroop or Go/NoGo tasks. Using this knowledge and the two aforementioned known parameters (SSD and go trial RT variability), it is possible to estimate the latency of the stop process (stop signal RT, SSRT, Figure 1B, indicated by vertical arrow) by comparing the observed sampling distribution of go RTs on trials in which the stop signal was presented (Figure 1B, black region) to the full go RT distribution on trials in which the stop signal was not presented (Logan and Cowan, 1984; Logan et al., 1984, Figure 1B, white region). While there are many methods for estimating SSRT, they all rely on this simple principle: any response that would be generated with an RT longer than SSRT will be captured by the stop process, canceled, and not observed in the go RT sampling distribution (Logan and Cowan, 1984; Logan et al., 1984). Therefore, by finding the slowest RT observed (assuming infinite data points; empirical methods for estimating SSRT must account for noisy data), we can know SSRT.

An important question is whether studying motoric inhibition is relevant for understanding non-motoric cognitive inhibition, as is assumed to be necessary for executive function. The answer to this question is that the study of stopping is concerned with both modification of ongoing premotor activity in motor regions and the modification of goals, stimuli, or rules held in working memory in largely non-motor regions (Bissett and Logan, 2012; Boucher et al., 2007a). The advantages of studying stopping are many: the neural circuits for producing motor behaviors are relatively well-understood in mammals, providing ample insight as to where to look for the effects of motor inhibition. In primates and humans, occulomotor

saccades are often used as primary task responses in the SST because the neural circuits for generating saccade are well-understood and provide an easy framework for understanding inhibition. Neurons in the supplementary eye field (SEF) and superior colliculus (SC) compete to either shift or maintain gaze: so-called fixation neurons are active when monkeys maintain gaze on a target, and so-called movement neurons accumulate activity to a threshold prior to eye movements (Brown et al., 2008; Everling et al., 1998; Hanes et al., 1998; Hanes and Schall, 1996; Paré and Hanes, 2003; Sparks, 1978). When stopping is required, the activity of fixation neurons increases and the accumulation of movement neurons is arrested prior to SSRT (Boucher et al., 2007a). This relatively simple circuit provides a rich framework for constraining the possible mechanisms of stopping: first, any neuron that controls movement initiation must differentially modulate its firing rate when stopping is and is not required, and second, this modulation must precede SSRT. Similar circuits for stopping skeletal movements are less well understood, but emerging theories suggest the involvement of large populations of neurons in the motor cortex (M1)(For review, see Stuphorn, 2014). Regardless, the same constraints apply to controlling skeletal movements as apply to controlling eye movements, even if the neural circuits underlying movement initiation are different. Note, however, the focus of these studies is on *movement initiation,* rather than *inhibition.* In future chapters, I will focus on the neural circuits underlying inhibition as a possible general mechanism to address how stopping is a case study of cognitive inhibition.

Cortico-Basal Ganglia Networks Underlying Cognitive Inhibition

This simple computational model has greatly facilitated study of the mechanisms underlying cognitive inhibition. Studies in humans with focal cortical damage have demonstrated a consistent relationship between damage to the prefrontal cortex, especially the right inferior frontal cortex (IFC), and elevated SSRT (Aron et al., 2003; Rieger et al., 2003). These studies are corroborated by functional imaging data demonstrating elevated BOLD signal in the IFC when stopping is required (Aron and Poldrack, 2006; Swann et al., 2009). In addition, functional connectivity studies show increased connectivity between the IFC and the subthalamic nucleus (STN) when stopping is required, and this connectivity is greater in more proficient stoppers (Aron and Poldrack, 2006; Aron et al., 2007) and degraded in aged individuals with impaired cognitive inhibition (Coxon et al., 2012). This distributed cortical-basal ganglia network is thought to underlie rapid stopping in humans and primates.

In rodents, the orbitofrontal (Eagle et al., 2008b; Schoenbaum et al., 2002a; Szatkowska et al., 2007) and medial prefrontal (Caetano et al., 2012; Isoda and Hikosaka, 2007) cortices (OFC and MFC) are both involved in cognitive inhibition and response selection. Lesion or inactivation of the OFC impairs the ability of animals to suppress an inappropriate response but does not impair response generation or learning (Burke et al., 2009; Eagle et al., 2008b; Schoenbaum et al., 2002a; Volle et al., 2011). By contrast, lesion of the MFC impairs response selection and cognitive flexibility (Maddux and Holland, 2011; Volle et al., 2011). The OFC has long been implicated in cognitive inhibition and the use of outcome

predictive information to guide behavior. This region is therefore likely to play a role in performance of the SST (Eagle et al., 2008b). The MFC, on the other hand, is important for linking actions to outcomes and necessary in order for organisms to select the appropriate action (Isoda and Hikosaka, 2007; Maddux and Holland, 2011). As in humans, these two cortical regions in conjunction with the basal ganglia (Haynes and Haber, 2013; Leventhal et al., 2012; Schmidt et al., 2013) are thought to form part of a distributed fronto-cortical network that contributes critically to selecting, generating, and inhibiting behavioral responses in rodents. Together, these studies establish a cortical-subcortical network between the IFC (in primates and humans), the OFC/MFC (in rodents), and the basal ganglia, especially the STN, important for performance in the SST.

The STN has long been thought to play a role in action suppression as part of the cortico-basal ganglia loop subserving action selection (Aron et al., 2007). Parkinson's patients with tardive dyskinesia show reduced markers for GABAergic neurons in the STN (Andersson et al., 1989), leading to the hypothesis that excessive STN activity contributes to loss of movement control in Parkinson's disease. Moreover, early studies using selective deep brain stimulation (DBS) of the STN provided support for these hypotheses. DBS in the STN was shown to help suppress spontaneous movements in primates (Beurrier et al., 1997) and humans (Benabid et al., 1994; Benazzouz et al., 1993; Kumar et al., 1998; Tsubokawa et al., 1995). These findings ultimately led to the hypothesis that selective stopping was achieved via top-down influence of cortical regions on the

basal ganglia, where the striatum and STN raced to control the output nuclei of the basal ganglia for control of behavior (Aron et al., 2007; Schmidt et al., 2013).

While there is strong theoretical reasoning for a role of the STN in selective stopping, more recent studies have suggested rather that the STN provides a more transient global motor pause to facilitate later selective stopping. More complete DBS studies in humans showed that DBS of the STN actually *impaired* stopping in Parkinson's patients with less severe clinical impairment, while improving stopping only in those patients with more severe impairment (Mirabella et al., 2011; Ray et al., 2012; van den Wildenberg et al., 2006). Additionally, in patients with essential tremor, DBS of either the STN or the ventromedial intermediate nucleus of the hypothalamus was equally effective in alleviating spontaneous tremors, suggesting that the STN may not be unique in facilitating suppression of inappropriate responses (van den Wildenberg et al., 2006). In rodents, a recent study utilizing single unit recording from the STN while rodents performed a variant of the SST showed a rapid, sensory-like response in STN neurons present on both go and stop trials, and the latency of this response greatly preceded and was not correlated with SSRT (Schmidt et al., 2013). The magnitude of this response was positively correlated with RT (i.e., more STN activity correlated with slower RTs) on both trial types, suggesting that this STN response may provide a rapid pause in the preparation of a movement to allow for more selective inhibition, should it be required (Schmidt et al., 2013). In support of this hypothesis, fiber sparing lesions of the STN in rodents do not impair their ability to cancel an ongoing movement, though the effect of such lesions on planned movements has not been investigated

(Eagle et al., 2008b). Together, these findings suggest a role for the STN in providing a transient global pause of motor activity, effectively delaying the generation of a response in order to facilitate more selective control of actions by other regions. It is then an open question what happens between when basal ganglia neurons are activated to provide a global motor pause and when cortical premotor neurons change their firing patterns to preclude movement initiation. In other words, the precise neural locus of the stop process (and hence of stopping in the SST) remains unknown.

Influence of Subcortical-Cortical Networks for Inhibition

In general, the studies discussed above fit nicely with the view that inhibition reflects the hierarchical organization of the brain (Smith, 1992). According to this framework, higher-level cortical structures suppress and control competing, lower-level subcortical structures in order to produce an appropriate behavioral output (Aron et al., 2007; Bryden et al., 2012; Haynes and Haber, 2013; Li et al., 2008; Smith, 1992; Zandbelt and Vink, 2010). This thinking has led to a wealth of studies demonstrating that cognitive inhibition is effected by a distributed fronto-cortical network (Aron et al., 2003; Aron and Poldrack, 2006; Bari et al., 2011a; Duann et al., 2009) via their connections with discrete subcortical regions (Aron et al., 2007; Rieger et al., 2003; Schmidt et al., 2013). While this framework is informative and supported by many studies, it overlooks the role of subcortical neuromodulatory regions in cognition. Instead, it is often seemingly implicitly assumed that these regions at best play a supporting role in cognition. Given that subcortical neuromodulatory networks can often exert rapid, powerful, and widespread

modulation of cortical circuits and of general behavioral states (Goard and Dan, 2009; Lin et al., 2006; Nguyen and Lin, 2014; Sara and Bouret, 2012; Sarter and Bruno, 1999), it seems plausible that these regions could influence cognitive inhibition.

One such subcortical neuromodulatory region, the basal forebrain (BF), is well-situated to rapidly and powerfully modulate ongoing cortical processing (Lin et al., 2006; Nguyen and Lin, 2014). The basal forebrain (BF) is one of the largest neuromodulatory networks in the mammalian brain, forming a continuum of magnocellular neurons extending from the midline of each hemisphere laterally and caudally along the base of the brain and forming the ventral border of the cerebrum. Neurons in this region express markers for a wide variety of neurotransmitters, most notably the modulatory neurotransmitter acetylcholine (ACh), inhibitory GABA, and excitatory glutamate, in addition to a variety of poorly-studied neuropeptides (Henny and Jones, 2008; Manns, 2002; Manns et al., 2001). Historically, the majority of research in the BF has focused on the population of cholinergic neurons. Early post-mortem analyses of tissue from Alzheimer's disease (AD) patients revealed that these patients had severe atrophy of cholinergic BF neurons (Whitehouse et al., 1982). Later studies using lesions of the BF or injection of cholinergic antagonists either systemically or into discrete cortical regions produced profound behavioral impairments similar to those observed in AD, establishing a role for this subcortical region in what was previously thought to be a cortical dementia (Drachman and Leavitt, 1974; Hepler et al., 1985; Hepler et al., 1985; Hepler et al., 1985; Herremans et al., 1995; Huston

and Aggleton, 1987; Muir et al., 1996; Olton et al., 1991). These anatomical and functional studies culminated in the development of the Cholinergic Hypothesis of Dementia, which stated that the cognitive decline observed in AD is partly caused by dysfunction or atrophy of cholinergic BF neurons (Coyle et al., 1983; Francis et al., 1999).

However, better pharmacologic agents were later developed, such as excitotoxins that largely spare noncholinergic neurons while damaging cholinergic neurons extensively (e.g., quinolinate, quisqualate, etc.), or 192-IgG saporin, a ribosome inactivating toxin conjugated to an antibody selective for the “low affinity” p75 neurotrophic factor receptor present only on magnocellular cholinergic neurons in the BF. A large body of work demonstrates that these specific cholinergic lesions fail to reproduce the pattern of impairment observed in AD, while toxins that nonpreferentially destroy cholinergic and GABAergic BF neurons (e.g., Ibotenate) resulted in profound impairment (Baxter et al., 1995; Baxter and Gallagher, 1996; Dornan et al., 1996; Dunnett et al., 1991, 1989; Fletcher et al., 2007; Gutiérrez et al., 1999; Kamke et al., 2005; Markowska et al., 1990; Olton et al., 1991; Robbins et al., 1989; Wenk et al., 1989). These studies led to the conclusion that the impairments observed following nonselective lesions of the BF were primarily due to damage to either the noncholinergic components of the BF, damage to the cholinergic projection to the amygdala (which is spared by infusions of 192-IgG saporin), or a combination of damage to multiple neuronal BF populations. While these studies did not provide support for the Cholinergic

Hypothesis of Dementia, they did pique interest in the BF noncholinergic population.

Ironically, the majority of studies assessing the function of BF noncholinergic neurons were those originally intended to assess the role of the cholinergic neurons using nonselective lesion techniques prior to the use of 192-IgG saporin. These lesion studies must be interpreted with caution, as a method for semi-selectively removing GABAergic projection neurons was only recently validated (Köppen et al., 2013; Pang et al., 2011; Roland et al., 2014; Roland et al., 2014). However, one can infer some function of these neurons by contrasting the behavioral consequence of selective cholinergic lesions from those produced by less selective toxins. Selective cholinergic lesion of the whole BF spares freezing but attenuates ultrasonic vocalizations in a fear conditioning preparation (Frick et al., 2004). This type of lesion also fails to impair performance on the Morris water maze (Baxter et al., 1995), and fails to impair conditioned taste aversion (Gutiérrez et al., 1999). However, rats with selective cholinergic lesions of the nucleus basalis of Meynert and substantia innominata (NBM/SI) complex (subregions of the basal forebrain) show reduced accuracy in tasks requiring sustained attention, especially the 5-choice serial reaction time task and vigilance tasks. Animals with such lesions typically exhibit a pattern of behavior consistent with a speed-accuracy tradeoff; that is, a decrease in accurate responses when there are time constraints or when the animal is under heavy attentional load (Burk and Sarter, 2001; Dalley et al., 2004; McGaughy et al., 2002, 1996). Therefore,

cholinergic neurons in the BF seem to be involved in sustaining attention relevant for task performance, especially under conditions of attentional load.

By contrast, lesion of GABAergic BF neurons produces no change in correct response rate but produces an increase in false alarms and an increase in response latency in both rats (Muir et al., 1993, 1996; Olton et al., 1988) and primates (Voytko et al., 1994). Furthermore, less specific ibotenic acid lesions of the NBM/SI in rodents and primates increase perseverative responding in the radial arm maze task (Hepler et al., 1985) and in reversals of previously acquired visual discriminations (Roberts et al., 1992). Additionally, lesions of the BF, especially when noncholinergic BF neurons are targeted, impair cognitive inhibition and cognitive flexibility as substantially as lesions of the OFC or MFC themselves (Muir et al., 1993, 1996; Olton et al., 1988; Roberts et al., 1992; Voytko et al., 1994). These neurons have dense projections to both the OFC and MFC where they form disinhibitory circuits with pyramidal cells via intra-cortical inhibitory interneurons (Freund and Gulyás, 1991; Gritti et al., 1997; Henny and Jones, 2008). They are therefore ideally situated to provide fast, powerful modulation of cortical information processing (Lin et al., 2006; Nguyen and Lin, 2014). Taken together, these studies implicate the non-cholinergic BF (likely the GABAergic system, Lin and Nicolelis, 2008; Lin et al., 2006) in a form of cognitive inhibition.

The Role of the Basal Forebrain in Cognitive Inhibition

In this thesis, I will describe a series of experiments exploring how putatively non-cholinergic neurons in the rodent BF influence cognitive inhibition. In Chapter 1, I will describe a novel rodent SST and method for estimating SSRT based on

continuous RT distributions. In Chapter 2 I will describe the first assessment of cognitive inhibition in aged rats using the SST. In this chapter, I will also examine the relationship in decline across different cognitive domains. Finally, in Chapter 3, I will describe a series of experiments using *in vivo* physiological recording of neuronal activity in the BF while rats perform the SST. In these experiments, I will demonstrate a clear link between a subset of BF neurons and stopping, providing new evidence for subcortical influences in what has been nearly exclusively studied as a cortically-driven behavior.

Chapter 1 – A Novel Rodent Stop Signal Task

Rationale

Cognitive inhibition is essential for meeting the shifting demands of complex environments (Logan et al., 1997). Successful cognitive inhibition can be achieved through both reactive and proactive control strategies, respectively involving preparation to stop prior to stimulus onset and stimulus-driven processing at stimulus onset (Aron, 2011; Li et al., 2006a). One important paradigm to study cognitive inhibition is SST. In the SST, subjects need to rapidly cancel a prepotent behavioral response when the go signal is occasionally followed by a stop signal. The SST is uniquely powerful in that it allows for the quantitative estimation of the latency of reactive inhibition, the SSRT (Logan and Cowan, 1984; Logan et al., 1984). Subjects also employ proactive inhibition in the SST to adjust response speed following errors or stop trials (Bissett and Logan, 2012; Emeric et al., 2007; Verbruggen and Logan, 2009a). Understanding the neural mechanisms of cognitive inhibition is critical because elevated SSRT is a widely observed feature

of cognitive impairment across many neuropsychiatric disorders, including Parkinson's disease (Gauggel et al., 2004; Mirabella et al., 2011), attention-deficit hyperactivity disorder (McAlonan et al., 2009), and normal cognitive aging (Andrés et al., 2008; Coxon et al., 2012).

Recent years have seen a surging interest in rodent versions of the SST (Bryden et al., 2012; Eagle and Robbins, 2003a; Leventhal et al., 2012) to leverage the advantages of rodent models, such as lesion, pharmacology and recording. However, important differences exist between current rodent and primate SSTs and pose a major challenge in comparing the two literatures. For example, while primates typically need to cancel the initiation of an action, rodents are commonly required to inhibit an ongoing movement (Beuk et al., 2014, Bryden et al., 2012; Eagle and Robbins, 2003a). Furthermore, while primate SSTs typically use multiple stop signal delays (SSDs), many rodent tasks employ only a single SSD (Leventhal et al., 2012; Schmidt et al., 2013), encouraging rats to adopt an alternative timing strategy in anticipation of the highly predictable stop signal. Finally, the implications of different behavioral strategies between rodents and primates, such as differing baseline response biases, on estimating SSRT have not been systematically investigated (Robinson et al., 2009). Reconciling these differences is an essential step toward establishing the rat as a valid model to study cognitive inhibition.

The goal of this chapter was to examine whether rats exhibit proactive and reactive cognitive inhibition as commonly described in primates in a novel rodent-appropriate SST. Specifically, we investigated how rats cancel the initiation of a

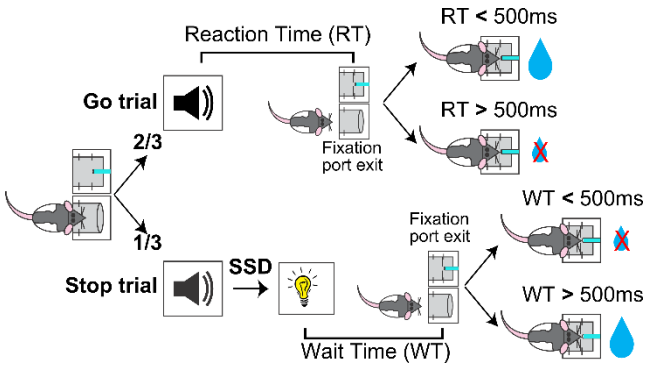

Figure 2 - Schematic of the rodent Stop Signal Task (SST)

Rats began each trial by inserting their nose into a fixation port. After maintaining fixation for a variable foreperiod, a tone was presented. Two-thirds of trials were Go trials, in which the tone was presented alone and the trial was rewarded if reaction time (RT, latency between tone onset and fixation port exit) was faster than 500ms. One-third of trials were Stop trials, in which the tone was followed by a Stop light and the trial was rewarded if wait time (WT, latency between light onset and fixation port exit) was longer than 500ms. The delay between the Go tone and Stop light, the Stop Signal Delay (SSD), varied between trials.

---

rapid nosepoke port exit response while incorporating multiple SSDs within each session. We found that, in addition to errors of stopping, rats often commit independent errors of waiting. The conflation of these two types of errors using current estimation methods systematically overestimates SSRT. This led us to develop and validate a novel method to estimate SSRT independent of the ability to wait.

Experimental Methods

Data for Chapter 1 have already been collected and published (Mayse et al., 2014). Methods will be briefly summarized here where possible. Behavioral training methods, description of the modified integration method for estimating SSRT and the yoking procedure are provided in full; these methods are identical to methods used for Chapters 2 and 3 and are provided here as a reference.

Subjects

Ten male Long-Evans rats were used for the experiments in Chapter 1. Animals were individually housed in a light-, temperature-, and humidity-controlled vivarium (12L:12D, lights on at 0700). All animals were food deprived to 85% of their free-feeding weight to motivate task performance.

Behavioral Training – Go Trial Shaping

Rats were initially trained to respond to a 6kHz tone (2 sec, 80dB) in the operant chamber to receive 3 drops of reward (30µl) in the reward port, delivered starting at the 3rd lick. Only trials with the three licks within a 3s reward window were considered successful and rewarded. Subsequently, rats were shaped to nosepoke in the fixation port and maintain fixation until tone presentation. Early fixation port exit before tone onset resulted in no reward delivery. The delay between fixation port entry and tone onset, or foreperiod, was adaptively increased until rats could reliably maintain fixation for 800ms in anticipation of the tone. After that point, four different foreperiods (350, 500, 650, and 800ms) were used, varied pseudo-randomly across trials, to minimize temporal expectation of stimulus onset. The inter-trial interval (ITI) was 1-3 sec, and not signaled to the rat. Premature fixation port entry and premature licking during ITI both reset the ITI timer. A cutoff of 500ms RT, the latency between tone onset and fixation port exit, was also imposed such that RTs longer than the 500ms were not rewarded. Animals were held at this stage for 10-14 sessions to encourage fast responding to the tone, until 90% RTs were faster than 500ms.

Behavioral Training – Stop Trial Shaping

After rats were trained to respond as fast as possible to the 6kHz go signal, they were trained to associate a light signal with reward if they responded after the light offset but not before. The overall organization of the task was the same as the previous shaping phase, except that the 6kHz tone was replaced by illumination of a white central panel light in each trial, which will later serve as the stop signal in the SST. Fixation port exit responses during light illumination led to forfeiture of reward, and only responses after light offset led to 3 drops of reward (30µl). The duration of light illumination was initially set at 350ms, such that some fixation port exit responses were slow enough to be rewarded. To provide an explicit feedback to animals that they had waited long enough in the fixation port and that reward was available, waiting for the duration of the light was coupled with an audible solenoid click similar to the click associated with reward delivery. The light duration was then adaptively increased until animals could reliably wait for 500ms light illumination (10-14 sessions). After that, rats received several refresher tone-alone sessions before transitioning to the SST.

Behavioral Training – Stop Signal Task

The general organization of the SST, including ITI, nosepoke port fixation, foreperiod and reward delivery, was the same as the two behavioral shaping phases. In the SST, the 6kHz go signal was presented on all trials, and on 1/3 of the trials the go signal was followed by the light stop signal after a variable SSD. In the tone-alone trials (2/3), or Go trials, animals were required to make fast go responses (RT<500ms) to receive reward, the same contingency as in the shaping

phase. In the Stop trials (1/3), reward contingency was dictated by the stop light as in the shaping phase, such that reward was available only if wait time (WT), the latency between stop signal onset to fixation port exit, was longer than the 500ms hold duration. The same amount of reward (30μl) was delivered in both fast Go trials and successful Stop trials. Five SSDs were determined before the start of each session based on performance in the previous session, and the SSD was chosen pseudorandomly from these five SSDs on each trial. Every session included a 0ms SSD such that the tone and light were presented simultaneously. The remaining four SSDs were evenly spaced in 40ms steps and adjusted by experimenters between sessions to ensure approximately 50% failed stop trials.

In Stop trials in which rats already made the fixation port exit response before the onset of stop signal (RT<SSD), we chose to omit the stop signal and rewarded the animal for the go response in order to encourage fast responses to the go signal. While animals subjectively perceived these 'converted' Stop trials as Go trials, these trials were treated as failure-to-stop errors in our analysis to ensure that the stochastic go process was sampled equally in both Go and Stop trials. This is important because these converted trials tended to have very fast RTs: classifying these trials as Go trials would result in a disproportionately fast Go trial RT distribution and slow Stop trial RT distribution from essentially transferring the fastest Stop trials to Go trials. The effect of such misclassification would be to bias the Go RT distribution leftward (i.e. faster) and under-estimate the percentage of failure-to-stop errors, resulting in the under-estimation of SSRT (i.e. faster SSRT). Note that, because converted trial RTs were faster than the SSD, classifying these

trials as failure-to-stop errors resulted in negative values when aligned to the Stop signal. These converted Stop trials were not included when determining the percentage of attempted reward collection in failure-to-stop errors and in the analysis of proactive cognitive inhibition in which only trials with stop signal presentation were included. Previous studies in rodents have treated these trials similarly by omitting stop signal presentation and rewarding fast go responses (Beuk et al., 2014; Eagle and Robbins, 2003a), with the exception of one study which did not address these trials directly (Schmidt et al., 2013).

Data Analysis

Data analysis included only sessions with (1) 50 or more Stop trials; (2) greater than 25% failed Stop trials; and (3) fewer than 25% Go trials with RTs exceeding the 500ms cutoff (n=257/507 sessions, 49% sessions excluded). Of all excluded sessions, 48% occurred in the initial 1/3 of training days, while only 10% were from the last 1/3 of training days.

Estimating SSRT Using Discrete Trial Outcomes: The Median and Integration Methods

Most existing methods for estimating SSRT, including the median and integration methods, require a binary classification of stop trials based on whether or not stopping was successful. This binary classification is needed to calculate the *p*roportion of *failure-to-stop* errors, p(failure-to-stop), per SSD. The median method estimates SSRT by first fitting the inhibition function, SSD vs. p(failure-to-stop), commonly with logistic regression, to determine the SSD_{50} associated with p(failure-to-stop)=0.5. SSRT is then estimated as the difference between the

median Go trial RT (RT_{50}) and SSD_{50}. For sessions in which p(failure-to-stop)=0.5 fell outside of the range of observed p(failure-to-stop), we did not provide a SSRT estimate to avoid errors in extrapolation. The integration method, on the other hand, estimates SSRT first for each SSD and then averages all estimates to produce the final SSRT estimate. For a particular SSD, e.g. SSD_{100ms}, the integration method finds the $100*p(\text{failure-to-stop})_{100ms}^{th}$ percentile in the Go trial RT distribution (RT_{100ms}), and estimates SSRT as $RT_{100ms} - SSD_{100ms}$. For instance, if $p(\text{failure-to-stop})_{100ms} = 0.25$, then to find SSRT one would find the 25^{th} percentile of the Go RT distribution (for instance, 180ms) and subtract the current SSD (100ms; SSRT = 80ms). This process is then repeated for each SSD and the separate estimates are averaged for a session-wide estimate.

Critical to both methods is how stop trials are classified into binary outcomes, which is equivalent to setting a WT cutoff in Stop trials. Conventionally, successful stopping in rats is indexed by whether or not they obtained reward in each Stop trial, which is equivalent to setting the WT cutoff as the entire duration of the required hold period (500ms). We explored varying the WT cutoff at different points of the hold period, as well as an ideal WT cutoff that perfectly distinguishes failure-to-stop errors from failure-to-wait errors in the RT simulation benchmark test. We also explored, with observed RTs in the SST, setting the WT cutoff as the conservative upper bound of the SSRT estimate determined in the third step of our method.

Estimating SSRT Using Observed Reaction Time Distributions: The Modified Integration Method

Because rodents are required to wait in addition to stop, *a priori* it is possible that rats could successfully stop but subsequently fail to wait. Including these failure-to-wait errors as failure-to-stop errors would theoretically increase p(failure-to-stop) artificially and bias SSRT estimates rightward. Our new method aims to estimate SSRT by directly comparing RT distributions in Stop trials and Go trials in order to determine the time point at which the stop signal begins to slow down RTs relative to Go trial RTs. Because SSRT estimates capture the relatively fixed latency for the brain to process the stop signal and cancel the planned go response (Logan et al., 1984). RTs faster than this fixed latency should be statistically indistinguishable on Stop and Go trials, while RTs longer than this fixed latency should be much slower on Stop than Go trials. By directly comparing Go and Stop trial RT distributions, SSRT should correspond to the earliest time point that Go and Stop trial RT distributions diverge and Stop trial RTs begin to significantly slow down.

This method was implemented in the following four steps: **First**, we drew *n* (where *n* is the number of stop trials) random samples (without replacement) from the approximately *2n* Go trials in a session, and subtracted from these *n* sampled Go trial RTs the SSDs associated with Stop trials. This procedure created a new RT distribution such that Go trial RTs were re-aligned to would-be stop signals in order to compare with the Stop trial RT distribution also aligned to the onset of Stop signal. **Second**, this sampling procedure was repeated 10,000 times to

construct a conservative 99.9% (0.05% - 99.95%) confidence interval (CI) of the cumulative re-aligned Go trial RT distribution. **Third**, we determined the earliest time point in the sorted Stop trial cumulative RT distribution at which RTs began to significantly slow down relative to the 99.9% CI. To guard against false positive discovery from noisy Stop trial RT distributions, significant slowing of the Stop trial cumulative RT distribution should be present in at least *~0.15n* consecutive Stop trials. This identified time point provided a WT cutoff that optimally separated failure-to-stop errors (which were statistically indistinguishable from Go trial RTs) from failure-to-wait errors. This WT cutoff also determined the proportion of failure-to-stop errors, p(failure-to-stop), among all Stop trials in a session. **Fourth**, the WT cutoff identified in the last step represented a conservative upper bound of the SSRT estimate, which was determined not only by the true SSRT but also affected by the number of Stop trials (*n*) and the chosen confidence interval (99.9%). To provide an unbiased estimate of the SSRT, we took the mean of the re-aligned cumulative Go trial RT distributions as the best estimate of re-aligned cumulative Go trial RT distribution, and determined the time point in this distribution that corresponded to the probability p(failure-to-stop). This time point was defined as the SSRT estimate because, according to the independent race model, the go process in *p(failure-to-stop)*n* trials would complete faster than SSRT and therefore escape inhibition. This procedure is conceptually equivalent to the commonly used integration method of SSRT estimation in which the time point in the Go trial RT distribution (relative to go signal onset) corresponding to p(failure-to-stop) is assumed to equal (SSD + SSRT). Thus, our method extended the

integration method of SSRT estimation to RT distributions aligned to both actual and would-be stop signal onset. We therefore refer to this new method as the "modified integration method".

This new method requires a few assumptions: **First**, Go trial RTs are generated by a stochastic go process that randomly draws from a static probability distribution represented by the observed Go trial RTs. It does not assume the shape of the RT distribution. **Second**, Stop trial RTs are generated by the same stochastic go process in competition with a stop process that begins to influence RT at the latency SSRT after stop signal onset. This assumption is validated by our empirical observation that the cumulative Stop trial RT distribution and the re-aligned Go trial RT distribution completely overlapped up until 130-150ms after stop signal onset. Note that, to ensure this assumption is met in practice, Go and Stop trials should represent independent and comparable sets of trials in the SST such that the stochastic go process is sampled equally in the two trial sets. **Third**, this method assumes that SSRT is independent of SSD so that data from all SSDs can be pooled together. This is not a stringent assumption because this method can be used to estimate SSRT for each SSD separately, but the fewer number of trials per SSD will dilute its power and make the estimate noisier. **Fourth**, this method does not assume that the Stop signal will necessarily slow down RTs. The method is in fact capable of detecting both significant RT speeding and slowing, but empirically we only observed significant RT slowing following the stop signal. This method also does not assume how the Stop signal will affect RT distributions *after* SSRT, it only works to detect the initial divergence between Go and Stop RT

distributions. As a result, two animals can have the same SSRT estimate but show widely differing proportion of failure-to-wait errors.

Median and Integration Methods of SSRT Estimation

Both the median and integration methods require a binary classification of stop trials based on whether or not stopping was successful. This binary classification is needed to calculate the proportion of failure-to-stop errors, p(failure-to-stop), per SSD. The median method estimates SSRT by first fitting the inhibition function, SSD vs. p(failure-to-stop), commonly with logistic regression, to determine the SSD_{50} associated with p(failure-to-stop)=0.5. SSRT is then estimated as the difference between the median Go trial RT (RT_{50}) and SSD_{50}. For sessions in which p(failure-to-stop)=0.5 fell outside of the range of observed p(failure-to-stop), we did not provide a SSRT estimate to avoid errors in extrapolation. The integration method, on the other hand, estimates SSRT first for each SSD and then averages all estimates to produce the final SSRT estimate. For a particular SSD, e.g. SSD_{100ms}, the integration method finds p(failure-to-stop)$_{100ms}^{th}$ percentile in the Go trial RT distribution, RT_{100ms}, and estimates SSRT as RT_{100ms} - SSD_{100ms}.

Critical to both methods is how stop trials are classified into binary outcomes, which is equivalent to setting a WT cutoff in Stop trials. Conventionally, successful stopping in rats is indexed by whether or not they obtained reward in each Stop trial, which is equivalent to setting the WT cutoff as the entire duration of the required hold period (500ms). We explored varying the WT cutoff at different points of the hold period, as well as an ideal WT cutoff that perfectly distinguishes

failure-to-stop errors from failure-to-wait errors in the RT simulation benchmark test **(Figure 6)**. We also explored, with observed RTs in the SST **(Figure 7)**, setting the WT cutoff as the conservative upper bound of the SSRT estimate determined in the third step of our method.

RT Simulation Benchmark Test

To directly compare our new method of SSRT estimation with the two commonly used methods – median and integration methods, we simulated RT distributions in the SST using the independent race model with the SSRT fixed at 150ms **(Figure 6A)**. For each of the 100 simulation runs, we simulated 300 Go trials and 150 Stop trials. These 100 runs were blocked in 10 blocks of 10 model iterations each for statistical comparison. The go process was simulated by randomly drawing from a distribution equivalent to the mean of Go trial RT distributions across all sessions (from **Figure 3A**). The stop process was simulated by randomly drawing from one of 5 SSDs (0, 65, 105, 145, 185ms) plus the duration of the preset SSRT (150ms). Go trial RTs were determined only by the go process, while Stop trial RTs were determined by an independent race between the go and stop processes. If the stop process completed earlier than the go process, WT was then simulated by randomly drawing from a distribution corresponding to the second peak of the bimodal Stop trial WT distribution in **Figure 3B**. The WT distribution in **Figure 3B** was truncated at the trough between the two RT peaks (225ms), and the area under the second peak was normalized to one. This second peak of the bimodal WT distribution corresponds to Stop trials that rats had successfully cancelled the planned go response, and may or may not

have waited for the entire hold period to receive reward. Therefore, the ideal WT cutoff that perfectly separated failure-to-stop and failure-to-wait errors in this simulation was 225ms. This simulation provided a close approximation of the empirically observed RT distributions in both Go and Stop trials, as well as the proportion of the two types of Stop trial errors. We used the simulated RTs to compare the accuracy and precision of SSRT estimation by all three methods against the preset SSRT (150ms).

Analysis of Proactive Inhibition

Proactive response adjustments were identified by comparing RTs on two Go trials (G_1, G_2) before and after a Go trial (G_1-G-G_2), a failure-to-stop trial (G_1-F-G_2), a failure-to-wait trial (G_1-W-G_2), or a successful stop trial (G_1-S-G_2). Only sessions with at least five trials for each of these four types of trial sequences were included in analyses (n=184/257 sessions). The RT difference between G_2 and G_1 was reported as percent change in RT to quantify response adjustments (Beuk et al., 2014). In addition, G_1 and G_2 RTs were normalized to the median Go trial RT in order to examine absolute RT changes. Statistical comparisons were performed only between G_1-G_2 trials **(Figure 8B)**. Intermediate (G, F, W, or S) trials were shown only for visualization and were not included in statistical analyses.

To investigate whether the frequency of Stop trials in recent trial history affects subsequent go response speed as well as stop success probability (Emeric et al., 2007; Ide et al., 2013), we identified sequences of seven trials that ended with a Go trial or a Stop trial **(Figure 9)**. We classified trial sequences into different categories based on the number of stop trials in trials 1-6. For trial sequences

ending with a Go trial, we normalized RTs in trial 7 associated with each trial sequence category by the session-wide median Go RT. A significant deviation of the median-normalized RT from one indicates a systematic fluctuation of RT based on recent trial history. For trial sequences ending with a Stop trial, we calculated the probability for each stop trial outcome – failure-to-stop, failure-to-wait and successful stop – in trial 7 associated with each trial sequence category. We determined whether the probability of stop success in each trial sequence category deviated from the session-wide stop performance after taking into account the contribution of SSDs. This was achieved by first determining the probability of each stop trial outcome associated with each SSD for the entire session, and then estimating predicted stop trial outcome probabilities in each trial sequence category based on the observed distribution of SSDs. The difference between the observed and predicted stop trial outcomes (Δp(Stop)) represents the influence of recent Stop trial frequency on subsequent stop performance beyond what would be expected given the observed distribution of SSDs for that 7-trial block. Both median-normalized RTs and Δp(Stop) were averaged across sessions within an animal to obtain estimates for each animal at each trial sequence category. Pearson correlation between normalized RTs and Δp(Stop) was used to infer the coupling between these measures of proactive response adjustments.

Because some sequences of trials, especially those with very few (0-1) or very many (5-6) Go or Stop trials, are uncommon and noisy, we only analyzed trial sequence categories with at least 5 trial sequences in a session. Furthermore, a trial sequence category in a session must have at least 5 sequences ending with

a Go trial and 5 sequences ending with a Stop trial. To ensure a robust estimate, we further limited our analysis on trial sequence categories that were observed in at least 10% sessions to minimize noise associated with very infrequent trial sequences containing many stop trials in a row. For this analysis, converted stop trials in trials 1-6 were considered as Go trials because the stop signal was not presented (i.e., for the animal, these trials were effectively Go trials). However, converted stop trials in trial 7 were considered as failure-to-stop errors to

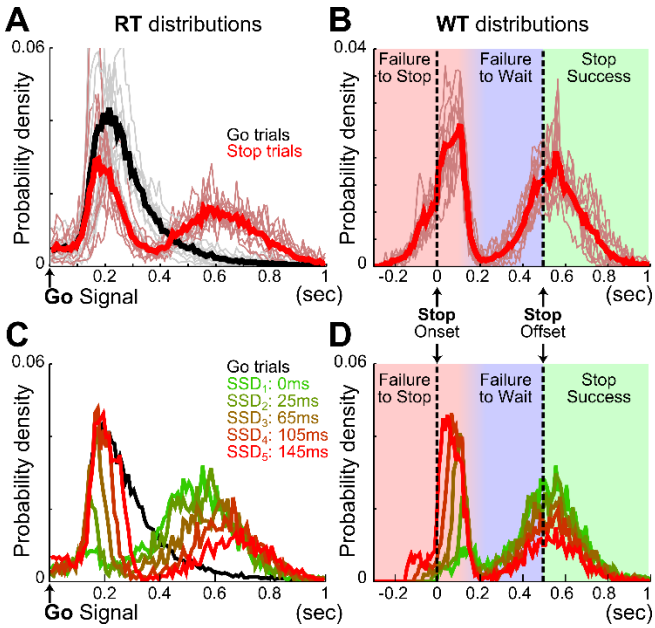

Figure 3 - Stop trial RTs are bimodally distributed

(A) Mean RT distributions in Go (black) and Stop (red) trials. Thin lines represent the mean RT distribution for individual animals (n=10). Stop trial RTs were bimodally distributed, with the fast RT peak largely overlapping with Go trial RTs. **(B)** Mean WT distributions in Stop trials. Thin lines represent the mean WT distribution for individual animals (n=10). Vertical black dashed lines indicate onset and offset of the stop signal and correspond to the duration of the hold period. WTs were bimodally distributed, with the fast WT peak abruptly truncated within 150-200ms after Stop signal onset. The color shadings indicate three types of Stop trials: failure-to-stop error (red), failure-to-wait error (blue) and stop success with reward (green). **(C)** Mean RT distributions in 95 sessions with the same SSDs for Go (black) and Stop (colored) trials. Stop trials were plotted separately for each SSD. This example illustrates that the relative proportion of the two RT peaks is a function of SSD. **(D)** WT distributions from the same Stop trials in **(C)** shows that the fast WT peak is truncated at the same time point after stop signal onset irrespective of SSD.

accurately estimate the entire range of stop trial outcomes. In addition, we did not constrain the order of trials in each sequence, only the number and types of trials. For instance, a trial sequence of Go-Stop-Go-Stop-Go-Stop-Go and Go-Go-Go-Stop-Stop-Stop-Go would both be similarly classified as having three stop trials preceding a Go trial.

Results

To develop a rodent appropriate version of the SST, we incorporated two key elements in the primate SST that have not been consistently incorporated in other rodent SSTs: stopping the preparation of an action instead of stopping an ongoing movement (Beuk et al., 2014, Eagle and Robbins, 2003b, 2003a), and the inclusion of multiple SSDs within a session (Eagle and Robbins, 2003a, 2003b; Leventhal et al., 2012; Schmidt et al., 2013). Specifically, each trial was initiated by rats inserting their nose into a fixation port and waiting for an auditory go signal **(Figure 2)**. On Go trials (67%), the go signal was presented alone and rats were rewarded in an adjacent port if the reaction time (RT), i.e. the latency between go signal onset and fixation port exit, was within 500 msec. On Stop trials (33%), the go signal was followed by a visual stop signal after a stop signal delay (SSD) randomly chosen from 5 possible latencies. In these trials, rats were rewarded only if the WT, i.e. the latency between stop signal onset and fixation port exit, was longer than 500ms. Exiting the fixation port before the end of the hold period (WT<500ms) resulted in forfeit of reward. Successful performance in stop trials required rats to cancel the planned go response and maintain fixation for the entire hold period.

We first examined reactive inhibitory control in rats. Ten Long Evans rats were trained in the SST and were able to complete on average 354.08 ± 4.18 Go and 177.01 ± 2.10 Stop trials within a 90-minute daily session (mean ± s.e.m. n=257 sessions). Rats modulated fixation port exit RT based on trial type, making slower responses on Stop than Go trials (Go: 287.27 ± 18.27ms, Stop: 431.04 ± 24.13ms, t_9 = -17.04, p=4.0x10^{-58}). Closer examination of RT distributions shows

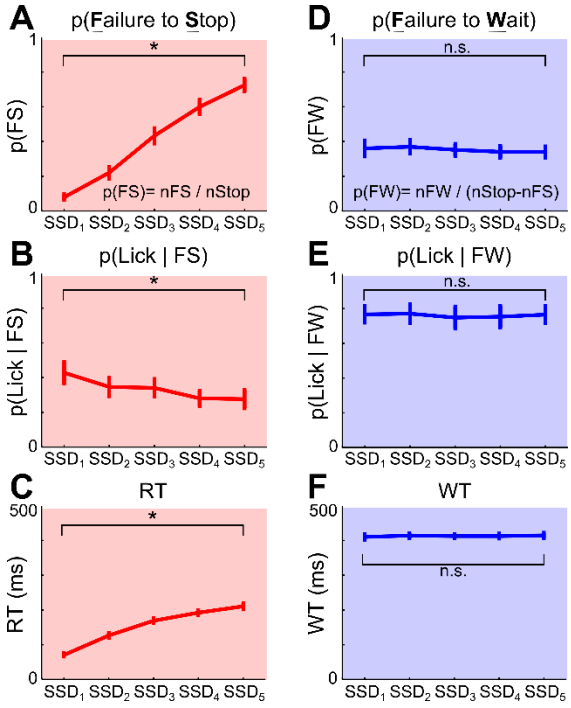

Figure 4 - Failure-to-stop and failure-to-wait represent independent errors

(A-C) Failure-to-stop (FS) errors. (**A)** Proportion of FS trials among all Stop trials increased as a function of SSD, reflecting that stopping is harder when SSD is longer. (**B)** Proportion of FS trials in which animals attempted to lick for reward at the sipper tube. (**C)** RT relative to Go signal onset in FS trials increased as a function of SSD. (**D-F**) Failure-to-wait (FW) errors. (**D)** Proportion of FW trials among the subset of Stop trials in which the fast Go response was cancelled as a function of SSD. Unlike FS errors, FW errors were unaffected by SSDs. (**E)** Proportion of FW trials in which animals attempted to lick for reward at the sipper tube. Unlike FS errors, FW errors were associated with a high percentage of attempted reward collection and unaffected by SSDs. (**F)** WT relative to Stop signal onset in FW trials was not affected by SSDs. Error bars represent s.e.m (n=10 rats). See methods for the definition of FS and FW errors. Asterisks denote main effect of SSD (repeated measures ANOVA).

that, unlike Go trial RTs, Stop trial RTs were bimodally distributed **(Figure 3)**. The first and fast mode of Stop trial RTs closely overlapped with the Go trial RT distribution **(Figure 3A, C)**, occurred well before the end of hold period, and were therefore considered as errors and not rewarded. This fast mode of Stop trial RT was abruptly truncated about 100-200ms after the onset of stop signal, which reflects a pause in behavioral response **(Figure 3B, D)**. This was followed by the second and slower mode of Stop trial responses, with WTs centered on the end of the hold period **(Figure 3B, D)**. A significant proportion of this second, slower mode of Stop trial responses occurred before the end of the 500ms hold period and therefore were considered as errors and not rewarded. The consistent pattern of bimodal stop trial RT distributions across animals shows that two types of Stop trial errors are categorically different.

We hypothesized that the first type of Stop trial error corresponded to trials in which animals failed to stop the planned go response, and therefore the RTs were highly similar to Go trial RTs. We refer to this type of error as failure-to-stop (FS). We further hypothesized that the second type of error arose after animals had successfully stopped the initial go response, but failed to wait for the entire duration of the 500ms hold period. We refer to this type of error as failure-to-wait (FW). According to this hypothesis, failure-to-stop errors in this task are analogous to non-cancelled trials in human and primate stop signal task studies, while failure-to-wait errors would represent successful stopping but a failure of post-stopping related processing, and may rely on separate neural mechanisms.

To test if the two types of Stop trial errors were independent of each other,

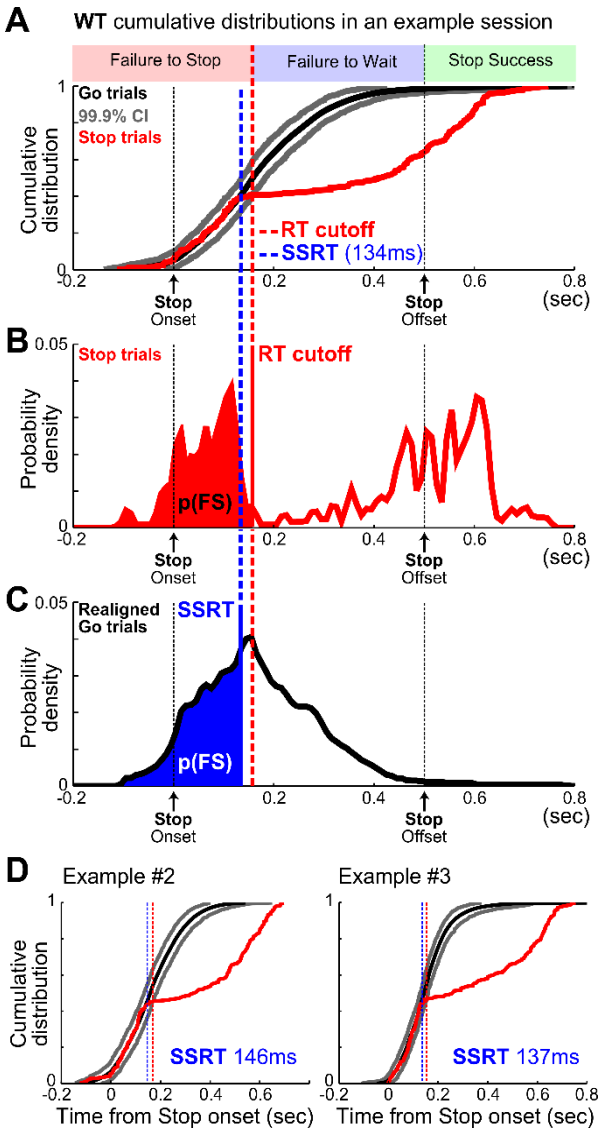

Figure 5 - A New Method to Estimate SSRT Independent of Failure-to-Wait Errors

A. Illustration of the new modified integration method by plotting the WT cumulative distributions from one example session. WT distributions relative to stop signal onset from Stop trials (red) and re-aligned Go trials (mean, black; 99.9% CI, gray). The intersection of Stop trial WTs (red) and the upper 99.9% CI bound (gray) defined an optimal WT cutoff (red vertical dashed line) that best separated FS and FW errors. **B.** The WT cutoff determined the proportion of FS errors, p(FS), indicated by the red area under the WT distribution from Stop trials. **C.** SSRT estimate (blue vertical dashed line) was defined as the time point in the WT distribution from re-aligned Go trials that corresponded to p(FS) under the curve. This is conceptually similar to the integration method of SSRT estimation, but aligned to stop signal onset. **D.** SSRT estimation from two other example sessions. Note that WTs from re-aligned Go trials and Stop trials overlapped completely up until SSRT.

we investigated whether the proportion and speed of each type of error changed as a function of SSD, and whether animals attempted to collect reward following each type of error. We found that longer SSDs were associated with higher percentages of failure-to-stop error (overall mean p(failure-to-stop) = 0.41 ± 0.03, main effect of SSD: $F(4,36) = 175.14$, $p=5.0x10^{-24}$, repeated measures ANOVA) (**Figure 4A**, see also **Figure 3C-D**). Furthermore, rats only attempted to collect reward in 33.44 ± 4.76% of these trials and were less likely to try to collect reward at longer SSDs (main effect of SSD: $F(4,36) = 5.98$, $p=0.0009$, **Figure 4B**). The mean RT in failure-to-stop errors increased with longer SSDs (overall mean = 153.77 ± 4.67ms, main effect of SSD: $F(4,36) = 102.27$, $p<10^{-20}$) but were faster than the mean RT in Go trials (Go vs. failure-to-stop: 287.27 ± 18.27ms vs. 153.77 ± 4.67ms, $t_9 = 7.20$, $p=9.1x10^{-22}$, **Figure 4C**). These features are consistent with key properties of stop failure error predicted by the independent race model between the go and stop process (Logan and Cowan, 1984; Logan et al., 1984).

In contrast, the proportion of trials in which animals successfully stopped and subsequently failed to wait (failure-to-wait errors) was little affected by SSDs (Overall mean p(failure-to-wait) = 0.35 ± 0.04, no main effect of SSD, $F(4,36) = 1.19$, $p=0.33$) (**Figure 4D**, see also **Figure 3C-D**). Rats attempted to collect reward in 76.00 ± 5.33% of these trials and attempted to collect reward with equal likelihood on all SSDs (no main effect of SSD, $F(4,36) = 0.38$, $p=0.82$, **Figure 4E**). Fixation port exit in these trials occurred close to the end of 500ms hold period and was not affected by SSD (mean WT = 412.85 ± 6.04ms, no main effect of SSD, $F(4,36) = 0.3$, $p=0.88$, **Figure 4F**). Therefore, while rats similarly forfeited reward

in these trials by responding during the 500ms hold period, this mode of failure is distinct from the failure-to-stop error. In contrast to failure-to-stop errors, failure-to-wait errors are more similar to successful stop trials because of their long RTs near the end of the hold period and high percentage of reward collection after fixation port exit. These properties support the idea that this type of error likely reflects failure-to-wait during the hold period, even though rats are able to successfully inhibit their planned go response.

The prevalence of failure-to-wait errors poses a unique challenge of adopting the SST in rodents because SSRT should be estimated based only on failure-to-stop errors while excluding failure-to-wait errors, even though both types of error led to forfeiture of reward. However, these two types of errors have been traditionally conflated in rat studies because whether rats successfully obtained reward is typically used as a proxy for whether the planned go response was

---

Figure 6 - Validating the new SSRT estimation method using simulated data

(A) Schematic of the RT simulation. Each of the 100 simulation runs consisted of 300 Go trials and 150 Stop trials. RTs in Go trials were randomly drawn from the mean RT distribution from Figure 2A. Stop trials were modeled as an independent race between a go process (as in Go trials) and a stop process consisting of the SSD randomly drawn from 5 SSDs and a fixed SSRT at 150ms. If the go process finished faster, RT was determined by the go process. If the stop process finished faster, the fast go response was inhibited and the WT was randomly drawn from the slow peak of the mean WT distribution from Figure 2B (red). This simulation produced RT and WT distributions similar to the empirical observation. **(B)** Summary of SSRT estimates (mean ± s.e.m) with varying amounts of FW errors mislabeled as FS errors for median (green) and integration (blue) methods, compared with SSRT estimated from the modified integration method. Conflation of FW errors as FS errors systematically overestimates SSRT using median and integration methods. Asterisks denote SSRT estimates significantly greater than the true SSRT (150ms) by independent t-test Bonferroni corrected for multiple comparisons (n=10 10-iteration blocks). **(C)** Scatter plot of estimated SSRTs over all model iterations between the modified integration method vs. the conventional median (green) and integration (blue) methods. For median and integration methods, the ideal WT cutoff (see Methods) was used to classify failed and successful stop trials. n=100 iterations. **(D)** Scatter plot of SSRT estimates using the 500ms WT cutoff, which mislabels all FW errors as FS errors. Convention as in **(C)** n=100 iterations.

canceled. To disambiguate these two types of error, we developed a new analytic method that estimates SSRT independent of failure-to-wait errors. Because SSRT represents the time it takes to process the Stop signal and to cancel the planned go response, RTs in Go and Stop trials should be statistically indistinguishable up to the point of SSRT: RTs faster than this time point should similarly result from the execution of the go response alone (G. D Logan et al., 1984) (Figure 4). Therefore, by directly comparing Go and Stop trial RT distributions, SSRT should correspond to the earliest time point that Go and Stop trial RT distributions diverge

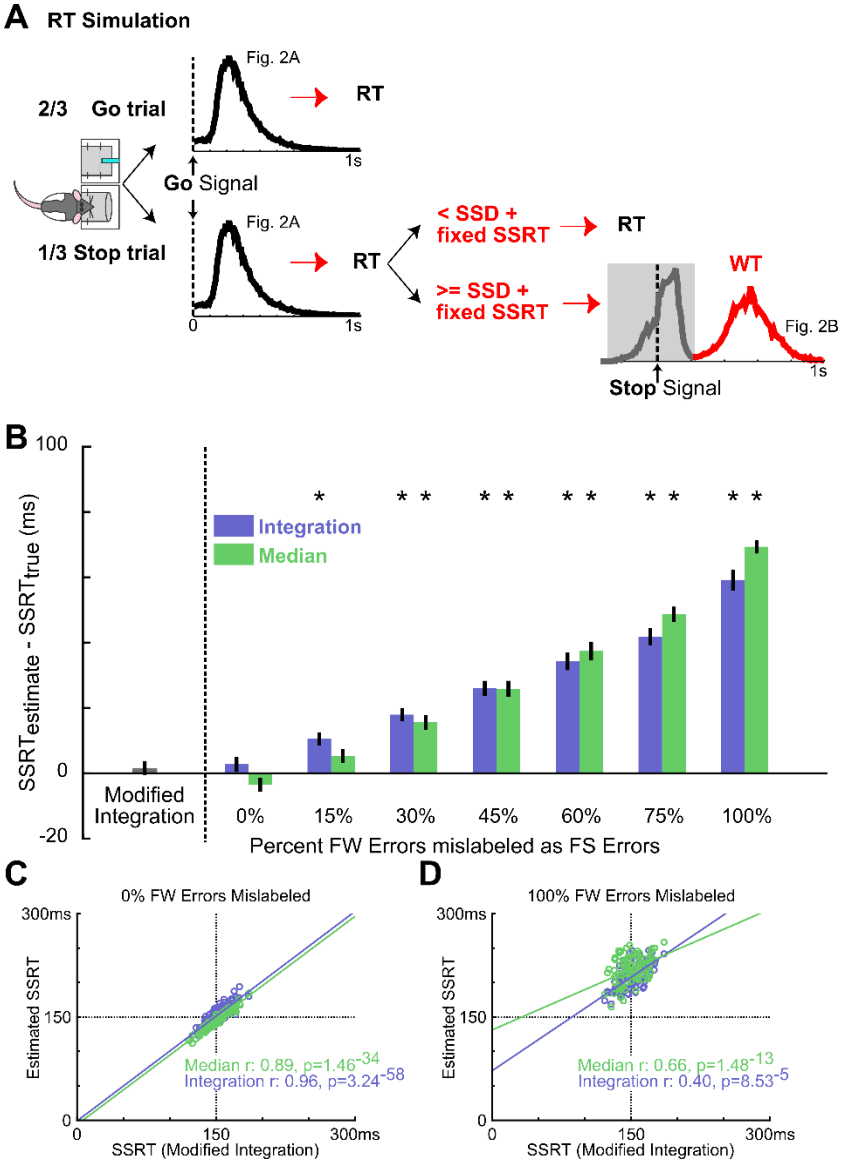

and Stop trial RTs begin to significantly slow down. We successfully implemented this method by extending the latency-matching procedure to generate Go trial RT distributions aligned to would-be stop signals, comparing the cumulative Go and Stop trial RT distributions, establishing statistical significance using a bootstrapped 99.9% confidence interval, and finally extending the integration method of SSRT estimation to RT distributions aligned to the onset of stop signal **(Figure 5)**. Importantly, this method does not require assumptions about the shape of RT distributions or how the Go and Stop process interact. Because of the conceptual similarity with the integration method, we refer to this new SSRT estimation method as the "modified integration method".

To validate our new modified integration method of estimating SSRT, we simulated RT distributions in the SST with a fixed SSRT of 150ms (**Figure 6A**, schematic of simulation). Using the simulated RTs, we then compared SSRT estimation between the modified integration method and two commonly used methods – median and integration methods. RT distributions in the SST were simulated using the independent race model between the go process (randomly drawn from the empirically observed go RT distribution) and the stop process (randomly drawn from one of five SSDs plus the duration of SSRT). If the stop process completed earlier than the go process, WT was then determined by the empirically observed WT distribution in trials that rats had successfully cancelled the go response (corresponding to the second peak of the bimodal Stop trial WT distribution). Therefore, the simulation matches the empirically observed RT distributions, including the proportion of the two types of Stop trial errors.

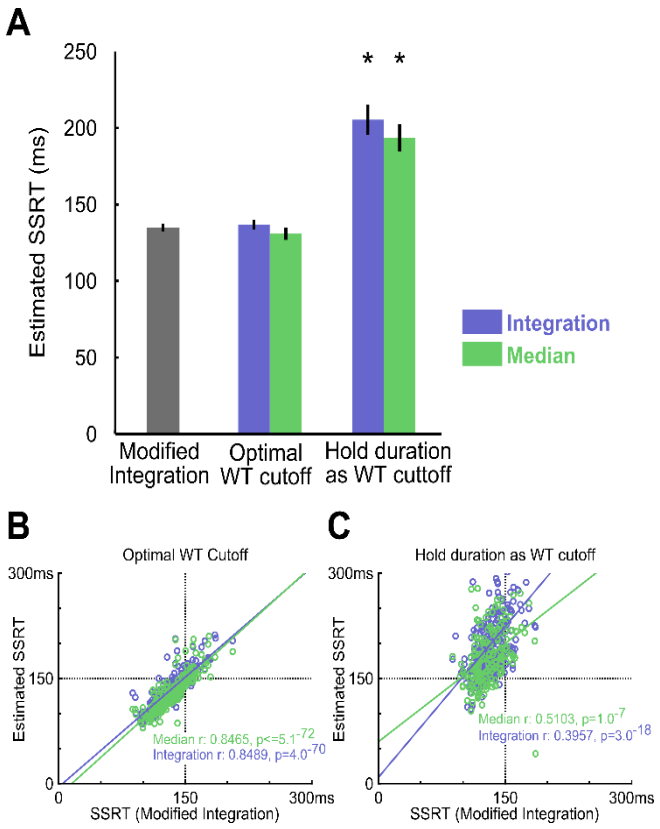

Figure 7 - Comparing three SSRT estimation methods in empirical data

(A) Summary of SSRT estimates using different methods and WT cutoffs (mean ± s.e.m). The optimal WT cutoff refers to the conservative upper bound of the SSRT estimate (see Methods), while the hold period WT cutoff corresponds to defining success in stop trials as obtaining reward. Asterisks denote estimates significantly different from the modified integration method estimate corrected for multiple comparisons (n=10 rats). **(B)** Scatter plot of estimated SSRTs over all behavioral sessions between the modified integration method vs. the conventional median (green) and integration (blue) methods, using the optimal WT cutoff. **(C)** Scatter plot of SSRT estimates using the entire hold period (500ms) as cutoff, which mislabels all FW errors as FS errors. Convention as in **(B)** n=257 sessions.

Our simulation shows that the median and integration methods produced SSRT estimates that were, respectively, 69.60 ± 2.98ms and 59.22 ± 3.02ms (mean ± S.E.M.) slower than the true SSRT when success in Stop trials was defined as successfully waiting for the entire 500ms hold period, as has been used in previous rodent SSTs **(Figure 6B)** (Bryden et al., 2012; Eagle and Robbins, 2003b; Leventhal et al., 2012). While overall SSRT estimates were similar between the median and integration method (no main effect of method, F(1,126) = 0.52,

p=0.64, repeated measures ANOVA, Method x Percent failure-to-wait Mislabeled), they were systematically overestimated with increasing inclusion of failure-to-wait errors (main effect of Percent failure-to-wait Mislabeled: $F(6,126) = 193.02$, $p<10^{-20}$, **Figure 6B**). Troublingly, the mislabeling of as few as 15-30% failure-to-wait errors (corresponding to 4-8 out of 150 Stop trials simulated) significantly biased the SSRT estimate by 10-20ms (Median method $SSRT_{Estimated} - SSRT_{Actual}$ ± s.e.m..; $Median_{15\%\ failure\text{-}to\text{-}wait}$: 6.48 ± 2.52ms, $t_9 = 2.56$, p=0.0304, n.s. vs. Bonferroni corrected α/n = 0.0036; $Integration_{15\%\ failure\text{-}to\text{-}wait}$: 10.58 ± 1.90ms, $t_9 = 4.31$, p=0.0003; $Median_{30\%\ failure\text{-}to\text{-}wait}$: 15.98 ± 12.49ms, $t_9 = 6.42$, p=0.0001; $Integration_{30\%\ failure\text{-}to\text{-}wait}$: 17.94 ± 1.93ms, $t_9 = 9.29$, $p=7.0x10^{-36}$; **Figure 6B**). The median and integration methods provided accurate estimates only when given an ideal WT cutoff that perfectly distinguishes failure-to-stop errors from failure-to-wait errors in the simulation **(Figure 6B)**, which converged with the estimates of the modified integration method (Median method Pearson's r: 0.8865, $p=1.5x10^{-34}$; Integration method Pearson's r: 0.9641, $p=3.2x10^{-58}$; **Figure 6C**). Using a cutoff that included 100% failure-to-wait errors significantly degraded this relationship (Median method Pearson's r: 0.6548, $p=1.5x10^{-16}$; Integration method Pearson's r: 0.4021, $p=8.5x10^{-5}$; **Figure 6D**). The modified integration method provided an accurate estimate of the true SSRT without the need for an arbitrary WT cutoff **(Figure 6B)**. This comparison shows that the conflation of the two types of stop errors leads to significant bias in SSRT estimation using the conventional methods, and validates our new modified integration method in providing an unbiased SSRT estimate independent of failure-to-wait errors.

In empirical data from rats performing the SST, the modified integration method estimated SSRT at 134.77 ± 2.48ms (mean ± S.E.M.), which was substantially faster than the estimates provided by median (193.72 ± 8.38ms, t_9 = -8.22, p=1.8x10^{-5}) and integration (205.40 ± 9.23ms, t_9 = -8.79, p=1.0x10^{-5}) methods using reward as the proxy for stop success **(Figure 7A)**. As our simulation results illustrated, such differences in SSRT estimates likely resulted from the conflation of the two types of errors. The modified integration method, however, can also provide a reliable WT cutoff that best separates the two types of stop errors such that median and integration methods produced similar SSRT estimates as the new modified integration method (Median method: 130.81 ± 3.72ms, t_9 = 1.86, p=0.0953; Integration: 136.80 ± 3.03ms, t_9 = -1.19, p=0.2632, **Figure 7A**). The SSRTs estimated by median and integration methods using this optimal WT cutoff were highly correlated with the SSRT estimated by the modified integration method (Median method: Pearson's r = 0.8489, p=5.1x10^{-72}; Integration: Pearson's r = 0.8465, p=4.0x10^{-70}, **Figure 7B**), suggesting a convergence of SSRT estimation by all methods under ideal conditions. This correlation was significantly degraded when SSRT estimated by median and integration methods was based on reward as the proxy for stop success (Median method Pearson's r = 0.3957, p=1.0x10^{-7}; Integration method Pearson's r = 0.5103, p=3.0x10^{-18}, **Figure 7C**). These results suggest that SSRT estimates in rats have been significantly overestimated by existing methods when failure-to-wait and failure-to-stop errors are conflated.

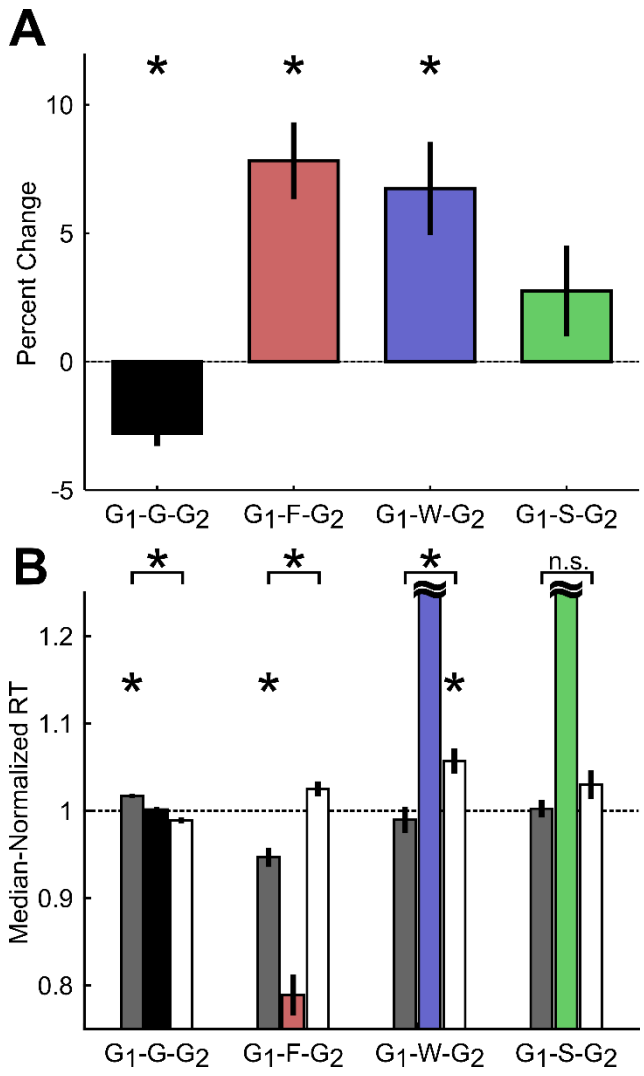

Figure 8 - Proactive adjustment of RT based on trial outcome

(A) Percent change in RT on Go trials preceding (G_1) and following (G_2) different trial outcomes. G_1-G-G_2 refers to three consecutive go trials (F: failure-to-stop; W: failure-to-wait; S: stop success). **(B)** Median-normalized RT for the Go trials preceding and following each trial outcome. Horizontal black dashed line indicates median RT. Intermediate trial data were included for visualization purposes only and not included in statistical analyses. Asterisks represent means significantly different than 1 or significant differences between groups, corrected for multiple comparisons. Error bars represent s.e.m. n=10 rats.

Having demonstrated that rats exhibited reactive inhibitory control similar to primates, we further examined whether rats also employed proactive control strategies in the SST by adjusting the speed of their responses based on the outcome of previous trials (Beuk et al., 2014; Bissett and Logan, 2012; Emeric et

al., 2007; Ide et al., 2013; Ide and Li, 2011; C. R. Li et al., 2008; Pouget et al., 2011; Verbruggen and Logan, 2009a). To this end, we first compared RTs in two Go trials (G_1, G_2) interleaved with either a Go trial (G), a failure-to-stop trial (F), a failure-to-wait trial (W), or a successful stop trial (S) as percent changes relative to G1 **(Figure 8A)** or as median-normalized RTs **(Figure 8B)**. We observed that rats speed up following sequential Go trials (Median-normalized RT on G_1-G trials: 1.02 ± 0.002; G-G_2 trials: 0.99 ± 0.003; t_9 = 5.86, p=2.4x10^{-4} vs. Bonferroni corrected α/n=0.0042). In addition, rats slowed down following both failure-to-stop (G_1-F: 0.95 ± 0.01; F-G_2: 1.03 ± 0.01; t_9 = -5.52, p=3.7x10^{-4} vs. corrected α/n=0.0042) and failure-to-wait (G_1-W: 0.99 ± 0.01; W-G_2: 1.06 ± 0.01; t_9 = -3.93, p=0.0034 vs. corrected α/n=0.0042) errors, but not successful stop trials (G_1-S: 1.00 ± 0.01; S-G_2: 1.03 ± 0.02; t_9 = -1.64, p=0.1365 vs. corrected α/n=0.0042). We further observed that, in Stop trials, only G_2 trial RTs following failure-to-wait trials (W-G_2) were significantly slower than the median RT (t_9 = 4.15, p=0.0025 vs. corrected α/n=0.0042), while only G1 trial RTs before failure-to-stop trials (G1-S) were significantly faster than the median RT (t_9 = -5.10, p=0.0006 vs. corrected α/n=0.0042). These results suggest that, in proactive inhibitory control, not only do Stop trial errors induce modifications in subsequent response speed (G2), but also that the baseline response speed (G1) predicts whether subsequent stopping, but not waiting, would be successful.

Recent studies in humans and monkeys have also shown that the frequency of Stop trials in the recent trial history affect subsequent speed of go responses as well as the probability of stop success (Emeric et al., 2007; Ide et al., 2013). To

further investigate whether similar effects are present in rats, we determined how Stop trial frequencies in any contiguous 6-trial sequence affected go and stop performance in the next trial, relative to the performance in the entire session. This was achieved by first identifying all 7-trial sequences that ended with a Go or a Stop trial (on trial 7), and categorizing trial sequences based on the number of Stop trials in trials 1-6 **(Figure 9)**. We found that RTs on Go trials following with no recent Stop trials were faster than median RT (t_9 = -3.91, p=0.0035 vs. corrected α/n=0.01), while RTs following blocks of trials with 3/6 and 4/6 Stop trials were slower (t_9 = 3.76, p=0.0045 and t_9 = 5.97, p=2.1x10^{-4} vs. corrected α/n=0.01) (**Figure 9A**, left). The pattern of proactive RT adjustment is consistent with other reports showing go RT speeding following infrequent recent Stop trials and go RT slowing following frequent recent Stop trials (Emeric et al., 2007; Ide et al., 2013) and our observations in **Figure 8**. However, we found that frequent recent Stop trials were followed by worse stop performance compared to session-wide performance level, and vice versa following infrequent recent Stop trials (**Figure 9A**, right). Furthermore, the extent of RT adjustment was significantly correlated with the extent of stop performance adjustment in the same trial categories (**Figure 9A**, right). In other words, frequent recent Stop trials resulted in slower response speed as well as worse stop performance in the following trial, and the extent of both adjustments were coupled. This observation was surprising because slower RTs are typically associated with better, not worse, stop performance, assuming that SSRT was not affected.

To further validate this surprising observation, and to delineate the respective contributions of three types of Stop trial outcomes, we sorted the same trial sequences by the number of failure-to-stop trials **(Figure 9B)**, failure-to-wait trials **(Figure 9C)** and successful stop trials **(Figure 9D)**. We found that trial sequence sorting based only on failure-to-stop trials did not result in significant RT modulations and only minimal stop performance adjustments that were not correlated with RTs, even in blocks with several failure-to-stop trials **(Figure 9B)**. On the other hand, sorting based on both failure-to-wait and successful stop trials showed RT modulations and correlated stop performance adjustments **(Figure 9C,D)**, patterns that were comparable to the findings in **Figure 9A**. These observations suggest that RT and stop performance adjustments were driven not by failure-to-stop trials but primarily by failure-to-wait and successful stop trials. Indeed, we observed the strongest correlation between RT and stop performance adjustments when trial sequences were sorted by the number of both failure-to-wait and successful stop trials **(Figure 9E, F)** ($r=-0.75$). Among the three possible Stop trial outcomes, the adjustment of stop success probability was consistently best correlated with RT adjustments. Together, the strong coupling between RT and stop performance adjustments suggests that both types of proactive adjustment were likely controlled by the same underlying mechanism. The commonality between failure-to-wait and stop success trials that were able to trigger these proactive adjustments is that both trial types involve successful stopping of the prepotent go response, while in failure-to-wait trials the conflict between the prepotent go response and the reactive stop response is reduced.

Discussion

In this study, we developed a novel, rodent appropriate stop signal task and characterized both reactive and proactive control strategies in rats. Our rodent SST incorporated key elements commonly used in the primate SSTs, including multiple SSDs and requiring subjects to cancel a planned action instead of stopping an ongoing movement **(Figure 2)**. For reactive inhibitory control, we showed that errors in Stop trials resulted from two independent sources: failure-to-stop the go response, or failure-to-wait after stopping was achieved **(Figure 3, 4)**. The conflation of these two types of errors systematically overestimates SSRT by at least 50ms both in a simulated race model and in practice **(Figure 6, 7)**. To address this issue, we developed and validated a novel modified integration method that provides an unbiased SSRT estimate independent of the ability to wait **(Figure 5, 6, 7)**. For proactive inhibition, we showed that rodents exert proactive control strategies following stop trials to increase their probability to stop **(Figure 8)**. In addition, we demonstrated that rats adjust their RTs and the probability of stopping based on recent trial history beyond the immediately preceding trials **(Figure 9)**. Together, these results establish the rat as a valid model that displays proactive and reactive inhibitory control as observed in monkeys and humans.

This study differs from previous attempts to translate the SST for rodents in several critical ways. While rats are required to cancel the initiation of an action in our task as in most primate and human studies, previous rodent studies from both Eagle and colleagues (Eagle and Robbins, 2003a) and Beuk and colleagues (Beuk et al., 2014) used a task in which rodents were required to inhibit an ongoing

movement following a stop signal. It is not clear if these tasks invoke the same task demands as in human and primate versions of the SST. While this is not a concern for Berke and colleagues (Leventhal et al., 2012; Schmidt et al., 2013), which required rats to cancel a fixation port exit response similar to the task design used here, their task design, as well as those used by Eagle and colleagues, used only a single, constant SSD per session. The practice of using a constant SSD makes the stop signal highly predictable and likely encourages rats to employ a timing strategy to improve stopping. Such a concern is minimized in primate SSTs, which typically use multiple SSDs or a tracking procedure to dynamically adjust SSD across trials. Our SST design addresses both issues and successfully translate the SST for rodents.

In SSTs studies of humans and non-human primates, proactive and reactive control each refers to preparation to stop prior to signal onset and stimulus-driven process at signal onset. In the context of understanding reactive inhibitory control in rodents, our results highlight the unique challenge in rodents to dissociate initial stopping from subsequent waiting in the SST. While the stop signal similarly instructs humans, monkeys and rats to withhold the prepotent go response for a short period of time (the hold period), rats are especially prone to committing errors during this period. Further, while failure-to-stop errors likely represent failures of reactive control **(Figure 4 A-C)** and are influenced by proactive adjustments **(Figure 8)**, failure-to-wait errors seem unaffected by SSD, RT, or proactive adjustments **(Figure 4D-F, Figure 8)**. This difference likely originates from two sources: First, rodents may be more impulsive than primates and less able to wait

for the entire duration of the hold period after they have successfully stopped the planned go response (Robinson et al., 2009). Second, the nature of behavioral responses generated by primates and rats in behavioral tests are fundamentally different and these differences must be accounted for. For instance, unlike in primates, rats needed to rapidly exit the fixation port to approach, collect, and consume the reward after they had successfully stopped the planned go response and waited for the entire hold period. In contrast, reward in primate SSTs is not directly associated with specific task-relevant behavioral responses such as saccade or button press, but is instead generally delivered without an instrumental requirement (e.g., licking). Therefore, in rodents this reward-approaching response likely commands a stronger motivational drive than in primates, especially toward the end of the hold period when reward availability is imminent.

Figure 9 - Proactive adjustments of RT and stop performance by recent stop trials.

(A) Comparison of 7-trial sequences ending with a Go trial (left) or a Stop trial (right), sorted by the total number of all stop trials in trials 1–6. The top three rows show the average trial composition in trials 1–6 in each trial sequence category (top row), the respective relative frequencies (second row) and sessions containing at least 5 sequences in each trial sequence category (third row). The bottom row shows, for each trial sequence category, the median-normalized RTs (left) and the difference between the observed and predicted stop trial outcomes (right) in trial 7. The difference between the observed and predicted stop trial outcomes [Δ*p*(Stop)] represents the influence of recent Stop trial frequency on subsequent stop performance beyond what would be expected given the observed distribution of SSDs for that trial sequence category. *P*-values for *t*-test (*n* = 10) are represented by the size of circles. *R* and *p*-values for Pearson correlation between median-normalized RTs and Δ*p*(Stop) are indicated next to each type of Stop trial outcome. **(B–E)** The same analysis as in **(A)**, sorted by the number of failure-to-stop trials **(B)**, failure-to-wait trials **(C)**, successful stop trials **(D)**, or the number of successful stop trials and failure-to-wait trials combined **(E)**. **(F)** Correlation between median-normalized RTs and Δ*p*(Stop Success) based on trial sequence categories in **(E)**. These results show that proactive adjustments of RT and stop performance are highly correlated and jointly driven by recent failure-to-wait and successful stop trials.

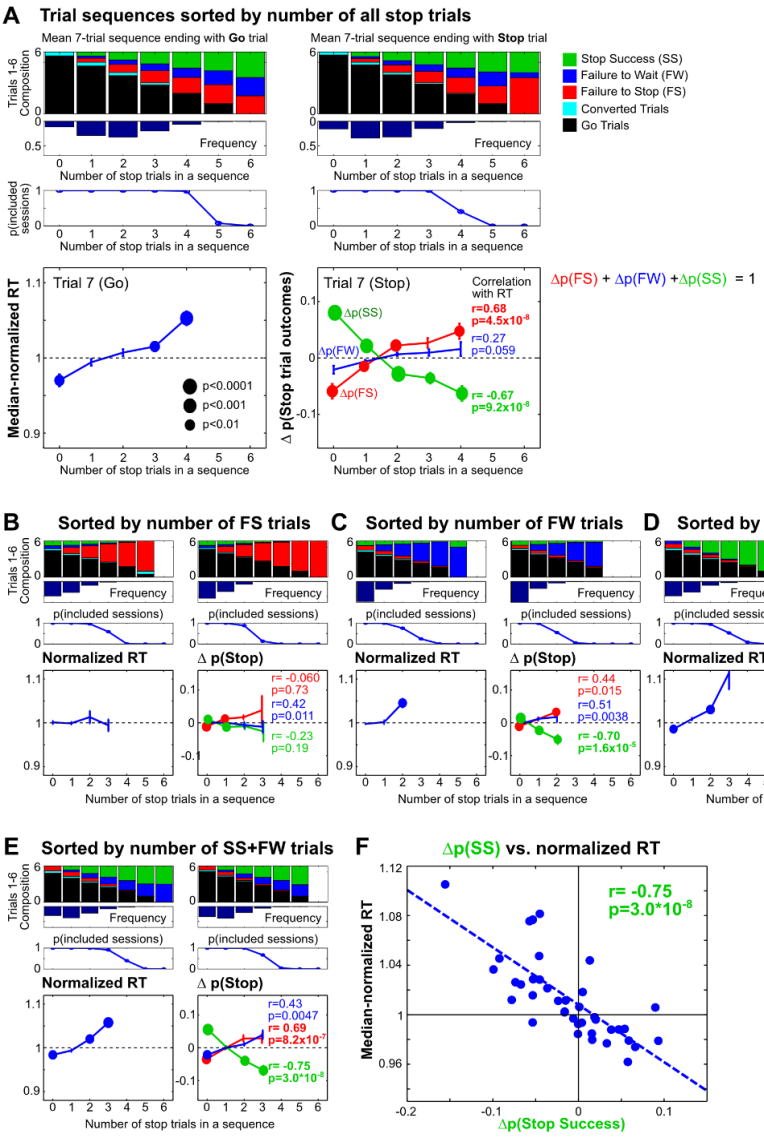

Our results support that failure-to-stop and failure-to-wait errors are generated independently. We show that failure-to-wait errors are associated with long WTs and a high frequency of reward collection attempts, but are not modulated by SSD **(Figure 4)**, properties that are very similar to successful Stop trials. By contrast, failure-to-stop errors are significantly modulated by SSD and their associated RTs are faster than Go trial RTs **(Figure 4)**, which recapitulate the key properties predicted by the independent race model (Band et al., 2003b; Logan

and Cowan, 1984). These findings are consistent with the interpretation that failure-to-stop errors result from failure of reactive inhibition to cancel the planned go response, while failure-to-wait errors represent premature attempts to collect reward after stopping was successful and are unrelated to factors affecting stopping. The presence of failure-to-wait errors likely represent a common feature of rodent SSTs that must be addressed when estimating SSRT (Bryden et al., 2012; Eagle and Robbins, 2003a; Leventhal et al., 2012; Schmidt et al., 2013). For example, RTs on failed Stop trials are similarly bimodally distributed in Figure 1 of Schmidt et al. and Figure 4B of Leventhal et al., 2012. The distinction between failure-to-stop and failure-to-wait errors is important because these two types of errors are under the control of distinct behavioral variables and therefore likely arise from distinct underlying neural mechanisms. It is important to also note that the distinction between failure-to-stop and failure-to-wait errors does not map onto the distinction between proactive and reactive inhibitory control. Rather, distinguishing failure-to-stop from failure-to-wait errors is relevant for correctly estimating SSRT, which embodies the reactive inhibitory control process. In addition, our rodent SST may also serve as a useful model to independently assess two forms of impulsive action in a within-task design (Broos et al., 2012; Eagle et al., 2008a; Worbe et al., 2014).

The conflation of these two types of errors in rodents not only significantly overestimates SSRT **(Figure 6, 7)**, such conflation may lead to incorrect mechanistic interpretations because manipulations such as psychostimulant administration (Fillmore and Rush, 2002; Groman et al., 2009; Li et al., 2006; Liu

et al., 2009) or prefrontal cortical lesion (Aron et al., 2003; Picton et al., 2007) may also affect impulsivity (Mar et al., 2011; Mendez et al., 2010) and therefore the ability to wait. In such cases, manipulations that affect the ability to wait will produce longer SSRT estimates when the two types of stop error are conflated, and likely would be misinterpreted as affecting the ability to stop instead. Even in cases in which such manipulations are not used, the mislabeling of as few as 15% failure-to-wait errors (corresponding to about 3% of all stop trials) as failure-to-stop errors significantly inflates the SSRT estimate. It is important to note that because most human and primate studies do not explicitly require subjects to wait after successfully stopping that these failure-to-wait errors are likely a rodent-specific phenomenon. Given the rapidly growing demand for an appropriate rodent SST to link the computational power of the SST to techniques too costly or not yet available in human and monkey studies, special attention must be placed on ensuring rodent SSRT estimates are valid, reliable, and comparable to primate estimates.

The new method developed in this study represents an extension of the commonly used integration method, and provides an unbiased SSRT estimate independent of the ability to wait, without assuming the shape of RT distributions or how the go and stop process interact **(Figure 5, 6)**. This modified integration method estimates SSRT by comparing RT distributions in Stop trials with appropriately resampled and realigned Go trials to would-be stop signals. The modified integration method provides a direct parallel with, and was in fact inspired by, neurophysiological data analysis where responses are aligned to the onset of

distinct events. Therefore, the modified integration method can potentially provide a unified framework for comparing behavioral and neural responses between Go and Stop trials, a major analytic advance applicable to rodents and primates alike.

Using this new modified integration method of SSRT estimation, we found that rats show a very robust and fast stopping behavior. Our estimate of SSRT is ~50-60ms faster than SSRT estimates using median or integration methods when the failure-to-stop and failure-to-wait errors are conflated, as has been the case in previous rodent studies (Bryden et al., 2012; Eagle and Robbins, 2003a). The use of a long RT cutoff to separate failure-to-stop from failure-to-wait errors by Leventhal and colleagues offered a sub-optimal solution and similarly produced substantially slower SSRT estimates than reported here (162.00 ± 12.65ms in Leventhal et al. vs. 134.77 ± 2.48ms here). This bias represents a significant percentage of the SSRT estimate and is of critical importance for existing and future rodent studies using the SST. More importantly, such a bias may also shift the temporal order and causal inference between neurophysiological responses and SSRT, such that a neural signal that was faster than conventional SSRT estimates in rodents may in fact occur after the true SSRT. Special attention must be paid to minimizing or eliminating the conflation of failure-to-stop and failure-to-wait errors.

Our analysis using RT simulations further shows that conventional methods of SSRT estimation can be salvaged by selecting an optimal WT cutoff that best separates failure-to-wait error from failure-to-stop error **(Figure 6)**. While setting such a WT cutoff in empirical datasets can be subjective and arbitrary because

substantial differences exist between subjects and between different training sessions within the same subject, our new modified integration method can also provide an unbiased WT cutoff so that SSRT estimates from all methods converge **(Figure 6, 7)**.

In the context of understanding proactive inhibitory control in rodents, we demonstrate that like primates, rats employ a proactive slowing strategy to increase stopping ability (Emeric et al., 2007; Nelson et al., 2010; Pouget et al., 2011; Rieger and Gauggel, 1999; Verbruggen and Logan, 2009a). In 3-trial sequences, we observe that RTs are slower than the median RT following failure-to-wait errors **(Figure 8B)**. In addition, we observe that RT on the previous trial predicts the outcome on the current trial: RT prior to a failure-to-stop trial was faster than the median RT, while RT prior to a successful Stop or failure-to-wait trial was not different from the median RT. These data suggest a complicated push-pull relationship in rats between the predisposition to respond quickly and the task-relevant requirement to stop.

We extend those findings in the longer 7-trial sequence **(Figure 9)** and observe that RTs following frequent recent Stop trials are slower than the median RT, while RTs following infrequent recent Stop trials can be faster than the median RT. Much to our surprise, however, the same trial sequences leading to slower subsequent RTs are associated with worse stop performance relative to session-wide stop performance level, even after controlling for the contribution of SSDs **(Figure 9)**. In the context of the independent race model, stop performance is completely determined by the go RT distribution, SSRT, and SSDs. In most

behavioral experiments, SSRT is assumed to be a session-wide constant, while SSD is often either constant, varied among constant values (as it is here), or varies tracking performance. With the exception of the latter case, slowing of Go RTs would necessarily improve stopping probability if SSRT and SSD were held constant. Therefore, our observation that slower RTs are associated with worse stop performance necessarily implies that SSRT slows down even more significantly than RT slowing. Together, these observations imply that, rather than being stationary stochastic processes, both the Go RT distribution and the SSRT are subject to trial-by-trial variation in their underlying parameters and are dynamically adjusted based on recent trial history (Bissett and Logan, 2012; Emeric et al., 2007). While such dynamic adjustments pose a serious challenge for accurately estimating SSRT, our analysis shows that a comparison with the session-wide performance level provides a viable way to identify systematic local dynamic adjustments in stop performance.

Two observations are important for interpreting the surprising finding that slower RTs following frequent recent stop trials are associated with worse stop performance. First, the extent of stop performance adjustment is tightly coupled with the extent of RT adjustment, suggesting that both effects arise from a common cause (though, importantly, they may not share a common neural mechanism). Second, both RT and stop performance adjustments are specifically driven by failure-to-wait errors and successful stop trials but not failure-to-stop errors, which share the common feature that the prepotent planned go response is successfully canceled. Such an observation also supports our conclusion that failure-to-wait

errors are similar to success stop trials and distinct from failure-to-stop errors and should not be conflated.

One possible hypothesis based on these observations is that the common driving force for both types of proactive adjustments is the conflict between the go response rule and the stop response rule in the context of relatively common Go trials and relatively infrequent Stop trials. In other words, following successful and repeated execution of stopping in recent past trials that takes place against the background of low Stop trial probabilities, rats are less certain about which of the two response rules to prepare for: the global and more probable go response or the recent but less probable stop response. As a result, rats are less efficient at executing either the go or the stop response. Such a conflict is not present, however, in failure-to-stop errors when rats failed to execute the stop response. Future studies are needed to reconcile the differences between the current finding with those in humans and non-human primates (Ide et al., 2013). Future studies may test this hypothesis directly in rats, humans, and non-human primates by varying the proportion of stop trials to test if making Stop trials equally likely as or more likely than Go trials eliminates or even reverses the effects observed here.

It is necessary to reconcile to apparent discrepancy between proactive adjustments based on immediate trial history (Figure 8) and distant trial history (Figure 9). We observed non-significant slowing on Go trials immediately following SS trials (Figure 8) and significant slowing on Go trials following blocks with a large amount of SS trials or FW and SS trials (Figure 9D & E). While these data are seemingly at odds, it is important to note that they likely represent highly non-

overlapping trials. When examining immediate trial history effects, we selected a very specific triplets of trials in which a trial of interest (Go, FS, FW, or SS) occurred intermediate to two Go trials. By contrast, when examining recent trial history, we selected blocks of trials with differing numbers of FS, FW, or SS trials that could occur in any order, a less selective set of trials. In fact, these two trial sets may be highly non-overlapping: blocks of six trials containing a Go-Stop-Go triplet would necessarily be less likely to contain many more stop trials in the remaining three trials. Therefore, it is difficult to directly compare proactive adjustments immediately following specific trials, which may reflect trial-by-trial adjustments, and adjustments following blocks of trials, which may reflect a more global behavioral state.

Together, the current study establishes the rat as a valid model that displays both proactive and reactive inhibitory control similar to monkeys and humans. This is especially important because SSRT estimates are elevated in individuals with deficient cognitive control, including adults (Bekker et al., 2005) and children (de Zeeuw et al., 2008) with Attention Deficit Hyperactivity Disorder, Obsessive-Compulsive Disorder (Lipszyc and Schachar, 2010), Parkinson's Disease (Mirabella et al., 2011), pathological gambling (Grant et al., 2011), Tourette syndrome (Goudriaan et al., 2005), schizophrenia (Hughes et al., 2012), drug abuse (Li et al., 2006b) and normal cognitive aging (Kramer et al., 1994). The current study therefore represents an important first step in connecting the computational and quantitative power of the SST paradigm for studying inhibitory control with the unique advantages of dissecting neural circuit mechanisms in

rodent models and easy access to disease models to advance research with both basic science and clinical implications.

Chapter 2 – Characterization of Age-Related Cognitive Impairment in the Stop Signal Task

Rationale

Cognitive inhibition, or the ability to suppress unwanted or unnecessary thoughts and actions, is critical for normal functioning and is an integral component of many cognitive functions. Impaired cognitive inhibition is a hallmark of many neuropsychiatric conditions, including normal cognitive aging (Coxon et al., 2012; Gamboz et al., 2009; Haaland et al., 1987; Kramer et al., 1994; Schoenbaum et al., 2002b). However, studying cognitive inhibition is often difficult because direct measurement of the inhibitory process is often difficult. The stop signal task (SST) is a powerful tool for studying cognitive inhibition because it provides a parametric estimate of the duration of the covert inhibitory process, the stop signal reaction time (SSRT, Logan et al., 1984). In the SST, subjects are required to make a rapid behavioral response following the presentation of a Go signal and cancel this planned response following the occasional subsequent presentation of an imperative Stop signal. Whether a subject is able to cancel their planned response depends on the experimenter-controlled delay between the Go and Stop signals, the speed at which the subject was preparing their response (Go RT), and the speed at which the subject can cancel their response (SSRT).

Like primary task RTs, SSRT estimates have proven to be powerful indicators of even minor insults to cognitive inhibition. SSRT estimates are elevated in individuals with deficient cognitive control, including in neuropsychiatric disorders such as Parkinson's Disease (Gauggel et al., 2004; Mirabella et al.,

2011) or Tourette syndrome (Goudriaan et al., 2005; Johannes et al., 2001; Lipszyc and Schachar, 2010), schizophrenia (Hughes et al., 2012), or healthy individuals with cognitive impairment, such as in pathological gambling (Goudriaan et al., 2005; Grant et al., 2011; Odlaug et al., 2011) and normal cognitive aging (Kramer et al., 1994). These conditions serve as useful case studies for understanding the specific neural mechanisms of cognitive inhibition and how they are altered to cause impairment; however, most require access to cumbersome or imperfect animal models of disease or patient populations. By contrast, normal cognitive aging is common and ubiquitous, and importantly naturally occurring animal models of aging have been shown to be highly valid models of human cognitive aging (Gallagher et al., 2011; Gallagher and Colombo, 1995; Gallagher and Rapp, 1997). Normal cognitive aging provides a useful backdrop for understanding both normal and impaired cognitive inhibition.

Aging is associated with impairment in many often overlapping cognitive domains. In particular, there is substantial evidence that aging is also associated with a global decline in the ability to rapidly process information (Burwell and Gallagher, 1993; Salthouse, 2000, 1996). Aged individuals frequently report longer RTs on a wide variety of tasks, suggesting that this decline is domain-general to some extent (Kail and Salthouse, 1994). A recent study in young adults performing a SST found that young individuals who are able to more rapidly process the Go signal are also able to more rapidly process the Stop signal, suggesting there is some degree of interplay of processing speed, non-decision factors (such as sensory or motor processing time), or both between the speed of going and

stopping, at least in young individuals (White et al., 2014). It is then an open question to what extent age-related declines in processing speed and slowing of SSRT represent overlapping or nonoverlapping cognitive impairments.

The goal of the current study was to utilize the variety of behavioral information provided by the SST to examine whether changes in various cognitive domains in aging are correlated. Specifically, we examined the domain specificity of cognitive impairment in processing speed (as measured by primary task RT), stopping (as measured by SSRT) and waiting/impulsivity (as measured how long animals are able to maintain noseport fixation after stopping).

Methods

General SST methods are identical to those used in the experiments in Chapters 1 and 2 with one notable exception: In these experiments, the stop signal was presented on converted trials (those trials where rats made a noseport withdrawal response before the stop signal was presented). This change was made to bring these studies in line with the majority of human and primate studies which use a similar procedure and did not have an overall effect on the experiment.

Subjects

Nine young (3mo) and 15 aged (16-19mo at start of shaping) male Long-Evans rats completed training in the SST. Of these, all nine young and 11/15 aged rats were subsequently tested in the Morris water maze (MWM). All animals were food deprived to 85% (young) or 80% (aged) of their free-feeding weight and maintained at this weight throughout training, except during MWM testing.

Morris Water Maze Testing

Both aged (24 months) and young (6 months) rats were characterized in a standardized place version of the Morris water maze. Training was conducted over eight consecutive days with each day consisting of three-90 second trials with a 60-second ITI. In each trial rats learned to locate a submerged escape platform in opaque water. The platform was maintained in a constant location throughout training, but start locations were varied so that rats were required to learn the location of the hidden platform in space in order to locate it. To assess how well rats could locate the platform, probe trials were conducted on every sixth trial (every two days) in which the platform was retracted for the first 30 seconds of the trial and then raised to allow escape. Performance was assessed using a learning index score called the spatial learning index (SLI). This score was a weighted average proximity-to-platform over the course of probe trials, with higher scores representing poorer localization of the platform. To control for age-specific effects on motivation, locomotion, and vision, animals were also tested in a cued version of the water maze in which the platform was raised above the surface of the water. Animals were trained in a single six-trial session in this task; any animal that failed to consistently locate the visible platform was excluded from any further analyses.

SST Data Analysis

SST data analysis was identical to that used in Chapters 1 and 2, including use of the modified integration method to estimate SSRT, and is reproduced here in brief. Animals were first shaped to lick a centrally-located sipper tube to receive reward. Subsequently, animals were shaped to attempt reward collection only

following the presentation of a pure tone. After animals reliably withheld licking except in the presence of the tone, they were trained to nosepoke in the right-located fixation noseport to receive tone presentation and reward availability in the central reward port. As animals learned to nosepoke for tone presentation, the delay between noseport entry and tone onset (foreperiod) was dynamically increased until animals could reliably wait for 800ms for the tone. At this point, animals were trained to respond as quickly as possible (<500ms) and we incorporated variable foreperiods (350-800ms, 150ms steps) to make tone presentation unpredictable. After ~two weeks of training on this version of the nosepoke task, we trained animals to respond to the presentation of a panel light by maintaining noseport fixation until an audible click (solenoid opening). As with foreperiod training, the duration of the hold period increased dynamically until rats could reliably wait for 500ms from the light; at this point, animals were given several refresher tone-alone sessions and then transitioned directly to the SST.

In the SST, animals were required to respond quickly following presentation of the Go signal (pure tone) and withhold responding following the presentation of the Stop signal (panel light). The stop signal delay (SSD), referring to the delay between Go and Stop signal presentation was varied randomly between five latencies within a session. The mean of the SSD distribution was changed between sessions to make stopping easier or more difficult. The outcome of stop trials was parsed into three nonoverlapping trial types, characterized by the latency of noseport exit relative to the stop signal (wait time, WT). Failure-to-stop trials were characterized as those trials with WT<SSRT; failure-to-wait trials were those trials

with SSRT<WT<500ms; successful wait trials were those trials with WT>500ms. To calculate the proportion of failure-to-wait and successful wait trials, we summed the number of each trial type divided by the number of trials in which the animal stopped; therefore, the proportion of failure-to-wait and successful wait trials sum to 1, rather than 1-P(failure-to-stop).

Timecourse Consideration

In order to ensure all animals were well-trained in the SST, aged animals began training in the SST between 16-20 months of age (discrepancies in age at start of training result from opportunistic acquisition of animals). Shaping and acquisition of asymptotic behavioral performance generally requires 3-6 weeks in aged animals. After this period, animals are transferred to the SST, where they generally require 2-4 weeks to reach behavioral asymptote. Therefore, only aged animals with at least 28 days of SST training were used in analyses in this chapter (11/15). The remaining four aged animals were removed from the experiment early for health complications and did not meet the criterion of 28 days of SST training.

Linear Accumulator Model Fitting

While RTs are sensitive measures of behavior, they are nonetheless composite measures that capture the total duration of all cognitive, sensory, and motoric processes occurring between the presentation of a stimulus and the generation of a response. These processes can be separately modeled using a simple linear accumulator model in which an arbitrary decision unit accumulates activity from a baseline to a response threshold. The rate at which this unit accumulates on a given iteration is constant and varies stochastically from trial to

trial. This model requires four parameters: the mean and variability (μ_R and σ_R, respectively) of the distribution of accumulation rates, the distance between the baseline and threshold of activation (Thr), representing an index of response caution, and the non-decision time (ND, with mean μ_{ND} and variance σ_{ND}), representing sensory and motor (i.e., non-decision) processing. Model parameters were initialized by fitting a robust regression to the inverse of the RT distribution on Go trials for the average of all sessions for an individual animal (LATER model, Carpenter, 1981). These average parameters were used as the starting point to optimize parameters in the linear accumulator model on a session-by-session basis for each rat. Parameters were optimized using a SIMPLEX routine (Nelder

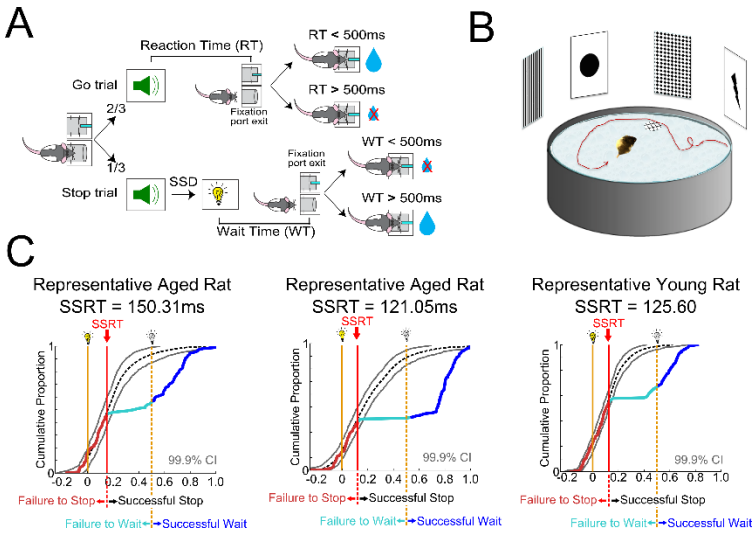

Figure 10 - Task Schematic and Representative Aged and Young Reaction Time Distributions

A. Schematic of the rodent stop signal task. Rats were required to rapidly withdraw from the noseport following an auditory go signal (2/3 trials) and maintain noseport fixation for 500ms following a visual stop signal (1/3 trials). **B.** Schematic of the Morris water maze. Rats were required to locate a submerged platform using extramaze cues. Performance was assessed using spatial learning index, a weighted proximity to platform measure. **C.** Representative aged (left two panels) and young (right panel) reaction time data from the rodent SST. For each animal, WT on Stop trials (colored traces) aligned to stop signal (vertical solid orange line) is compared to yoked Go RTs (black traces). SSRT was defined as the point at which Stop and yoked Go diverged (vertical red line). Trials were classified as failure-to-stop if WT<SSRT; failure-to-wait if WT>SSRT<500ms (stop signal offset, vertical dashed orange line), or successful wait if WT>500ms.

and Mead, 1965, MATLAB fminsearch function). Goodness-of-fit was assessed by minimizing chi-squared

$$\chi^2 = \sum \frac{(Expected - Observed)^2}{Expected^2}$$

for the 10th, 30th, 50th, 70th, and 90th RT quintiles and the proportion of slow (>500ms) RTs.

Results

To examine the effect of chronological aging on cognitive inhibition, we trained and tested aged and young Long-Evans rats in the rodent SST **(Figure 10)**. We first examined reactive, or stimulus-driven, inhibitory control. Both aged (n = 11 rats and 585 sessions) and young (n = 9 rats and 461 sessions) rats rapidly acquired the stop signal task, completing 586.22 ± 13.12 (mean ± s.e.m.; Go: 391.17 ± 8.75; Stop: 195.05 ± 4.36) and 451.81 ± 10.22 (Go: 301.48 ± 6.81; Stop: 150.34 ± 3.41) trials, respectively. Young rats completed more Go (paired t-test, $t_{22} = -7.89$, $p = 7.50 \times 10^{-8}$) and Stop (paired t-test, $t_{22} = -7.87$, $p = 7.75 \times 10^{-8}$) trials that aged rats. As predicted, aged rats were considerably slower to both go and stop than young rats. Both average Go trial RTs (Young: 174.16 ± 7.61ms; Aged: 222.58 ± 15.24ms, $t_{17} = -2.77$, $p = 1.3 \times 10^{-2}$) and SSRT estimates (Young: 128.10 ± 3.07ms, Aged: 155.38 ± 10.34ms, $t_{17} = -2.42$, $p = 2.7 \times 10^{-2}$, **Figure 11A)** were considerably slower for aged rats in the last five days of training, suggesting that this deficit was present even after rats reached behavioral asymptote. Moreover, aged rats had significantly slower Go RTs and SSRTs throughout training (Go RT:

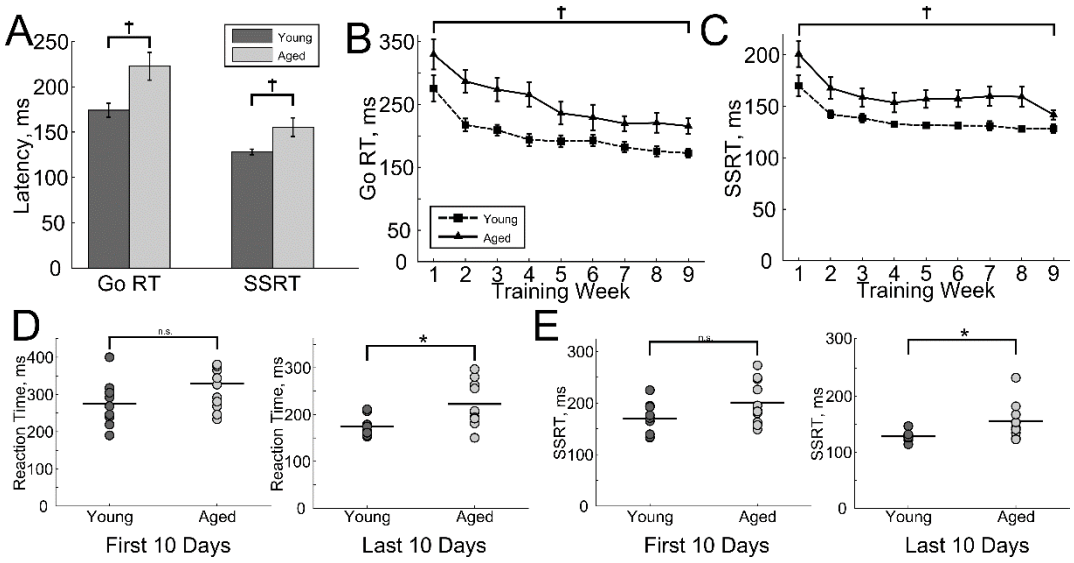

Figure 11 - Aging is accompanied by Persistent Slowing of Go RT and SSRT

A. Mean Go RTs and SSRTs for young (dark grey) and aged (light grey) rats. Aged rats had significantly slower Go RTs and SSRTs as compared to young (paired t-test, $p<0.05$). **B.** Comparison of Go RTs for aged (solid line, triangle markers) and young (dashed line, square markers) rats. Aged rats had significantly slower Go RTs throughout training. **C.** Comparison of SSRTs for aged and young rats. Aged rats had substantial slower SSRTs throughout training. Convention as in **B**. **D.** Left panel: distribution of Go trial reaction times during the first 10 days of training. Right panel: distribution of Go trial reaction times during the last 10 days of training. **E.** Same as **D.**, but for SSRT.

---

main effect of Age, $F(1,158)=47.78$, $p<1x10^{-10}$; SSRT: main effect of Age, $F(1,158)=42.57$, $p<1x10^{-10}$; **Figure 11B & C**). Both groups improved similarly over the course of the training (Go RT: main effect of Week, $F(8,158) = 9.47$, $p<1x10^{-10}$, no Age x Week interaction, $F=0.37$, $p=0.93$; SSRT: main effect of Week, $F(8,158)=6.53$, $p<1x10^{-10}$, no Age x Week interaction, $F=0.24$, $p=0.98$). As expected, we found considerable individual variability in both Go RT (**Figure 11D**) and SSRT (**Figure 11E**) late but not early in training, suggesting even after extensive training, some aged animals showed significant impairment, while others maintained performance on par with young counterparts. These data suggest that slower Go RT and SSRT are stable phenotypes of the aged rats that reflect an

increase in population variability in aging. In support of this, we found considerable test-retest reliability for individual rats over the course of training (**Tables 1 & 2**).

Young Rats	*Block 1*	*Block 2*	*Block 3*	*Aged Rats*	*Block 1*	*Block 2*	*Block 3*
Block 1	-	0.6301 (0.0689)	0.5499 (0.1251)	***Block 1***	-	0.7613 (0.0105)	**0.7739 (0.0086)**
Block 2	-	-	**0.8166 (0.0072)**	***Block 2***	-	-	**0.9646 (<1x10^{-4})**

Table 1 – Test-Retest Reliability in Go RT in the Rodent SST
Pearson's R (p-value) between blocks of three training weeks for Go RT. Young animal data is presented in the left panel and aged animal data is presented in the right panel. P values are indicated in parentheses and significant correlations (p<0.01 to correct against multiple correlations) are bolded. After reaching asymptotic performance (Block 2), measures for individual rats were highly reliable.

Young Rats	*Block 1*	*Block 2*	*Block 3*	*Aged Rats*	*Block 1*	*Block 2*	*Block 3*
Block 1	-	0.7122 (0.0313)	0.6786 (0.0445)	***Block 1***	-	**0.9174 (0.0020)**	**0.8721 (0.0010)**
Block 2	-	-	**0.8264 (0.0060)**	***Block 2***	-	-	**0.9655 (<1x10^{-4})**

Table 2 – Test-Retest Reliability in SSRT in the Rodent SST
Pearson's R (p-value) between blocks of three training weeks for SSRT. Young animal data is presented in the left panel and aged animal data is presented in the right panel. P values are indicated in parentheses and significant correlations (p<0.01 to correct against multiple correlations) are bolded. After reaching asymptotic performance (Block 2), measures for individual rats were highly reliable.

However, it is unclear to what degree these impairments reflect overlapping or nonoverlapping cognitive impairment. To examine this, we compared Go RTs, SSRTs, and spatial learning index scores (SLIs) for aged and young rats during the last 10 days of training when performance was asymptotic (**Figure 12**). We found no relationship between Go RT and SSRT (p's>0.210, **Figure 12A**), SLI and SSRT (p's>0.619, **Figure 12B**), or SLI and Go RT (p's>0.182, **Figure 12C**) for either aged or young rats. These data are in agreement with previous studies suggesting that aging is accompanied by domain independent cognitive decline in multiple domains.

Other than latency measures, overall task performance was similar in young and aged rats, with some notable differences **(Figure 13)**. A SSD x Age repeated measures ANOVA revealed differences in the inhibition functions for aged and young rats. As predicted, the proportion of failure-to-stop errors increased with

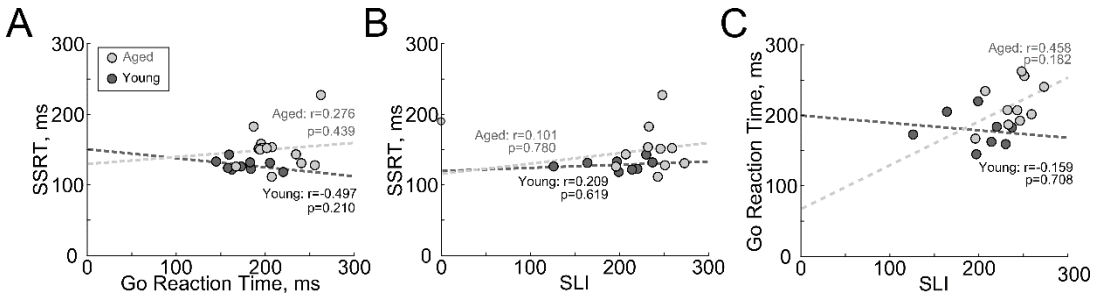

Figure 12 – Domain Independence of Cognitive Decline in Aging

A. Scatter plot of Go RT (abscissa) and SSRT (ordinate) during the last 10 days of training for aged (light circles) and young (dark circles) rats. **B.** Same as in **A**, but comparing SLI and SSRT. **C.** Same as in **A**, but for SLI and Go RT. No relationships were found between any variables for either aged or young rats.

SSD (main effect of SSD, F(4,85)=153.73, p<1x10-4). Aged rats overall failed to stop less often than young rats (main effect of age F(1,85) = 17.7, p = $1x10^{-4}$) and increased the proportion of failure-to-stop trials less at longer SSDs than young rats (Age x SSD interaction, F(4,85) = 3.19, p = 0.017), though this effect is likely due to our SSD matching procedure (see Discussion). As in Chapter 1, neither failure-to-wait errors nor successful wait trials (**Figure 13A**) changed as a function of SSD or age (all F's < 1.9, all p's > .17). To more closely examine how rats made errors, we investigated the response latencies on failure-to-stop, failure-to-wait, and successful wait trials in the last 10 days of training. We found, as predicted, that both aged and young rats similarly increased RT on failure-to-stop trials as SSD increased (main effect of SSD, F(4,85)=44.94, p<$1x10^{-4}$, no main effect of Age, F(1,85)=2.3, p=0.13, no Age x SSD interaction F=0.86, p=0.49). Additionally, we observed no main effect of Age on failure-to-wait trial WTs nor any Age x SSD interaction (wait times, latency from stop signal presentation to noseport withdrawal, all p's>0.096), suggesting that aging is not associated with a slowing of all response latencies in the SST. Noseport exits on failure-to-wait trials

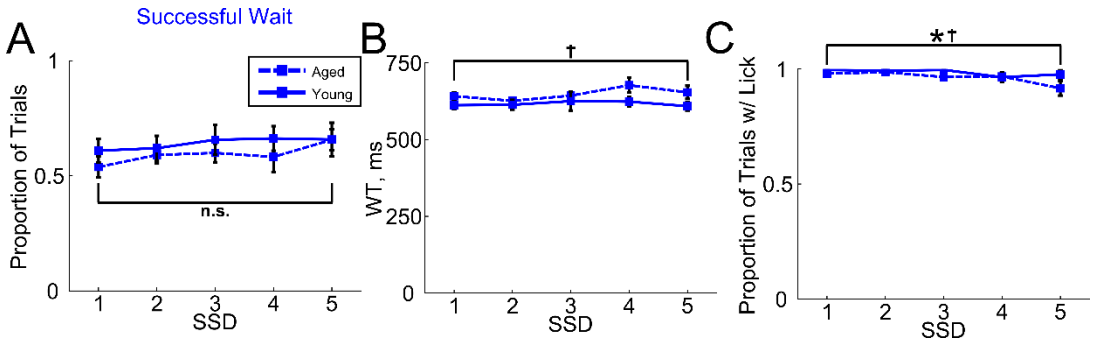

Figure 13 – Aged Rats Wait Longer when Stopping is Successful than Young Rats

A Proportion of successful wait trials for aged (solid line) and young (dashed line) rats. Aged rats successfully waited as often as young rats. **B.** WT on successful wait trials, calculated as the latency of noseport exit relative to Stop signal onset. Aged rats were slower over all SSDs than young rats on successful wait trials. **C.** Proportion of successful wait trials with a reward collection attempt. Aged rats made fewer reward collection attempts on successful wait trials than young rats. Asterisk: main effect of SSD. Single cross: main effect of age. Double cross: Age x SSD interaction.

occurred around the end of the hold period, and aged and young WTs on failure-to-wait trials were similar, suggesting that aged rats also make failure-to-wait errors by incorrectly timing the duration of the hold period. However, aged and young rats responded markedly differently on successful wait trials. As in Chapter 1, WTs on successful wait trials did not change as a function of SSD for either aged or young rats (no main effect of Age nor Age x SSD interaction, all F's<1, all p's>0.55); however, aged rats were significantly slower than young rats on these trials (main effect of Age, $F(1,85)=7.47$, $p=7.6\times10^{-3}$; **Figure 13B**). In contrast to the global slowing of the Go RT distribution, the increase in successful wait trial WT was caused by a selective increase in the number of very long WTs in aged animals (90^{th} percentile of WT distribution collapsed across SSD: Aged: 767.16 ± 17.34ms; Young: 706.24 ± 24.54ms, $t_{17} = 2.03$, $p=0.058$). While there was no change in WT on failure-to-wait trials, this is because the maximum latency on these trials is constrained by the 500ms hold period, likely masking any effect. This data

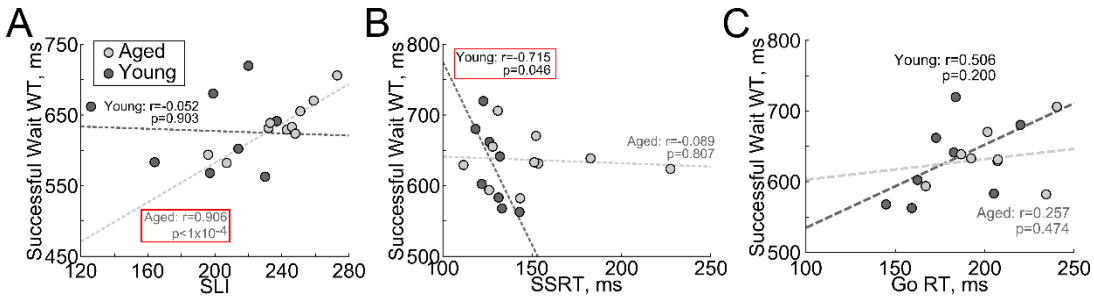

Figure 14 – Impulsive Responding on Successful Wait Trials is Correlated with SLI in Aged Rats and SSRT in Young Rats and is Independent of Go RT
A. Scatter plot comparing SLI and Successful Wait trial WT in aged (light circles) and young (dark circles) rats. For aged but not young rats a strong correlation was found between SLI and Successful Wait trial WT. **B.** Relationship between SSRT and Successful Wait WT. For young but not aged rats, a strong relationship was found between SSRT and Successful Wait WT. **C.** Relationship between Go RT and Successful Wait WT. No correlation was found for either aged or young rats, suggesting increased WT in aged rats is not caused by slowing of Go RTs.

suggests longer WTs on successful wait trials represent a decrease in vigilance and/or increase in variability of the speed of decision making, causing aged animals to occasionally make very slow responses on successful wait trials.

We next investigated how often rats attempted reward collection on failure-to-stop, failure-to-wait, and successful wait trials, a measure of whether rats expect reward. Both aged and young rats were less likely to attempt reward collection following a failure-to-stop error as a function of SSD (main effect of SSD, $F(4,85)=13.12$, $p<1x10^{-4}$, with no main effect of Age or Age x SSD interaction, all p's>0.48). As in Chapter 1, both aged and young rats were much more likely to attempt reward collection following a failure-to-wait error than a failure-to-stop error (paired t-test, collapsed across SSD, Aged: $t_{18}=21.39$, $p=3x10^{-14}$, Young: $t_{18} = 24.33$, $p=3.18x10^{-15}$), and this effect was similar across all SSDs for failure-to-wait errors (no main effect of Age, SSD, or SSD x Age interaction, all p's>0.15). Surprisingly, for successful wait trials we found that all rats attempted to collect reward less at long delays (main effect of SSD, $F(4,85)=2.8$, $p=0.03$) and aged rats

were slightly less likely than young rats to attempt to collect reward (main effect of Age, $F(4,85)=5.29$, $p=0.02$, no Age x SSD interaction, $p>0.26$; **Figure 13C**). However, this effect is difficult to interpret, because these trials were rare, as rats typically successfully stopped and waited on very few trials at long delays, where the largest difference between aged and young rats occurred. Regardless, these data show that both aged and young rats modulate their behavior after noseport exit differently as a function of whether they expect to receive reward. The finding that WTs on successful wait trials are longer in aged than young rats, and aged rats attempt to collect reward less often than young rats on these trials, suggests that aging is associated with changes in pre-SSRT and post-SSRT behavior in the SST.

We next examined whether the age-related changes in waiting behaviors were related to changes in Go RT, SSRT, or spatial navigation (spatial learning index, SLI) were domain-independent (**Figure 14**). SLI was included as an index of cognitive impairment because aging is associated with a profound and reliable decrease in performance in the Morris water maze in a subset of rats and this aged phenotype of hippocampal-dependent cognition has been shown to have test-retest reliability (Gallagher et al., 1993). In aged but not young rats SLI was nearly perfectly correlated with WT on successful wait trials (Aged: $r=0.906$, $p<1x10^{-4}$, Young: $r=-0.052$ $p=0.903$, **Figure 14A**), whereas for young rats SSRT was strongly correlated with RT on successful wait trials (Aged: $r=-0.089$, $p=0.807$, Young: $r=-0.715$, $p=0.046$, **Figure 14B**). Go trial RT was not correlated with WT on successful trials in either aged or young rats (all p's>0.200, **Figure 14C**), suggesting that the

amount of time rats are willing to wait is unrelated to the speed of their Go RTs. The finding that the ability to wait is exclusively correlated with SLI in aged but not young and SSRT in young but not aged suggests different neuronal mechanisms for waiting in young and aged animals.

One important behavioral phenotype of cognitive inhibition is observed in corrective noseport reentries. We examined whether aged rats attempted corrective noseport reentry responses **(Figure 15A,B)**. We found that young rats made corrective noseport reentries primarily around SSRT, with noseport reentries occurring immediately after SSRT and following noseport exits immediately before SSRT (Mean noseport exit latency relative to SSRT: 0.63 ± 5.56ms, blue triangles; Mean noseport reentry relative to SSRT: 151.96 ± 11.77ms, cyan triangles; **Figure 15C**). However, aged rats tended to reenter following noseport exits in a much wider distribution around SSRT, though this difference did not reach statistical significance (Mean noseport exit latency relative to SSRT: 17.15 ± 7.11ms, paired t-test against young t_{22}=-1.69, p=0.11; Mean noseport reentry relative to SSRT: 164.29 ± 9.12ms, t_{22}=-.86, p=0.40; **Figure 15D)**. It is important to note that the increased width of the reentry distributions for aged compared to young animals likely reflects increased estimation error because of slower Go RTs and SSRTs in aged rats, rather than a true increase in the variability of these distributions. This is supported by the finding that the time between noseport exit and reentry was similar for aged and young rats (blue solid horizontal lines; Young: 151.33 ± 13.77ms; Aged: 147.14 ± 7.52ms, t_{22}=0.31, p=0.76), suggesting that the characteristics of the reentry events themselves are preserved in aging. Both aged

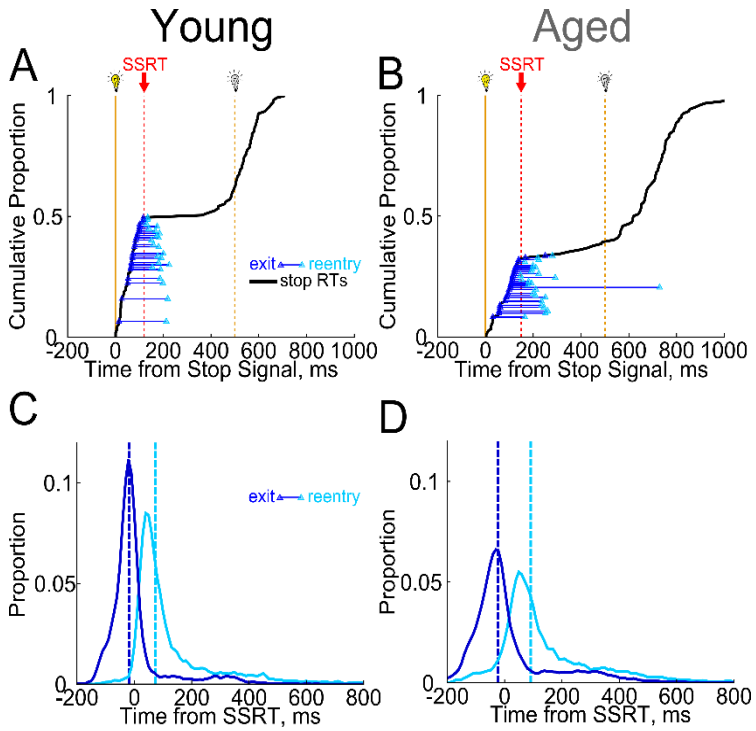

Figure 15 - Both Aged and Young Rats Similarly Attempt Corrective Noseport Reentry Responses around SSD

A. Representative example session from a young rat. Black: stop trial WTs. Blue triangles: noseport exits. Cyan triangles: noseport reentries. Convention as in **Figure 10C**. **B.** Representative example session from an aged rat. Convention as in **A**. **C.** Histogram of noseport exits preceding reentries (blue) and reentry events (cyan) relative to SSRT for all young rats. Exits leading to reentries preceded SSRT, while reentries selectively followed SSRT. **D.** Histogram of noseport exits preceding reentries and reentry events relative to SSRT for all aged rats. Vertical blue and cyan line represent the mean latency of noseport exits preceding reentry and reentry events respectively. No differences between aged and young rats (paired t-test, $p>0.05$).

and young rats frequently and similarly attempt corrective noseport reentries following erroneous noseport withdrawal around SSRT, suggesting these behaviors are a robust feature of the rodent SST.

Finally, we investigated whether aged rats employ proactive inhibition to adjust RTs based on recent trial history in order to improve subsequent performance. We first compared the change in RT on a pair of Go trials as a function of the interleaving trial (GGG: Go-Go-Go; GFG: Go-Failure-to-Stop-Go; GWG: Go-Failure-to-Wait-Go; GSG: Go-Successful-Wait-Go) over the course of

training. Only GGG and GFG trials were reliable enough to be compared week-to-week; therefore, GWG and GSG trials are not considered for this analysis. A 3-way repeated measures ANOVA (Trial Type x Training Week x Age) found that aged and young rats similarly modulated RTs on GGG and GFG trials overall (main effect of Trial Type, $F(1,315) = 158.11$, $p<1x10^{-10}$, no main effect of Age, $p = 0.79$ or Trial Type x Age interaction, $p = 0.30$, **Figure 16A**). However, while both aged and young rats adjusted GFG but not GGG RT over the course of training (Trial Type x Week interaction, $F(8,315) = 4.09$, $p=1x10^{-4}$), aged rats took slightly longer to make this change than young rats (marginal Trial Type x Week x Age interaction, $F(8,315) = 1.92$, $p=0.057$). However, by Week 5 of training, aged and young rats were largely indistinguishable in their proactive adjustments (post-hoc t-tests comparing GFG and GGG values for aged and young from Week 5 onward, Week

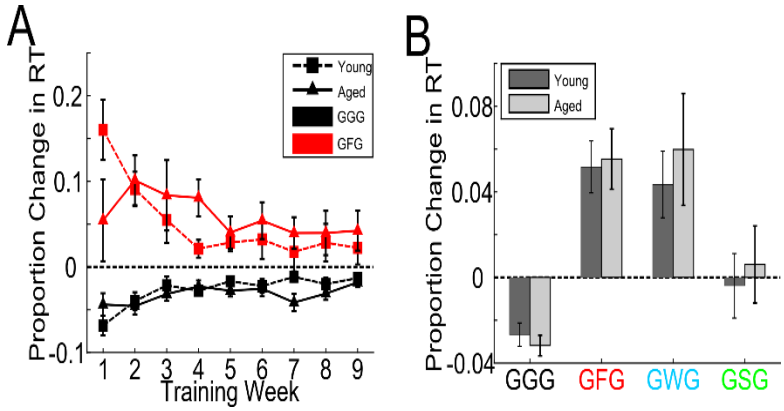

Figure 16 - Aged and Young Rats Similarly Utilize Proactive Control Based on Immediate Trial History Early in Training

A. Comparison of proactive adjustment on pairs of Go trials with either a Go trial (GGG; black) or failure-to-stop trial (GFG; red) in between. Data are plotted as the proportion change in RT from the first to the last Go trial in a GGG or GFG sequence. Both aged (solid line, triangle markers) and young (dashed line, square markers) rats proactively adjusted RT more on GGG and GFG trials early in training; no difference in aged vs. young adjustments late in training. **B.** Quantification of change in RT from the first to the last Go trial in a GGG (left), GFG (left-middle), Go-Failure-to-Wait-Go (GWG, right-middle), and Go-Successful-Wait-Go (GSG, right) trials across all nine training weeks. Both aged (light grey) and young (dark grey) rats significantly speeded RT on GGG trials and slowed RT on GFG and GWG trials.

7 GGG p=0.026, all other p's>0.22 against Bonferroni-corrected α/10 of 0.005). Comparing RT adjustments on all four trial types across all nine weeks of training revealed no significant age-related differences (main effect of Trial Type, $F(3,72) = 14.16$, $p<1x10^{-10}$, all other F's<1; **Figure 16B**). These data suggest that both aged and young rats utilize proactive control early in training, and rely on it less after extensive training in the task. Overall, these data demonstrate that both aged and young perform similarly in the SST and impairments observed in aged animals are likely not compensatory strategy shifts (which might be expected to alter gross task performance) but performance alterations.

RT is a composite measure of all of the decision and non-decision (i.e., sensory/motor) processing that occurs in the interval between Go signal presentation and noseport exit. While aging is associated with an increase in RT, it is not possible to dissociate age-related changes in the individual components of RT based on descriptive measures alone. To examine these components we constructed a linear accumulator model to describe the decision process leading up to a response in aged and young rats **(Figure 17A)**. In this model, a decision unit accumulates activity from a baseline to a threshold of activation (Thr, a measure of decision caution), at which time a response is made. The rate of this accumulation is stochastically drawn from a rate distribution with mean μ_R and variance σ_R. Finally, accumulation begins only after a variable non-decision time representing sensory and motor processing time. As with accumulation rate, the duration of this non-decision time is drawn stochastically from a distribution with mean μ_{ND} and variance σ_{ND}. We found that our model fit the empirical RT data well

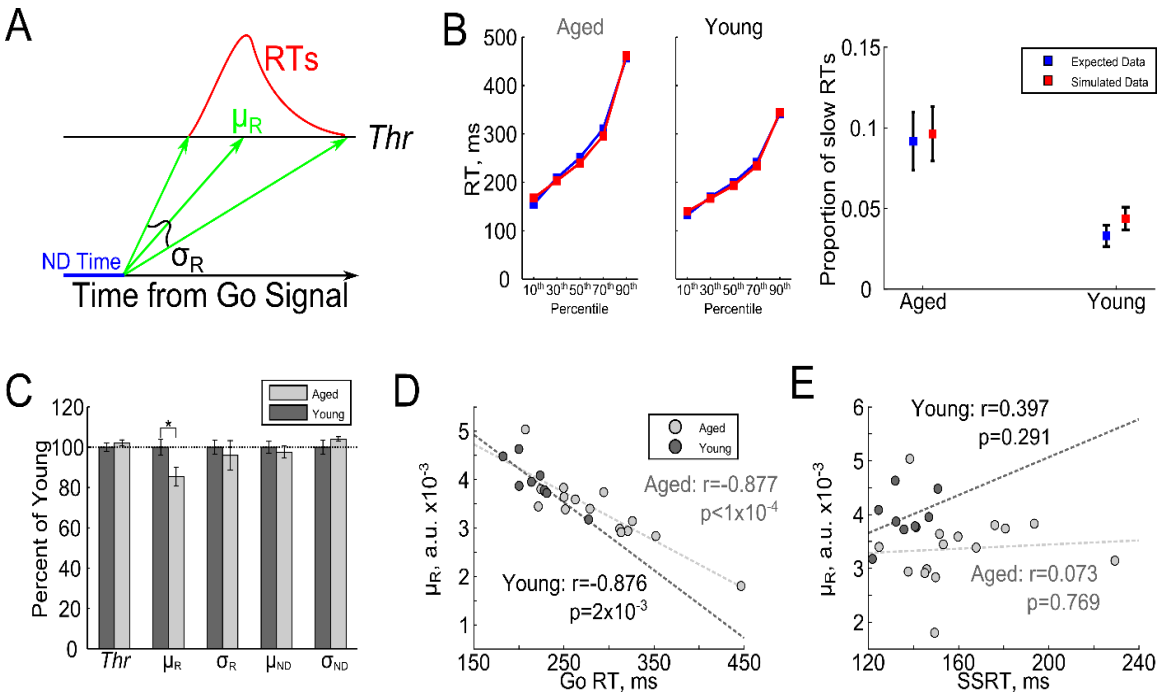

Figure 17 - Slower Processing Speed in Aged Animals Underlies Age-Related Increase in Go RT but not SSRT
A. Schematic of the linear accumulator model. Activity in an artificial decision unit accumulates from a baseline to a threshold of activation (Thr), at which point a response is made. Accumulation rate is constant on a given trial and drawn stochastically from a distribution with mean μ_R and variance σ_R. Accumulation begins following a variable non-decision time, drawn stochastically from a separate distribution with mean μ_{ND} and variance σ_{ND}. **B.** Model fit. Left panels: comparison of simulated (red) and expected (observed; blue) RT data. Data are plotted as the 10th, 30th, 50th, 70th, and 90th RT percentiles. For both aged and young animals the expected data was well-fit by the model. Right panel: comparison of simulated and expected proportion of trials with RT>500ms (slow RTs). No significant differences were found. **C.** Comparison of model-derived decision parameters for young (dark grey) and aged (light grey) rats. The mean accumulation rate μ_R was significantly decreased in aged animals. **D.** Relationship between μ_R and Go RT. For both aged and young animals μ_R was strongly negatively correlated with Go RT. Units for μ_R are arbitrary. **E.** Relationship between μ_R and SSRT. For both aged and young animals SSRT and μ_R were uncorrelated.

(minimized Chi^2, no main effect or interactions with Simulated vs. Expected as a factor, all p's>0.81) and found no differences in the expected vs. simulated number of slow RTs (paired t-tests, all p's>0.26; **Figure 17B**). We first examined whether aging was accompanied by changes in any of the model parameters of interest and found a selective decrease in μ in aged rats compared to young (t_{22} = -2.25, p = 0.037; all other p's>0.17; **Figure 17C**). As expected given age-related declines

in processing speed, we found strong negative correlations between μ_R and Go RT in aged ($r=-0.877$, $p<1x10^{-4}$) and young rats ($r=-0.876$, $p=2x10^{-3}$). Interestingly σ_R was negatively correlated with RT in aged ($r=-0.572$, $p=0.026$) but not young ($p>0.6$ rats, suggesting that variability in accumulation rate is an important factor in determining RT in aging. We similarly found a positive relationship between μ_{ND} and RT in aged ($r=0.628$, $p=0.012$) but not young ($p>0.8$) rats, suggesting again that non-decision time is an increased factor in controlling RT in aged but not young rats, while decision boundary and variability in non-decision time did not play a significant role (all p's>0.12). We found no correlation between any model parameters and SSRT in aged or young animals (all p's>0.1), providing further evidence that age-related changes in SSRT are independent of declines in processing speed in age.

Discussion

In the current chapter we examined the effects of aging on performance in two tasks, the rodent SST and the Morris water maze (**Figure 10**). We found a substantial and persistent impairment in both going and stopping, as measured by Go RT and SSRT in aged rats **(Figure 11)**, and these impairments reflected decline in independent cognitive domains (**Figure 12**). Overall SST performance, including the proportion of errors **(Figure 13)**, was similar in aged and young rats; however, we found a surprising age-related change in waiting behavior that was strongly correlated to spatial navigation in aged rats and response inhibition in young rats (**Figure 14**). Other behavioral features such as corrective reentry attempts **(Figure 15)** and proactive RT adjustments **(Figure 16)**, were similar for

aged and young rats. We found that slower Go RTs in aged rats were accompanied by slower and more variable processing speed, in addition to slower sensory/motor processing, but that age-related changes in SSRT were independent of these factors **(Figure 17)**, providing additional evidence that the impairments observed here reflect reduced integrity in nonoverlapping cognitive domains. Together, these data provide evidence that aging is accompanied by independent impairments in the speed of going and stopping.

Aged animals were slightly less likely to fail to stop overall, and tended to have slower RTs on failure-to-stop trials; however, this effect is likely caused by our SSD procedure. In our rodent SST, SSDs are adjusted between sessions and randomly sampled within sessions to titrate task difficulty to individual rats' baseline RT. Stopping in the SST is determined by only three parameters: speed of going (Go RT), speed of stopping (SSRT), and the delay between when an animal is instructed to go and, subsequently, to stop (SSD). When rats slow down, stopping becomes easier if SSRT and SSD are held constant. Therefore, to account for age-related increases in Go RT we increased SSD for aged rats. Longer SSDs mean that more trials will escape inhibition and increase the RT on failure-to-stop trials, accounting for the age-related slowing of failure-to-stop RT. However, this adjustment procedure is imperfect and likely accounts for the age-related difference in the proportion of failure-to-stop errors. The alternative explanation requires that aged rats are able to adopt a strategy to overcome a substantial slowing of SSRT and overall increased SSD in order to successfully stop more often, an unlikely explanation given that aged rats do not proactively

adjust RT more than young rats (which would suggest a dynamic speed-accuracy tradeoff).

While we titrated SSD to Go RT to make stopping easier or more difficult, this procedure is unlikely to affect post-SSRT behavior (i.e., waiting) because stopping and waiting are independent in our rodent SST (Chapter 1, Mayse et al., 2014). This makes the differences in waiting between aged and young animals quite interesting, because the rodent stop signal is essentially a reactive inhibition task combined with a sustained attention task. After animals stop, they must wait until an audible cue signals the end of the hold period to generate a response, incorporating a sustained attention requirement. The finding that the increase in WT on successful wait trials was greatest for the slowest WTs is in contrast to the overall increase across all percentiles of the Go RT distribution, suggests that increased WTs on successful wait trials are at least partially nonoverlapping with the overall age-related slowing effect. This finding is supported by the lack of a correlation between Go RT and WT on successful wait trials. While several studies have reported increased ability to sustain attention in aged individuals (Staub et al., 2014a, 2014b), other studies have reported a decrement in this ability, often when cognitive inhibition is required in the same task (Parasuraman et al., 1989; Staub et al., 2014c), suggesting that task demands may reveal either an age-related enhancement or impairment in sustained attention. Additionally, lesion of BF cholinergic neurons induces attentional vigilance decrements in young rats (McGaughy et al., 1996), and attentional vigilance decrements in aged rats are

alleviated by pro-cholinergic drugs (Grottick et al., 2003; but see Turchi et al., 1996).

Finally, we found that age-related slowing of Go RT is caused by a selective decrease in the mean rate-of-rise of a simple linear accumulator model. This parameter corresponds to the speed of information processing (White et al., 2014) and has been previously shown to be impaired in aging (Rush et al., 2006; Salthouse, 2000). However, age-related slowing of SSRT was not accounted for by slower information processing or any other model terms. These data provide additional evidence that age-related changes in Go RT and SSRT represent non-overlapping impairments (Coxon et al., 2012; Kramer et al., 1994). This finding is important in the light of recent findings suggesting a role for the basal forebrain (BF) in both speed of going (Avila and Lin, 2014) and stopping (Mayse et al., 2015, submitted; Chapter 3). Aging is commonly associated with reduced integrity of the BF cholinergic and noncholinergic system alike (Düzel et al., 2010; Bañuelos et al., 2013), and damage to the noncholinergic BF especially has been linked to both slower response speed and impaired response inhibition (Muir et al., 1996; Robbins et al., 1989; Voytko et al., 1994). The data in the current study suggest that the inputs mediating the BF's role in controlling the speed of going and stopping arise from independent sources. One hypothesis arising from the current data is that aged animals with slower Go RTs but intact SSRTs should show a reduced BF bursting response to the Go signal but an intact inhibitory response to the stop signal, whereas aged rats with intact Go RTs but slower SSRTs should show the opposite phenotype. Additionally, it may be possible that the BF is

functionally intact in the aged animal, but the effect of BF signaling on downstream circuits is diminished or altered. Future studies will need to utilize multisite recording in the aged rat to determine the locus of nonoverlapping impairments in Go RT and SSRT in aging.

Chapter 3 – Role of Basal Forebrain Bursting Neurons in Stopping

Rationale

Inhibitory control is an essential aspect of executive function that allows humans and animals to rapidly suppress actions inappropriate for the behavioral context. One important paradigm to study inhibitory control is the SST, in which subjects must rapidly cancel a prepotent behavioral response when a Go signal is occasionally followed by a Stop signal. The SST is uniquely powerful in that it allows for the quantitative estimation of the latency to stop, the stop signal reaction time (SSRT, Logan et al., 1984; Logan and Cowan, 1984). Understanding the neural mechanisms that determine SSRT is critical because SSRT is elevated in disorders characterized by deficient inhibitory control, including Parkinson's disease (Gauggel et al., 2004; Mirabella et al., 2011) and attention-deficit hyperactivity disorder (McAlonan et al., 2009), as well as in normal cognitive aging (Andrés et al., 2008; Coxon et al., 2012; Hu et al., 2013).

Recent studies have implicated a distributed corticostriatal network as a candidate neural circuit mechanism underlying inhibitory control. In particular, neuronal recordings in the SNr identify an early gating mechanism that transiently pauses the planned action and likely contributes to stopping, albeit well in advance of SSRT (Schmidt et al., 2013). The competition between Go and Stop processes ultimately involves cortical premotor or motor regions, where movement initiation signals are differentially modulated in cancelled trials only moments before SSRT (Boucher et al., 2007a). However, the neural processes that occur during the large temporal gap between the early SNr gating signal and the ultimate movement

initiation signals in motor regions remain unclear, and the precise neural circuit mechanism that determines SSRT is currently unknown.

In the current study, we explored an alternative hypothesis outside of the corticostriatal network and investigated the role of basal forebrain (BF) in inhibitory control. The BF is a large neuromodulatory system comprised of magnocellular cholinergic and GABAergic cortico-projection neurons (Freund and Gulyás, 1991; Gritti et al., 1997). The BF may play an under-appreciated role in inhibitory control: BF neuronal activity controls the speed of response generation (Avila and Lin, 2014), and BF lesion impairs response inhibition (Muir et al., 1996; Robbins et al., 1989). The current study focused on a physiologically homogeneous group of noncholinergic BF neurons that respond to motivationally salient stimuli with robust bursting responses (Lin and Nicolelis, 2008; Richardson and DeLong, 1990). Because the strength of the BF bursting response is tightly coupled with the speed of making a behavioral response, measured by RT (Avila and Lin, 2014), here we asked whether BF neuronal activity is also coupled with the speed of stopping, measured by SSRT (Mayse et al., 2014). We tested two opposing predictions about the potential role of BF neurons in response inhibition: one possibility is that BF neurons may show strong bursting responses to the motivationally salient Stop signal to facilitate stopping (Lin and Nicolelis, 2008). Alternatively, since stronger BF bursting is coupled with faster RT (Avila and Lin, 2014), arresting the preparation of the planned response in the SST may require inhibition of BF activity.

We found that, irrespective of whether stopping was rewarded, BF neurons that showed bursting responses to the Go signal were inhibited by the Stop signal. The latency of BF neuronal inhibition was coupled with, and slightly temporally preceded, SSRT. Furthermore, artificially inducing BF inhibition generated stopping in the absence of the Stop signal. These results identify a novel neural correlate of SSRT in the BF that is outside of corticostriatal circuits.

Material and Methods

Subjects

Long-Evans rats (Charles River, NC), weighing 250-350g at the start of the experiment, were used in this study. Nineteen rats were trained in the Stop Reward Task, four of which subsequently underwent surgery to record BF neuronal activity. A separate group of eight rats were trained in the Stop No Reward Task, four of which underwent surgery to record BF neuronal activity. Another group of seven rats were trained to associate the go sound with reward only, and were subsequently used in BF electrical stimulation experiments.

Animals were housed individually in a temperature- and humidity-controlled vivarium on a 12L:12D cycle. Animals in the Stop Reward condition were provided *ad libitum* access to water and food restricted to 85% of their free-feeding weight. Animals in the Stop No Reward condition and stimulation experiments were provided *ad libitum* access to food and water restricted with body weight maintained at least 90% of their free-feeding weight. These animals received free access to water for fifteen minutes daily at the end of the day and were provided 48 hours free access to water weekly.

All experimental procedures were conducted in accordance with the National Institutes of Health (NIH) Guide for the Care and Use of Laboratory Animals and approved by the National Institute on Aging Animal Care and Use Committee.

Apparatus

Behavioral training and neurophysiological recording took place in identical chambers to those described in Chapters 1 and 2 and are not described here.

Stop Signal Task

Behavioral shaping and training procedures for the Stop Reward Task have been described in detail previously (Chapter 1, Mayse et al., 2014). Briefly, all rats were first shaped to enter the central fixation port. After a variable foreperiod, selected pseudorandomly from [0.35, 0.5, 0.65, 0.8]s, a 6kHz tone (80dB, 2s) was presented, signaling reward availability. If rats began licking within 3s of tone onset, they receive 30µl of reward starting at the third lick. The inter-trial interval (ITI) was 1-3 sec and was not signaled to the rat. Either premature fixation port entry or premature licking during ITI both reset the ITI timer. Animals were held at this stage for 10-14 sessions to encourage fast responding to the tone before they underwent additional training.

After the initial behavioral shaping, rats in the BF electrical stimulation experiment did not receive any additional training **(Figure 24B).** Rats in the Stop No Reward task were transitioned to the full Stop No Reward contingency without any intermediate training. In this task, a stop signal (central panel light, 0.5s) was presented in one-third of trials after a variable stop signal delay (SSD). Rats were

not rewarded on those stop trials **(Figure 18B)**. The five SSDs were determined before the start of each session based on animals' performance in the previous session, and the SSD was chosen pseudorandomly from these five SSDs on each trial. Every session included a 0ms SSD such that the tone and light were presented simultaneously. The remaining four SSDs were evenly spaced in 40ms steps and adjusted by experimenters between sessions to ensure approximately 50% failed stop trials.

Rats in the Stop Reward condition underwent additional shaping to associate a light signal with reward if they responded after, but not before, light offset. The overall organization of the task was the same as the previous shaping phase, except that the 6kHz tone was replaced by illumination of a white central panel light in each trial. This light would subsequently serve as the stop signal in the SST. Fixation port exit responses during light illumination led to forfeiture of reward, and only responses that occurred after light offset led to 30µl of reward. The duration of light illumination was adaptively increased until animals could reliably wait for 500ms (10-14 sessions). Rats were provided with explicit feedback for successfully waiting for the entire light duration in the form of an audible solenoid click similar to the click associated with reward delivery. After this training phase, rats received several refresher tone-alone sessions before transitioning to the Stop Reward Task.

In the Stop Reward Task, the 6kHz tone (go signal) was presented on all trials, and on 1/3 of the trials the go signal was followed by the light stop signal after a variable stop signal delay (SSD) **(Figure 18A)**. In tone-alone trials (2/3), or

go trials, animals were required to make fast go responses (RT<500ms) to receive reward. In the stop trials (1/3), reward was available only if wait time (WT), the latency between stop signal onset to fixation port exit, was longer than the 500ms hold duration (equivalent to RT>SSD+500ms). The same amount of reward (30µl) was delivered in both fast Go trials and successful Stop trials. SSDs were determined similarly as in Stop No Reward Task.

Subjects were trained in one daily session (60-90 minutes) and underwent stereotaxic surgery for implantation of chronic recording electrodes after reaching behavioral asymptote. Following 7-14 days of recovery, animals were again food or water restricted and behavioral training resumed.

Stereotaxic Surgery for Implantation of Recording Electrodes

The stereotaxic surgery procedures were similar to those reported previously (Avila and Lin, 2014; Nguyen and Lin, 2014). After reaching behavioral asymptote, rats were removed from food or water restriction for 3d before undergoing stereotaxic surgery. Rats were anesthetized with isoflurane (3-5% induction followed by 1-3% maintenance), placed in a stereotaxic frame (David Kopf Instrument, CA) that was fitted with atraumatic ear bars and a heating pad to maintain body temperature at 37° C. Multiple skull screws were inserted first, with one screw over the cerebellum that served as the common electrical reference, and a separate screw over the opposite cerebellum hemisphere that served as the ground. A custom-built 32-wire multi-electrode moveable bundle was implanted into bilateral BF. The electrode consisted of two moveable bundles each ensheathed in a 28-guage stainless steel cannula. Each bundle contained 16

polyimide-insulated tungsten wires (38 μm diameter) (California Fine Wire, CA), with impedance ranging from 0.1-0.3 MΩ at 1kHz (niPOD, NeuroNexusTech, MI). The two cannulae of the electrode were precisely positioned to target the BF on both hemispheres at AP –0.6 mm, ML ±2.25 mm relative to Bregma. The cannulae were lowered to DV 6–6.3 mm below cortical surface using a micropositioner (Model 2662, David Kopf Instrument), and the electrodes were advanced to 7 mm below the cortical surface. After reaching target depth, the electrode and screws were covered with dental cement (Hygenic Denture Resin). Rats received acetaminophen (300 mg/kg, aq. oral delivery) post-surgery and allowed 7-14 days to recover. Cannulae and electrode tip locations were verified with cresyl violet staining of histological sections at the end of the experiment and were compared with reference anatomical planes.

Recording

Each recording session lasted 60-90 minutes. Several recording sessions were collected at each electrode depth (separated by 125 μm), and a single session was included in data analysis according the quality of behavioral and physiological data. Therefore, each recording session represents a distinct sample of BF single neuron ensembles. Electrical signals were referenced to a common skull screw placed over the cerebellum, filtered (0.03 Hz-7.5 kHz), amplified using Cereplex M digital headstages, and recorded using a Neural Signal Processor (Blackrock Microsystems, UT). Single unit activity was further bandpass filtered (250 Hz-5 kHz) and recorded at 30 kHz. Spike waveforms were sorted offline using OfflineSorter V.3 (Plexon Inc, TX). Only single units with clear separation from the

noise cluster and with minimal (<=0.1%) spike collisions (spikes with less than 1.5ms interspike interval) were used for further analyses. Additional cross-correlation analyses were used to remove duplicate units recorded simultaneously over multiple electrodes. Only neurons with at least 0.1Hz baseline firing rates were included in the analysis. A total of 494 well-isolated BF single units were recorded from 36 sessions across 8 rats in the SST (Stop Reward: 4 rats, 17 sessions, 235 neurons; Stop No Reward: 4 rats, 19 sessions, 259 neurons).

Estimation of SSRT using modified integration method

SSRT was estimated using the modified integration method that we have previously developed and validated (Chapter 1, Mayse et al., 2014). This new method provides an estimate of SSRT by directly comparing RT distributions in Stop trials and Go trials in order to determine the time point at which the stop signal begins to slow down RTs relative to Go trial RTs **(Figure 18C-D)**. Specifically, we randomly sampled *n* go trials (*n* = the number of stop trials in a session) and subtracted from the sampled go trial RTs the SSDs associated with stop trials. This procedure created a new RT distribution such that go trial RTs were re-aligned to would-be stop signals in order to compare with the stop trial cumulative RT distribution aligned to the onset of stop signal. This sampling procedure was repeated 10,000 times to construct a conservative 99.9% (0.05% - 99.95%) confidence interval (CI) of the cumulative re-aligned go trial RT distribution. We determined the earliest time point in the sorted Stop trial cumulative RT distribution at which RTs began to significantly slow down relative to the 99.9% CI, representing a conservative upper bound of the SSRT estimate ($SSRT_{UpperBound}$).

Failure-to-stop (FS) trials were defined as trials in which WT was less than $SSRT_{UpperBound}$. Successful stop (SS) trials had WTs longer than $SSRT_{UpperBound}$. In the Stop Reward Task, successful stop trials were further divided into failure-to-wait (FW) trials ($SSRT_{UpperBound}$<WT<500ms; not rewarded) and successful-wait (SW) trials (WT>500ms; rewarded). Finally, to provide an unbiased estimate of the SSRT, we took the mean of the re-aligned cumulative Go trial RT distributions, and determined the time point in this distribution that corresponded to the probability p(failure-to-stop) as the SSRT estimate. The resulting SSRT was not affected by the number of stop trials in a session and the choice of confidence interval, and provided an unbiased estimate, as was validated by using simulated data(Mayse et al., 2014).

Identification of BF Bursting Neurons

Peri-stimulus time histograms (PSTHs) were generated for each BF single neuron against each behavioral event using a 10ms bin. To determine whether BF neurons showed significant responses to the go signal, we compared PSTHs to the go signal (in go trials) with foreperiod-matched PSTHs during the nosepoke fixation period before go signal onset. This difference in firing rates between the two conditions **(Figure 20A)** allowed us to control for fluctuations in firing rates associated with nosepoke fixation, and to identify true responses to the go signal as significant deviations in the difference PSTH from the zero baseline. The response amplitude to the go signal **(Figure 20C-D)** was defined as the average firing rate of the difference PSTH at the [0.05, 0.2]s window.

BF bursting neurons were identified according to two criteria: (1) the presence of a significant excitatory response in the [0.01, 0.2]s window after go signal onset, and (2) baseline firing rates less than 12 spikes/s (**Figure 20C,** Avila and Lin, 2014; Lin et al., 2006; Lin and Nicolelis, 2008). The baseline firing rate was defined as the mean firing at [-2, -1]s before onset of the go signal. The statistical significance of the difference PSTHs was determined by comparing cumulative frequency histograms (CFHs) of PSTHs after tone onsets against the cumulative sum distribution of baseline PSTHs before tone onset ({−1.5, 0}s), estimated based on 1,000 bootstrapped samples (p = 0.01, two-sided, Wiest et al., 2005). A minimum response amplitude of 0.05 spikes per response was required to be considered a significant response.

To determine whether the population PSTHs on go trials and foreperiod-matched control trials were significantly different, we used paired t-tests at each 10ms bin, with Bonferroni's correction for multiple comparisons (α/n, where α = 0.01 and $n=40$ is the number of 10ms bins). The same method was used to compare population PSTHs in **Figures 20-24**, with statistical significance indicated by horizontal bars.

BF Neuronal Responses to the Stop Signal

To determine whether BF neurons showed significant responses to the stop signal, it is important to control for neuronal responses to the go signal that preceded the stop signal by a variable SSD. For this purpose, we compared PSTHs to the stop signal against latency-matched go trial controls using a random permutation method **(Figure 20B)**. Specifically, we randomly sampled *n* go trials

(*n* is the number of stop trials) and added to the timestamp of go signal the SSDs associated with the stop trials. We calculated PSTHs aligned to this new set of would-be stop signals that had the same SSDs relative to go signals. The random sampling procedure was repeated 10,000 times, and the mean of 10,000 PSTHs was taken as the PSTH for latency-matched go trial controls. Deviations of the difference PSTH (stop minus latency-matched controls) from zero baseline indicate significant responses to the stop signal. The response amplitude to the stop signal **(Figure 20D)** was defined as the average firing rate of the difference PSTH at the [0.1, 0.5]s window. Similar procedures were employed to calculate BF responses aligned to the estimated SSRT **(Figure 21B)**.

To determine how BF neurons respond to the stop signal in FS and SS trials, we modified the random permutation method and identified latency-matched go trial controls separately for FS and SS trials **(Figure 22A-B)**. Specifically, in each random sample of *n* go trials, we computed WT for each trial as the difference between its go trial RT and the randomly assigned SSD. Trials with WT less than $SSRT_{UpperBound}$ were used as latency-matched controls for FS trials, while trials with WT longer than $SSRT_{UpperBound}$ were used as controls for SS trials.

For post-SSRT neuronal responses, we directly compared the mean firing rates at the [0.05, 0.2]s post-SSRT window between different trial types **(Figure 23A)**. Note, however, that for direct comparisons of PSTHs such as in **Figure 23B** and **Figure 23C**, differences before SSRT likely reflected different distributions of SSDs associated with FS and SS trials, which were respectively not different from latency-matched go trial controls before SSRT **(Figure 22A-B)**.

Estimating BF neuronal inhibition latency

To determine BF neuronal inhibition latency and to compare this latency with estimates of SSRT in the same session **(Figure 21C)**, we developed a new method to using cumulative PSTHs that was based on the same principles of the modified integration method used to estimate SSRT. Specifically, we first pooled the activity of all BF bursting neurons recorded in a session as a multiunit, including only BF bursting neurons that were significantly inhibited by the stop signal (n=255/275). To ensure sufficient sampling of BF activity, we only analyzed sessions with at least four such BF bursting neurons (n=24/36 sessions). We then calculated the PSTH of the pooled multiunit to the stop signal in 1ms bins within the [0, 0.5]s window after stop signal onset, and the corresponding cumulative sum of the PSTH. Similar cumulative sums were generated for 10,000 permutations of latency-matched go trial controls in 1ms bins to calculate the average cumulative sum of PSTH and its 99.98% CI (0.01-99.99%). Significant inhibition by the stop signal was defined by a stop signal PSTH lower than 0.01% CI, that crossed 0.01% CI at time *t1*. The timepoint at which the stop signal PSTH exceeded the 1% CI was designated as *t2*. We then linearly regressed the cumulative sum of stop signal PSTH at [*t2*, *t1*+0.1s] window, and defined the onset of BF neuronal inhibition as the time point at which the regression line intersected the average cumulative sum of PSTH of the 10,000 latency-matched permutations.

This method was also applied to individual BF neurons, and identified the 255/275 BF bursting neurons that showed significant inhibition toward the stop signal. Results were similar to the number (253/275) identified by applying the

method described earlier that used cumulative sums in the baseline period (Wiest et al., 2005). However, the current method has several distinct advantages: (1) finer temporal resolution with bin sizes of 1ms; (2) reduced influence of the number of trials and the choice of parameters in the algorithm, such as the α level or minimum response amplitude for significant responses; (3) a higher correlation with earlier estimates of BF neuronal inhibition latency compared to the other method for determining significant inhibition (Wiest et al., 2005).

BF Neuronal Responses to fixation exit in FW and SW trials

Fixation port exits in FW and SW trials occurred under very different circumstances: in FW trials, rats exited the fixation port during the waiting period in the absence of an audible solenoid click. In contrast, while in SW trials, rats exit the fixation port after hearing the audible solenoid click that signaled reward availability. Therefore, the responses time-locked to fixation exits in FW and SW trials cannot be compared with each other directly. Instead, we realigned SW trials to would-be fixation exits that were latency-matched to the WT in FW trials **(Figure 23D)**. This allowed us to compare the activity of FW and SW during the same epochs in the waiting period prior to fixation exit in FW trials.

Reentry Behavior

Reentry behavior in stop trials **(Figure 22C-D)** and in stimulation trials **(Figure 24E)** was defined by two criteria: (1) the latency between fixation port exit and reentry must be less than 1s; and (2) rats must reenter the fixation port before entering the reward port.

Accelerometer Signals

A three-axis accelerometer (ADXL327, Analog Devices) was attached to the Cereplex M digital headstage and signals were digitized at 1kHz and recorded simultaneously with neural signals. Accelerometer signals were recorded from 3 rats over 15 sessions (Stop Reward Task, 1 rat, 2 sessions; Stop No Reward Task, 2 rats, 13 sessions).

Since accelerometers also detect gravity, and the projection of gravity on the three axes changes depending on the orientation of the accelerometer at any given moment, accelerometer signals alone are not sufficient to reconstruct the speed and position of the animal. The influence of gravity also makes it difficult to interpret the sign and amplitude of accelerometer signals. As a result, we only compared accelerometer signals between failure-to-stop trials and latency-matched go trial controls to identify when accelerometer signals began to diverge. Our goal was to test the specific hypothesis that rats began to reverse their fixation port exit behavior in failure-to-stop trials right around SSRT.

We used the same random permutation method to identify latency-matched go trials for failure-to-stop trials, and aligned accelerometer signals at SSRT **(Figure 22E)**. Accelerometer signals in failure-to-stop trials were significantly different from latency-matched controls if they exceeded 0.2% [0.1, 99.9] confidence interval (5,000 permutations) **(Figure 22E-F)**.

Electrical Stimulation

Seven rats were tested in the BF electrical stimulation experiment (20 sessions) after initial behavioral shaping procedures and without any additional training. The behavioral task **(Figure 24B)** had the same structure as the Stop No Reward Task, except that the visual stop signal was replaced by brief BF electrical stimulation. Individual stimulation pulses were biphasic charge-balanced pulses (0.1ms each phase) delivered through a constant current stimulator (stimulus isolator A365R, World Precision Instruments, FL), driven by a Mater-8-VP stimulator (A.M.P.I., Israel). Each stimulation train consisted of 1 or 3 pulses delivered at 100 Hz (10 ms interstimulus interval). The stimulation was delivered through all 32 electrodes in the BF, the same electrode configuration as used in the recording experiment. This was intended to mimic the widespread presence of BF bursting neurons throughout the recording region, representing an ensemble bursting event of the entire population (Avila and Lin, 2014). Stimulation current level was set at 24 - 48 μA per electrode.

In a subset of sessions (n=11, 4 rats), BF electrical stimulation was delivered only through half of electrodes (8/16) within each bundle (in each hemisphere), while single unit activity was recorded on the remaining wires to verify the effect of microstimulation on BF neuronal activity (n = 44 single units). These 44 single units were further classified into bursting (n=21) and non-bursting (other) neurons (n=23) based on their responses to the go signal **(Figure 20A)**.

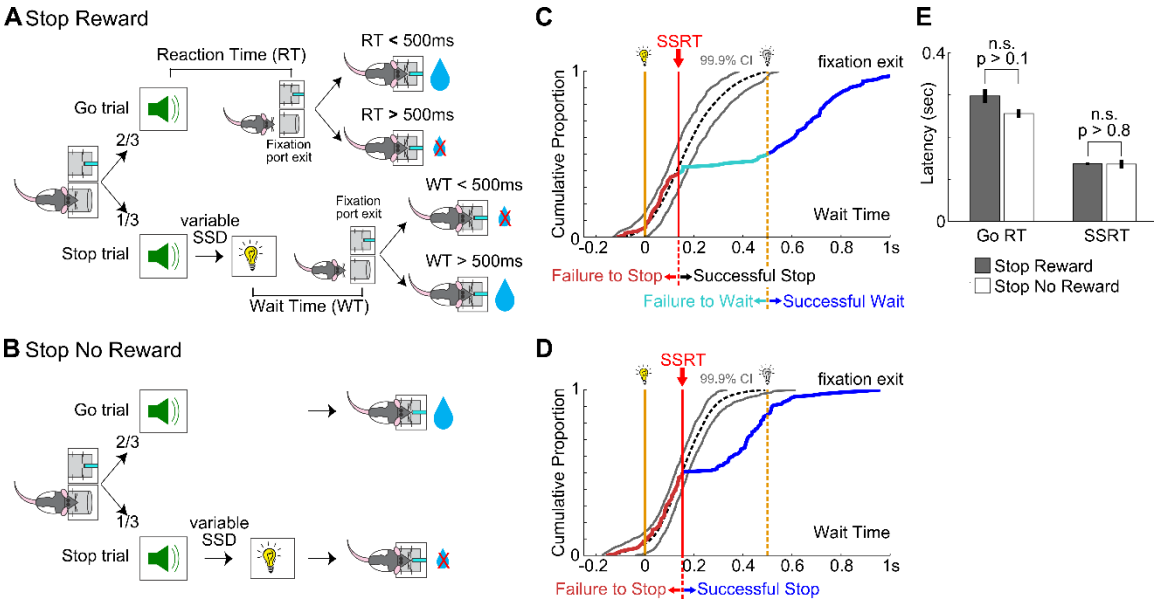

Figure 18 - Similar rapid behavioral stopping in two variants of SST

A-B. Schematic of the Stop Reward Task **(A)** and Stop No Reward Task **(B)**. In the Stop Reward Task, each trial started with the rat entering the fixation port, followed by the same Go sound in all trials signaling reward in the adjacent port if reaction time (RT) was < 500ms. On stop trials, the Go sound was followed by a Stop light after a variable stop signal delay (SSD). Rats were rewarded on these trials if they canceled the Go response and the wait time (WT) was > 500ms. Yellow dashed line indicates the offset of the Stop signal and the end of waiting period. The Stop No Reward Task had the same sequence of events, except that Stop trials were never rewarded. **C-D.** Example sessions from the Stop Reward Task **(C)** and the Stop No Reward Task **(D)** showing cumulative WT distributions. SSRT was determined by comparing the cumulative WT distribution in Stop trials with latency-matched Go trials (see Methods for details). Fixation port exits before SSRT were classified as failure-to-stop trials while those after SSRT were classified as successful stop trials. Successful stop trials in the Stop Reward Task were further classified into failure-to-wait and successful wait trials depending on whether rats waited long enough to receive reward. **E.** Go RT and SSRT were not significantly different between the two SST variants (Stop Reward: n = 19 rats, 543 sessions; Stop No Reward: n = 8 rats, 466 sessions).

Results

To study the neural mechanism of inhibitory control, we have recently adopted the primate SST and developed a rodent-appropriate SST (Mayse et al., 2014). In the SST, rats are required to rapidly generate a behavioral response following an imperative Go signal (sound), and to cancel the preparation of this response following an infrequent Stop signal (central panel light). Successful

performance in stop trials requires rats to cancel the planned Go response and maintain fixation for an additional 500ms wait period to receive reward **(**Stop Reward Task, **Figure 18A)**. By comparing the timing of fixation port exit in Go and Stop trials, we found that rats rapidly inhibited their prepotent go responses in stop trials, and that SSRT can be estimated without bias by using the novel modified integration method **(Figure 18C,** Mayse et al., 2014). As a result, stop trials can be partitioned into failure-to-stop trials (fixation exit before SSRT, whose RT distribution was indistinguishable from go trial RTs) and successful stop trials, which are further partitioned into failure-to-wait trials (not rewarded) and successful wait trials (rewarded) **(Figure 18C,** Mayse et al., 2014).

While the SST is a powerful task for studying inhibitory control, it is difficult to dissociate stop-related neuronal activity from reward-related neuronal activity using this task alone. Successful stopping commonly leads to, and is therefore closely associated with, reward delivery. To address this potential issue, and to dissociate stop- from reward-related activity, we developed a variant of SST in which stopping is not rewarded (Stop No Reward Task, **Figure 18B**). This task was identical to the Stop Reward task except that animals do not receive reward in Stop trials regardless of the outcome of stopping. While rats were not required to stop in the Stop No Reward Task, they showed fast behavioral stopping to the stop signal, **(Figure 18D)** with equivalent SSRT estimates as in the Stop Reward Task (**Figure 18E,** independent samples t-test, $p>0.8$). In contrast, subsequent to SSRT, rats behaved differently in the two tasks: when stopping was successful, rats stayed in the fixation port significantly longer in the Stop Reward Task than in

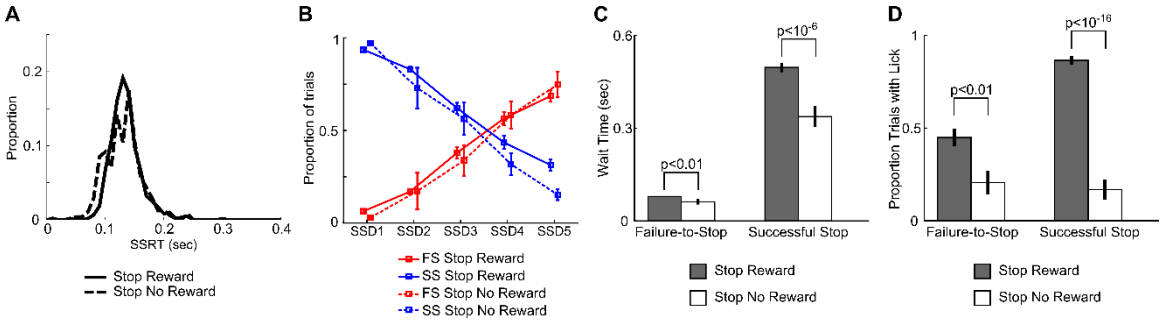

Figure 19 - Comparison of behavioral performance in two variants of SST.

A-B. Animals in the Stop Reward and Stop No Reward conditions have similar SSRT estimates **(A)** and inhibition functions **(B)**. **C-D.** Animals in the Stop Reward condition are slightly slower when they fail to stop (left) or successfully stop (right) **(C)** and attempt to collect reward more on both failure-to-stop and successful stop trials **(D)**.

---

the Stop No Reward Task, whereas animals almost always attempted to collect reward, but rarely did so, in the Stop No Reward Task **(Figure 19)**. The similarities and differences between the two SST variants allowed us to dissociate stop-related neuronal activity from reward-related neuronal activity. We predict that the neural correlate of stopping should be common to both SST variants at epochs leading up to SSRT, while neural signals related to reward expectancy that emerge subsequent to SSRT should be present only in the Stop Reward Task.

We recorded 494 well-isolated BF single units in 8 rats across 36 sessions while animals performed one of the two SST variants (4 rats each). The majority of recorded BF neurons (275/494) showed a rapid phasic excitatory response to the Go signal **(Figure 20A)** with baseline firing rates less than 12 spikes/s **(Figure 20C)**. Bursting neurons were similarly found in the Stop Reward Task (161/235) and the Stop No Reward Task (114/259). The properties of these neurons are consistent with the properties of salience-encoding noncholinergic BF neurons in previous studies (Avila and Lin, 2014; Lin and Nicolelis, 2008; Nguyen and Lin, 2014) and are the focus of subsequent analyses.

We first examined how BF neurons with bursting responses to the Go signal respond to the Stop signal. By comparing BF neuronal responses in stop trials to the activity of the same neurons in go trials at matching delays, we found that these BF neurons were rapidly and nearly completely inhibited by the stop signal **(Figure 20B)** in both SST variants. The stop signal led to significant inhibition in 93% (255/275) of BF bursting neurons (**Figure 20B,D**, see Methods). These neurons also constituted 83% (150/180) of BF neurons that were strongly inhibited by the stop signal (with a decrease of at least 4 spikes/s) and did not induce additional excitation at the population level at any time point **(Figure 20B)**. These results

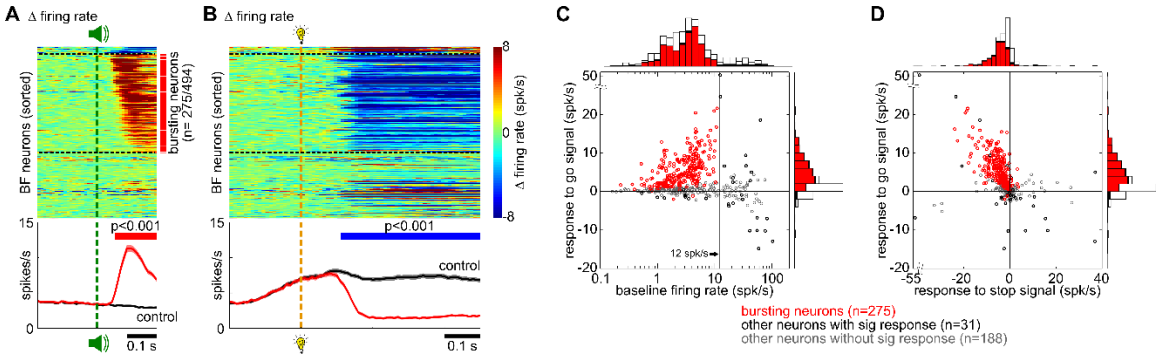

Figure 20 - BF neurons with bursting responses to the go signal were inhibited nearly completely by the stop signal, irrespective of the consequence of stopping

A. (top) Responses of individual BF neurons in both SST variants to the Go signal, shown as the difference between go trials and foreperiod-matched controls. Individual BF neurons were sorted by the latency of the first significant response within 200ms of Go signal onset. Significant responses were found in 21 (inhibitory) and 285 (excitatory) of 494 BF neurons (separated by black dotted lines). Bursting neurons were identified as BF neurons with excitatory response and baseline firing rate less than 12 Hz (275/285) (red bar). (bottom) Population PSTH for bursting neurons in go trials and foreperiod-matched controls, with significant excitation indicated by the red horizontal bar (Bonferroni-corrected paired t-test for each 10ms bin). **B.** Response of individual BF neurons to the stop signal, shown as the difference between stop trials and latency-matched go trial controls. Blue horizontal bar indicates significant inhibition. Conventions are the same as in **A**. **C.** Scatter plot of the go signal response in the [0.05, 0.2]s window after the Go signal vs. baseline firing rate for individual BF neurons, and corresponding marginal distributions. **D.** Scatter plot of the go signal response in the [0.05, 0.2]s window after the Go signal vs. the stop signal response in the [0.1, 0.5]s window after the Stop signal for individual BF neurons, and corresponding marginal distributions. Bursting neurons are indicated in red, other neurons with significant responses are indicated in black, and neurons with no significant responses are indicated in gray.

support that the go and stop signal induced opposite responses – bursting and complete inhibition, respectively – in the same BF neuronal population, irrespective of the consequence of stopping.

Given that the amplitude of BF bursting response is tightly coupled with RT, we next investigated whether the onset of BF neuronal inhibition may be coupled with SSRT. We observed that, in most BF bursting neurons, the onset of rapid and near complete neuronal inhibition was tightly coupled with SSRT (example in **Figure 21A**), irrespective of whether stopping was rewarded **(Figure 22)**. On the population level, BF bursting neurons began to be inhibited immediately (at least10 ms) before SSRT **(Figure 21B)**. Additionally, between-session variability in BF inhibition latency was tightly correlated with between-session variability in SSRT in both variants of SST **(Figure 21C)**. Together, these data show that BF neuronal inhibition was coupled with, and occurred at, or slightly before, SSRT regardless of the consequence of stopping. This observation suggests that BF neuronal

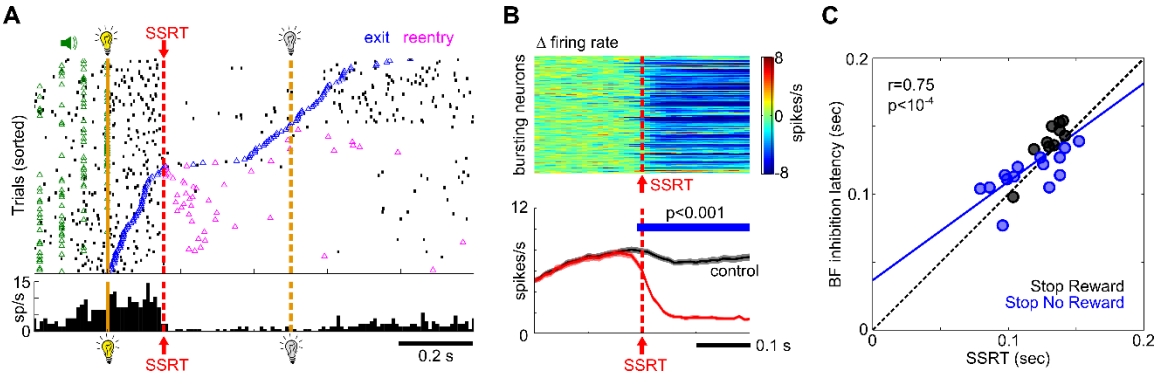

Figure 21 - The latency of BF neuronal inhibition was coupled with and slighted preceded SSRT

A. Raster plot of an example BF bursting neuron in the Stop Reward Task. Stop trials were aligned to stop signal onset and sorted by fixation port exit time. Near complete neuronal inhibition started around SSRT. **B.** Response of BF bursting neurons to the stop signal, aligned at SSRT. At the population level, the onset of BF inhibition precedes SSRT by at least 10msec. Conventions are the same as in Figure 2b. (n=275) **C.** The onset of BF neuronal inhibition in each session is strongly correlated with SSRT for both SST variants, in sessions with at least 4 BF bursting neurons (n=24 sessions).

inhibition provides a novel neural correlate of SSRT outside of commonly assumed corticostriatal circuits.

We next investigated whether BF neuronal inhibition was differentially engaged in successful and failed stop trials by comparing BF responses around SSRT **(Figure 22)**. In both the Stop Reward and Stop No Reward conditions, significant neuronal inhibition began around SSRT both when stopping was not successful (**Figure 22A-B,** left panels), and when it was (**Figure 22A-B,** right panels). The presence of near-complete BF inhibition in failure-to-stop trials in both SST variants is interesting because BF inhibition continued even after rats had failed to cancel the go response. This observation raised the question of whether behavioral stopping was also engaged in failure-to-stop trials after animals have executed the prepotent go response before SSRT. We found that rats frequently engaged in rapid reversal of their fixation port exit behavior (i.e. reentry) in failure-to-stop trials, especially when they exited the fixation port right before SSRT **(Figure 22C-D)**. The timing of the fixation port exit and reentry were centered around SSRT **(Figure 22D)**, suggesting a delayed engagement of stopping outside of the fixation port that took place around SSRT. In support of this idea, analysis of accelerometer signals showed that, while outside of the fixation port, rats began to reverse their head withdrawal motion right around SSRT **(Figure 22E-F)**. These results suggest that BF inhibition represents a robust and invariant stop process that is engaged even when it is too late to cancel the prepotent go response, and that the effects of the stop process persist even after the initial competition between going and stopping is resolved.

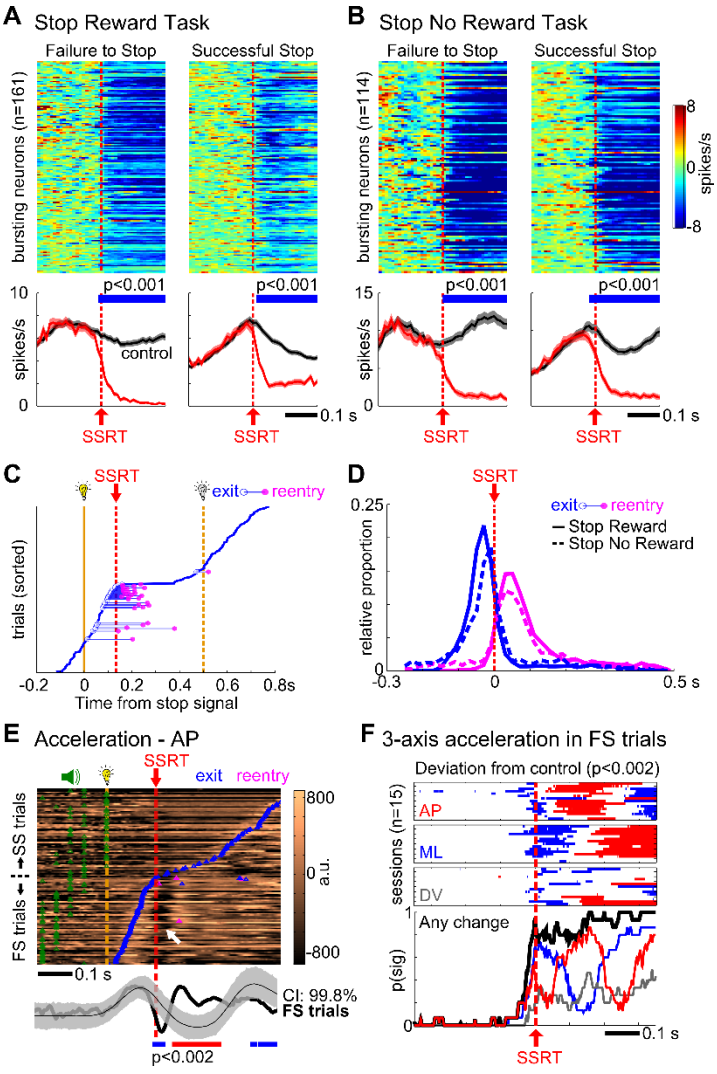

Figure 22 - BF neuronal inhibition in failure-to-stop trials was associated with corrective fixation port reentries and reversal of head movements at SSRT

A-B. Response of BF bursting neurons to the stop signal aligned at SSRT, plotted separately for failure-to-stop (left) and successful stop trials (right), and separately for the Stop Reward **(A)** and Stop No Reward task **(B)**. Conventions are the same as in Figure 20b. BF neuronal inhibition was present and time-locked to SSRT in both failure-to-stop and successful stop trials in both SST variants. **C.** An example session from the Stop Reward Task showing frequent fixation port reentry events in failure-to-stop trials, especially when rats exited fixation port right before SSRT. **D.** The distribution of fixation port exit and reentry events in all reentry trials. For both SST variants, fixation port exit and reentry events are centered on SSRT. **E.** Head-mounted accelerometer signal from an example session in Stop No Reward Task. Prominent reversal of movement acceleration in failure-to-stop trials occurred at SSRT (white arrow), which is significantly different (p<0.002) from the accelerometer signals in matching go trial controls (see Methods for details). **F.** The time course of when accelerometer signals in failure-to-stop trials were significantly different from matching go trial controls. Significant bins were plotted separately for 3 accelerometer axes in 15 sessions, with the aggregate probabilities shown below. Significant differences in accelerometer signals in failure-to-stop trials began at SSRT.

In contrast to the highly similar onset of BF inhibition at SSRT observed in

both failure-to-stop and successful stop trials, irrespective of whether stopping was rewarded, BF activity began to diverge subsequent to SSRT in failure-to-stop and successful stop trials. We observed that post-SSRT BF activity was similar between failure-to-stop and successful stop trials in the Stop No Reward task (paired t-test, p=0.78) **(Figure 23A-B)** where both trial types were not rewarded. However, in the Stop Reward Task, post-SSRT BF activity was significantly different between trial types: while failure-to-stop trials were associated with sustained BF inhibition, BF activity began to rebound in both types of successful stop trials (failure-to-wait and successful wait trials) that could lead to reward **(Figure 23A-C)**. Furthermore, the post-SSRT ramping activity in failure-to-wait trials was significantly greater than in successful wait trials **(Figure 23A-C)**. Activity

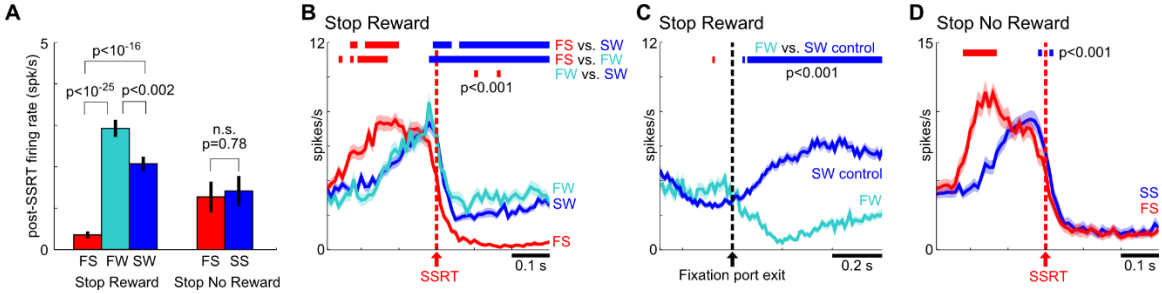

Figure 23 - Post-SSRT BF activity tracked reward expectancy and behavioral performance

A. Comparison of BF activity at the [0.05 0.2]s post-SSRT window between different trial types in both SST variants (n=161 for Stop Reward Task, n=114 for Stop No Reward Task). **B.** Population PSTH of BF bursting neurons in Stop No Reward task for the two trial types. There was no significant difference in neuronal activity between failure-to-stop and successful stop trials after SSRT. Activity differences before SSRT disappeared once SSDs were properly matched (Figure 22B). **C.** Population PSTH of BF bursting neurons in Stop Reward task for the three trial types. Activity in failure-to-stop trials was significantly lower than the other two trial types after SSRT. Activity in failure-to-wait trials was significantly higher than successful wait trials during the waiting period after SSRT. Significant differences in activity before SSRT disappeared once SSDs were properly matched (Figure 22A). **D.** Population PSTH of BF bursting neurons in Stop Reward task for failure-to-wait and successful wait trials, aligned at fixation port exit of failure-to-wait trials (see Methods for details). Activity in failure-to-wait trials was significantly higher than latency-matched successful wait trials, and peaked right before fixation port exit. After fixation port exit, activity in failure-to-wait trials immediately decreased, relative to successful wait trials.

in failure-to-wait trials peaked right before the premature fixation port exit, and immediately began to decrease after fixation port exit **(Figure 23D)**. These results are consistent with the interpretation that post-SSRT BF activity tracks the rising expectation of reward during the waiting period, which potentially led rats to exit prematurely in failure-to-wait trials. These results highlight the importance in distinguishing neural activity associated with the fast stopping response occurring near SSRT from the post-SSRT activity that likely reflects dynamic reward expectation.

Finally, we tested whether BF inhibition was sufficient to cause behavioral stopping. To test this hypothesis, we utilized precisely-timed electrical microstimulation of the BF to inhibit BF bursting neurons. This experiment was based on the observation that electrical microstimulation of the BF led to differential responses between bursting neurons and other BF neurons **(Figure 24A)**. A short pulse of BF electrical stimulation that minimized the potential excitatory effect and RT speeding (Avila and Lin, 2014) was able to selectively inhibit BF bursting neurons for up to 1s after a brief rebound excitation **(Figure 24A,C)**. We therefore tested whether artificially inducing BF inhibition in place of the visible stop signal may lead to behavioral stopping in rats that had never been trained in the SST **(Figure 24B)**. We found that the brief BF electrical stimulation induced rapid behavioral stopping in 18/20 sessions (7 rats) **(Figure 24C-D)**, and was therefore sufficient to replace the stop signal. In sessions with simultaneous BF recording and microstimulation, the onset of BF neuronal inhibition was closely associated with estimated SSRT **(Figure 24C)**. Furthermore, animals often

attempted to reenter the fixation port in failure-to-stop trials **(Figure 24C,E)**, similar to the reentry behavior observed in the SST **(Figure 22C-D)**. Reentry occurred despite the absence of an overt stop signal, and despite the fact that neither stopping nor reentry carried any behavior consequence. Together, these results provide causal evidence that BF inhibition is sufficient to produce stopping.

Discussion

Inhibitory control - the ability to suppress actions inappropriate for the behavioral context - is essential for animals' survival, and can be studied in rodents using a modified version of the stop signal task (SST). In this study, we examined the role of the basal forebrain (BF) in inhibitory control while rats perform two variants of a SST **(Figure 18)**. We found that, irrespective of whether or not

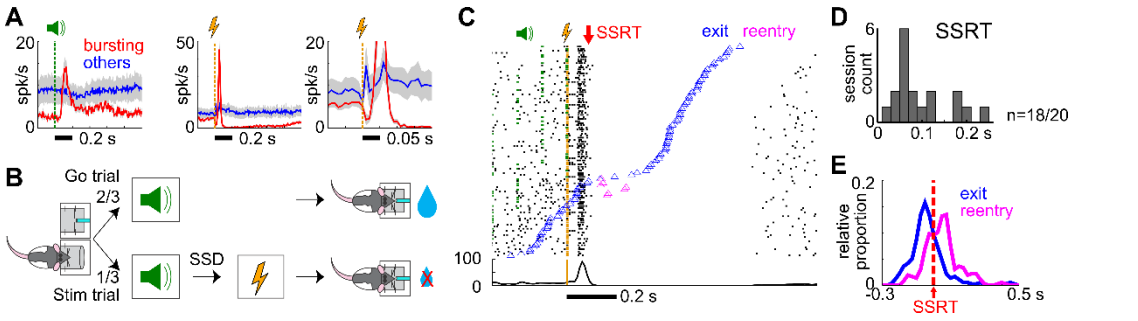

Figure 24 - Induced BF inhibition in place of a stop signal reproduced behavioral stopping and reentry behavior in rats naive to SST training

A. Response of bursting (n=21) and other (n=23) BF neurons to go sound (left panel) and brief BF electrical stimulation (middle and right panels, 11 sessions from 4 rats). BF bursting neurons, but not other neurons, demonstrated near complete inhibition in response to BF electrical stimulation after a brief rebound excitation. **B.** Schematic of the electrical stimulation experiment, which was the same as Stop No Reward task except that the stop signal was replaced by brief BF electrical stimulation. **C.** An example BF bursting neuron in stimulated trials. The onset of sustained BF inhibition coincides with estimated SSRT. Reentry was observed in trials where rats exited the fixation port right before SSRT, similar to the reentry behavior in SST (Figure 22C). **D.** Distribution of estimated SSRT from 18/20 sessions (7 rats) showing significant slowing of fixation port exit in response to BF electrical stimulation. **E.** The distribution of fixation port exit and reentry events in all reentry trials in the stimulation experiment. Fixation port exit and reentry events centered on SSRT.

successful stopping was rewarded, BF neurons with bursting responses to the go signal demonstrated near complete inhibition in response to the stop signal **(Figure 20)**. The onset of BF inhibition was tightly coupled with, and slightly preceded, the latency of behavioral inhibition, or stop signal reaction time (SSRT) **(Figure 21)**. Further, BF inhibition was similarly present in failure-to-stop trials, and was coupled with behavioral reversal of go responses at SSRT **(Figure 22)**. In successful stop trials, BF inhibition at SSRT was quickly replaced by ramping activity during the waiting period, which closely tracked whether animals successfully waited and thus expected to receive reward **(Figure 23)**. Finally, artificially inducing BF inhibition via precisely-timed microstimulation produced stopping in the absence of an overt stop signal **(Figure 24)**. Taken together, these results indicate that BF neuronal inhibition provides a novel neural correlate of SSRT, and plays a causal role in rapid inhibitory control.

The similar SSRTs in both SST variants suggest that the initial behavioral stopping is a rapid and automatic process that occurs irrespective of whether stopping was rewarded. This similarity extended to failure-to-stop trials, where rats in both SST variants displayed reversal of accelerometer signals in the direction of fixation port exit that was time-locked to SSRT, oftentimes resulting in corrective reentry into the fixation port **(Figure 22)**. The main behavioral difference between the two SST variants emerged only after the rapid initial stopping at SSRT: rats waited significantly longer in the fixation port, and approached the reward port more frequently when successful waiting led to reward. The similarities and differences of behaviors in the two SST variants allowed us to differentiate neural

responses that were associated with SSRT, and thus common to both tasks from neural responses associated with a post-stopping reward expectancy signal, and thus specific to the Stop Reward task.

Our results support the hypothesis that BF neuronal inhibition provides a novel neural correlate of SSRT, as BF inhibition was present in both SST variants, and was temporally locked to SSRT in both successful- and failure-to-stop trials. Our results further suggest that, even when it was too late to cancel the go response, BF neuronal activity still processed the stop signal, and the resulting BF inhibition similarly corresponded to behavioral stopping, irrespective of whether rats maintained fixation. It is important to note that BF inhibition did not lead to freezing, as rats were able to exit the fixation port under complete BF inhibition in both SST variants, as well as during stimulation-induced BF inhibition. This suggests that BF inhibition only stops and reverses the actions associated with the go signal, rather than inducing global motor suppression.

The presence of similar BF inhibition in both successful-stop and failure-to-stop trials indicates that successful stopping is not determined by the invariant BF neuronal inhibition. Instead, stop success is largely determined by the intrinsic variability of the go response, where considerable reaction time variability remains in response to the same well-learned and supra-threshold sensory stimuli (ref Irene). In other words, stop success is determined largely by the relative timing between the stochastic go process and the highly consistent stop process. This idea has important implications for identifying neural mechanisms for stopping because comparing neural responses between successful- and failure-to-stop

trials will not identify neural correlates of the invariant stop process, such as BF inhibition. Instead, this comparison will identify neural correlates associated with the stochastic variability of the go process, as well as neural correlates of a post-SSRT reward expectancy signal that is present only in successful stop trials, such as the BF ramping activity that follows the initial BF inhibition (Schall and Godlove, 2012).

BF neuronal inhibition was observed primarily in the subset of BF neurons with prominent bursting response to the go signal. These results highlight the functional significance of this group of BF neurons, and add to the growing list of cognitive functions that these neurons may mediate. Recent studies show that this physiologically homogeneous population of BF neurons is non-cholinergic (Hassani et al., 2009; Lin et al., 2006; Lin and Nicolelis, 2008), that their bursting responses encode the motivational salience of stimuli (Lin and Nicolelis, 2008), and that the presence of BF bursting is coupled with the detection of near-threshold stimuli (Goard and Dan, 2009; Lee and Dan, 2012). Furthermore, stronger BF bursting responses are linked to faster, and more precise reaction times (Avila and Lin, 2014). These behavioral effects are mediated, at least in part, via the generation of a frontal cortex event-related potential (ERP) response (Nguyen and Lin, 2014).

Our observation that the stop signal induced neuronal inhibition in BF without eliciting additional excitatory responses indicates that neuronal inhibition and bursting activity can be independently controlled in these non-cholinergic BF neurons. These findings suggest that neuronal inhibition is an equally important

dimension as is the phasic bursting responses in the BF, and support the hypothesis that BF neurons control the decision process bidirectionally: while BF bursting leads to faster decision speed, BF inhibition halts and reverses the preparation of the planned action. We suggest that BF activity may provide the gain signal of the decision unit in the rise-to-threshold model of decision making **(Figure 1,** General Introduction**)**. The correlation of BF bursting amplitude with reaction time suggests that BF bursting determines the slope of activity accumulation in the decision unit. On the other hand, the sudden inhibition of BF activity removes this gain signal, thus halting further activity accumulation, and inducing the animal to stop his prepared response. This model suggests that the delay between BF inhibition and SSRT can be very short, which is consistent with the short temporal delay (~20ms) that we observe between the onset of BF inhibition and SSRT in both SST variants, and in the electrical stimulation experiment (Boucher et al., 2007a). Consistent with this model, we have shown that BF can provide fast modulation of cortical activity, as evidenced by the generation of a frontal cortex ERP response within 5-10 msec of the BF bursting response (Nguyen and Lin, 2014).

These results reveal that BF neurons respond to motivationally salient go and stop signals in opposite directions, rather than by generating a similar bursting response to these stimuli that encodes their motivational salience, as previously suggested (Lin and Nicolelis, 2008). This discrepancy is likely due to multiple factors: First, Lin & Nicolelis found that BF neurons show a phasic bursting response to all motivationally salient stimuli in a Go/Nogo task. The initial bursting

is followed by a subsequent phase of tonic activity that is excitatory when rats make go responses, and inhibitory when the response is NoGo. Our current findings are consistent with that report, in that BF inhibition is associated with stopping of the prepotent go response in NoGo trials. Second, unlike previous studies where motivationally salient stimuli are presented alone, stop signals always follow a preceding go signal in the SST. We suggest that, in the presence of the go signal, rats likely have little uncertainty about what and when the next signal may occur. This low level of uncertainty likely underlies the lack of BF bursting response to the stop signal. Similarly, context dependent omission of bursting response in the presence of a preceding cue is also observed in midbrain dopaminergic neurons (Bromberg-Martin et al., 2010).

Together, our results support that the hypothesis that BF is a novel node of the inhibitory control circuitry outside of the commonly studied corticostriatal circuit. BF neurons likely work in concert with corticostriatal regions to determine the outcome of the competition between the go and stop process. The existing literature suggests that, when faced with a stop signal, STN/SNr likely provide an initial global pause signal, while SSRT is determined by the coordinated actions between BF inhibition and their modulation on other cortical determinants of SSRT.

General Discussion

Brief Summary and Novel Advances of the Current Work

Cognitive inhibition is an integral component of normal cognitive functioning. This thesis represents a significant step towards a greater understanding of the neural circuits underlying cognitive inhibition. In Chapter 1, we established a novel rodent version of the SST, linking a powerful behavioral paradigm for studying a form of cognitive inhibition to the advantages of rodent models. We utilized this novel rodent SST in Chapters 2 and 3 to examine a novel node in the neuronal circuits underlying stopping, the BF. In Chapter 2, we examined whether age-related slowing of processing speed and SSRT were independent in a naturally-occurring rodent model of normal cognitive aging, and whether these changes related to altered BF integrity. In Chapter 3 we utilized this rodent SST and in vivo electrophysiological recording to study the role of bursting neurons in the BF in stopping. Together, these studies make several critical advances towards the study of cognitive inhibition.

The establishment of a valid rodent SST is a significant advance for the study of stopping. While previous attempts have been made, all have failed in a number of ways to appropriately adapt the SST for rodents (Bari et al., 2011b; Beuk et al., 2014; Schmidt et al., 2013). By contrast, our task design reproduces all of the features of the SST in humans and primates. We show an increased proportion of failure-to-stop trials as SSD increases, and RTs on failure-to-stop trials are indistinguishable from the faster portion of the Go RT distribution, central tenets of the race model (Logan and Cowan, 1984; Verbruggen and Logan,

2009b). Additionally, we establish a method for unbiasedly separating errors of stopping and waiting in rodents, and show that failing to do so systematically biases SSRT estimates to be too long. In addition to reproducing the overall features of primate and human behavior in the SST, rodents reproduce many subtle behavioral features. First, we observed that rats make extensive use of proactive control to adjust RTs based on immediate trial history. Proactive control of RTs has been observed in both humans and primates and represents a strategic choice to slow RTs following stop trials or errors to improve subsequent performance (Chen et al., 2010; Verbruggen and Logan, 2009c). Second, we observe that rats often attempt corrective reentry responses, similar to corrective responses observed in humans and primates instructed to cancel skeletal movements (Boucher et al., 2007b; Chen et al., 2010; Logan and Irwin, 2000). Together, these results provide compelling evidence that not only are rodents capable of performing the SST, but that they perform it in a manner that is qualitatively indistinguishable from humans and primates once steps are taken to adapt the task appropriately for rodents.

Here we leverage two advantages of rodent models made possible by the development of the rodent SST laid out in Chapter 1. First, in Chapter 2, we use a rodent model of normal cognitive aging to study whether changes in performance in the SST in aged animals is related to impairment in other cognitive domains. Both humans and rodents show increased population variability on a variety of cognitive measures in age, including working memory (Salthouse et al., 1991; Wang et al., 2011), spatial navigation (Gallagher et al., 1993; Squire, 1992),

processing speed (Burwell and Gallagher, 1993; Salthouse, 2000), cognitive flexibility (Barense et al., 2002; Haaland et al., 1987), and cognitive inhibition (Kramer et al., 1994; Schoenbaum et al., 2002b). In this work we examined whether age-related impairment in three of these domains (spatial navigation, processing speed, and cognitive inhibition) were related to each other and to dysfunction in the BF cholinergic system. In line with previous studies, we found that impairment in these three domains were independent. However, we found a strong novel dissociation between the ability to sustain attention in anticipation of a salient stimulus and spatial navigation in the aged rat, and this same sustained attention ability and cognitive inhibition in the young rat. Furthermore, we found strong correlations between the number of medial BF ChAT+ neurons and waiting/navigation in aged rats, while the number of lateral BF ChAT+ neurons and waiting/stopping were correlated in young rats. These data suggest that, though aged and young rats seem to stop similarly in the SST, post-stopping behavior is achieved differently.

In Chapter 3, we explored the novel hypothesis that stopping is subserved by a subset of neurons in the BF that elicit strong, phasic “bursting” responses following motivationally-salient stimuli (Avila and Lin, 2014; Lin and Nicolelis, 2008). In young rats performing the rodent SST, we found that these BF bursting neurons differentially encoded the Go signal with phasic bursting and the Stop signal with phasic inhibition, followed by sustained tonic encoding that predicted whether the animal would receive reward. Phasic inhibition of BF neurons by the stop signal preceded and was correlated with SSRT, and the characteristics (i.e.,

magnitude and latency) of this inhibition did not predict the outcome of stopping before SSRT. We hypothesized that BF inhibition represents a putative stop process; that is, a neuronal signal capable of causing stopping but that itself does not encode the outcome of stopping. Such a stop process is analogous to the relationship between a red traffic light and an inattentive driver: the traffic light is itself simply instructing the driver to stop and is indifferent to whether he does so. Whether the driver stops depends on how fast the car is going and the delay between when the light turns red and when the driver attends to the light. In the same way, we find that artificially-inducing BF inhibition via precisely-timed electrical microstimulation causes animals to stop in a delay-dependent manner (i.e., inducing inhibition at short delays causes stopping, while inducing inhibition at long delays does not). These data provide compelling evidence that the BF is a novel node in the neuronal circuits underlying stopping. However, notably these BF bursting neurons are likely non-cholinergic (Hassani et al., 2009; Lin et al., 2006; Lin and Nicolelis, 2008), suggesting that the BF cholinergic (Chapter 2) and non-cholinergic (Chapter 3) populations overlap somewhat in their role in the SST. However, there is substantial intra-BF interaction between cortically-projecting cholinergic and GABAergic neurons, suggesting that age-related impairment linked to BF cholinergic neurons in Chapter 2 may in fact reflect impairment in the local BF microcircuit, rather than a discrete function subserved by the cholinergic neurons themselves (Yang et al., 2014). Future studies using optogenetic tagging of ChAT+ and Parvalbumin+ neurons in the BF can dissociate the functions mediated by these two neuronal populations.

A persistent problem with analyzing neuronal signals related to stopping in the SST is the requirement that multiple, variable delays between the go and stop signal be used to create variability in the outcome of stopping. While this restriction is necessary to prevent subjects from slowing their go responses in anticipation of a highly-predictable stop signal and for accurate estimation of SSRT (Band et al., 2003a), it complicates alignment of neuronal signals to the stop signal. Because the stop signal occurs at a variable time relative to the go signal, it is difficult to establish an appropriate go or no-stop baseline to which to compare neuronal responses to the stop signal. To circumvent this, many studies examine neuronal responses to the stop signal separately for each SSD and use latency-matched neuronal responses to the go signal as a baseline, severely reducing the power of statistical analyses. Here, we establish a novel method for yoking continuous distributions of physiological data to stimuli with different onset latencies. This method can be applied to behavioral data (Chapter 1, Mayse et al., 2014), neuronal recordings, or any other continuous data distributions and is a powerful addition to neurophysiological methods in general and the SST in particular. In this method, we collapse across SSD to analyze both behavioral and physiological data. Simply, this method allows us to create an estimate of the stop-aligned (i.e., yoked or latency-matched) continuous go trial distribution that would have been observed had the stop signal never been presented. For behavioral data, the yoked go distribution represents the RTs relative to the stop signal that would have been observed had the stop signal never been presented. For neuronal data, the yoked go distribution represents the activity of BF neurons relative to the stop signal that

would have been observed had the stop signal never been presented. Critically, in all cases the yoked go and empirical stop distributions overlap before time zero, demonstrating the effectiveness of our latency-matching and bootstrapping procedures in creating distributions that are otherwise equal except for the effect of the stimulus being yoked to. This method is an important and computationally-simple tool for analysis of physiological correlates of SST performance and has broad applications outside of the SST for any preparation in which there is a variable stimulus onset asynchrony.

Integration of the Basal Forebrain into Existing Neuronal Networks for Stopping

Executive control necessitates the capability to inhibit irrelevant or inappropriate responses in a context- or rule-dependent manner. A wealth of studies have implicated a distributed fronto-cortical network in such response inhibition (Aron and Poldrack, 2006; Aron et al., 2007; Aron et al., 2004, 2003; Duann et al., 2009; Muggleton et al., 2010). This fronto-cortical network is thought to effect stopping via its connections with the basal ganglia, where competing neural circuits race for control of basal ganglia output nuclei. The current study expands this literature by implicating neurons in the BF as a physiological instantiation of the stop process, an important finding and, to our knowledge, the first study to find such a correlate for stopping complex skeletal movements. BF neurons are inhibited before SSRT, and the latency of this inhibition correlates with SSRT. Additionally, replacing the overt stop signal with BF inhibition causes stopping, suggesting a causal relationship. Finally, BF inhibition is similar before SSRT regardless of the outcome of stopping. This finding is consistent with the

notion that the stop process is similarly activated even when stopping is unsuccessful and it is only the latency of this activation relative to the finish time of the go process that determines stopping (Boucher et al., 2007a; Logan and Cowan, 1984). An important question raised by this study is how the BF can be integrated into the established fronto-basal ganglia circuits thought to underlie stopping. We suggest that stopping is effected via a two-stage process in which basal ganglia neurons respond rapidly to delay motor action, while BF neurons provide a slower response possibly used by cortical regions involved in stopping to selectively guide behavior. A recent study in rodents performing the SST found that neurons in the STN and striatum race to control the SNr, an output nucleus of the basal ganglia (Schmidt et al., 2013). However, these STN neuronal responses were fast, sensory-like, and were time locked to both the go and stop signals but not SSRT. Additionally, the latency of STN activity did not correlate with SSRT, but instead with RT such that greater STN activity correlated with slower responses. These authors suggested that the STN neurons act rapidly in situations of response conflict to provide a brief, global motor pause in order to allow other regions to selectively control behavior. By contrast, here we show that BF neurons have much slower responses that differ to the go and stop signals, and the latency of the stop-specific BF response correlates well with SSRT. In fact, such a two stage model is supported by modeling of behavioral and neurophysiological data (Boucher et al., 2007a). Taken together, the current work is a powerful addition to the literature that provides a unified framework for stopping.

Current models suggest that competing pro- and anti-movement BG circuits are rapidly driven by cortical input (Aron and Poldrack, 2006; Aron et al., 2007). Here, we suggest that BF neurons exert their effect by modulating ongoing cortical processing on a longer timescale than the BG competition. If stopping is achieved via the actions of these two or more circuits with common cortical connections operating on different timescales as we suggest, then it remains unclear how the BF modulation observed here could exert its effect on stopping after the BG. One might instead have predicted that the BF first modulates cortex, which then drives competition in the BG. Instead, we observe late BF modulation in the SST, in contrast to the rapid modulation of the BG. However, while most studies have explored the hypothesis that stopping is subserved by an increase in the activity of anti-movement neurons (e.g., omnipause neurons in the superior colliculus, STN neurons in the BG, etc.), stopping could also be effectively achieved by cessation of pro-movement activity (Boucher et al., 2007a). For instance, it is possible that the BF acts to remove or modulate the goal or stimulus driving going, rather than cancelling the motor plan itself, leading to a decrease in the activity in pro-motor BG circuits rather than an increase in the activity of anti-motor BG circuits (Boucher et al., 2007a). Importantly, this modulation could occur relatively late in the process of generating a response. This hypothesis is consistent with the finding that whereas STN activity is rapid and sensory-like, activity in the striatum is tightly locked to movement and differentially modulated when stopping is and is not successful (Schmidt et al., 2013; Zandbelt and Vink, 2010).

We propose that the BG and BF act in concert on different timescales to modulate different portions of the decision process. In further support of this, one study found a dissociation between the effects of deep-brain stimulation (DBS) of the STN and BF in a patient with Parkinson's disease: whereas DBS of the STN ameliorated ataxic and motoric symptoms of Parkinson's, DBS of the BF restored the patient's higher-order non-motoric cognitive deficits and apraxic symptoms (Barnikol et al., 2010; Freund et al., 2009), similarly to the finding that DBS of the BF alleviates some cognitive deficits in Alzheimer's disease (Hardenacke et al., 2013). A relatively simple experiment to test this hypothesis would be to inhibit neurons in the BF (either optically or electrically, as was done here) while recording from striatal neurons in animals performing either the SST or a simple Go task (as we did in the microstimulation studies in Chapter 3). By randomly presenting either the Stop signal or inducing BF inhibition on each trial, it would be possible within-subject and within-session to observe whether BF inhibition is sufficient to drive modulation of striatal pre-motor activity, and whether this modulation is equivalent to the Stop-signal evoked striatal modulation. The results of this experiment would elucidate whether the role of the BF in stopping is to modulate inputs that drive response generation or some other component of the competition between going and stopping in the SST.

Because the BF does not directly innervate the BG, it is unlikely that any proposed BF-BG circuit is direct; rather, it is much more likely that the BF influences the BG via their common cortical connections (Aron et al., 2007; Gritti et al., 1997; Haynes and Haber, 2013; Henny and Jones, 2008). Therefore, a

primary research goal should be to understand how BF bursting neurons can modulate ongoing cortical processing. This is an especially pressing issue because there is relatively little topography to the BF-cortical connections: individual BF neurons often innervate wide regions of cortex (Gritti et al., 1997; Henny and Jones, 2008). These data suggest that the BF-cortical connection subserves a general function, and that this function in the SST is linked with stopping. One possible mechanism linked with the BF is regulation of cortical state and cortical synchrony. In support of this, several studies have found that requiring subjects to stop a response increases gamma activity in the same medial prefrontal regions (Swann et al., 2013, 2012) where BF stimulation has been shown to induce a local event-related potential (Nguyen and Lin, 2014). Activation of the BF has been strongly linked with increased cortical gain and increased gamma band activity (Fournier et al., 2004; Fu et al., 2014; Lin et al., 2006). Considering BF noncholinergic neurons synapse preferentially on putative fast-spiking cortical inhibitory interneurons capable of inducing gamma in cortex (Cardin et al., 2009; Henny and Jones, 2008), it seems plausible that the general function of the BF may be to regulate widespread cortical states and their transitions (Gervasoni et al., 2004). This role seems consistent with the function of the BF-medial temporal lobe connections, where BF neurons in the medial septum and vertical limb of the Diagonal Band of Broca preferentially innervate inhibitory interneurons involved in regulation of hippocampal oscillatory activity (Freund and Antal, 1988; Gulyás et al., 1991). This BF-hippocampal connection has been strongly linked to regulation of hippocampal theta (as opposed to cortical gamma)

rhythms (Chapman and Lacaille, 1999; Roland et al., 2014). The BF therefore may act in general to control coordinated activity in distributed neuronal networks via populations of inhibitory interneurons themselves specialized to produce local circuit dynamics specific to the local information processing demands.

References

Andersson, U., Häggström, J.E., Levin, E.D., Bondesson, U., Valverius, M., Gunne, L.M., 1989. Reduced glutamate decarboxylase activity in the subthalamic nucleus in patients with tardive dyskinesia. Mov. Disord. Off. J. Mov. Disord. Soc. 4, 37–46. doi:10.1002/mds.870040107

Andrés, P., Guerrini, C., Phillips, L.H., Perfect, T.J., 2008. Differential effects of aging on executive and automatic inhibition. Dev. Neuropsychol. 33, 101–123. doi:10.1080/87565640701884212

Aron, A.R., 2011. From reactive to proactive and selective control: developing a richer model for stopping inappropriate responses. Biol. Psychiatry 69, e55–68. doi:10.1016/j.biopsych.2010.07.024

Aron, A.R., Behrens, T.E., Smith, S., Frank, M.J., Poldrack, R.A., 2007. Triangulating a cognitive control network using diffusion-weighted magnetic resonance imaging (MRI) and functional MRI. J. Neurosci. Off. J. Soc. Neurosci. 27, 3743–3752. doi:10.1523/JNEUROSCI.0519-07.2007

Aron, A.R., Durston, S., Eagle, D.M., Logan, G.D., Stinear, C.M., Stuphorn, V., 2007. Converging Evidence for a Fronto-Basal-Ganglia Network for Inhibitory Control of Action and Cognition. J. Neurosci. 27, 11860–11864. doi:10.1523/JNEUROSCI.3644-07.2007

Aron, A.R., Fletcher, P.C., Bullmore, E.T., Sahakian, B.J., Robbins, T.W., 2003. Stop-signal inhibition disrupted by damage to right inferior frontal gyrus in humans. Nat. Neurosci. 6, 115–116. doi:10.1038/nn1003

Aron, A.R., Poldrack, R.A., 2006. Cortical and subcortical contributions to Stop signal response inhibition: role of the subthalamic nucleus. J. Neurosci. Off. J. Soc. Neurosci. 26, 2424–2433. doi:10.1523/JNEUROSCI.4682-05.2006

Aron, A.R., Robbins, T.W., Poldrack, R.A., 2004. Inhibition and the right inferior frontal cortex. Trends Cogn. Sci. 8, 170–177. doi:10.1016/j.tics.2004.02.010

Avila, I., Lin, S.-C., 2014. Motivational salience signal in the basal forebrain is coupled with faster and more precise decision speed. PLoS Biol. 12, e1001811. doi:10.1371/journal.pbio.1001811

Band, G.P.H., van der Molen, M.W., Logan, G.D., 2003a. Horse-race model simulations of the stop-signal procedure. Acta Psychol. (Amst.) 112, 105–142.

Band, G.P.H., van der Molen, M.W., Logan, G.D., 2003b. Horse-race model simulations of the stop-signal procedure. Acta Psychol. (Amst.) 112, 105–142.

Bañuelos, C., LaSarge, C.L., McQuail, J.A., Hartman, J.J., Gilbert, R.J., Ormerod, B.K., Bizon, J.L., 2013. Age-related changes in rostral basal forebrain cholinergic and GABAergic projection neurons: relationship with spatial impairment. Neurobiol. Aging 34, 845–862. doi:10.1016/j.neurobiolaging.2012.06.013

Barense, M.D., Fox, M.T., Baxter, M.G., 2002. Aged rats are impaired on an attentional set-shifting task sensitive to medial frontal cortex damage in

young rats. Learn. Mem. Cold Spring Harb. N 9, 191–201. doi:10.1101/lm.48602

Bari, A., Mar, A.C., Theobald, D.E., Elands, S.A., Oganya, K.C.N.A., Eagle, D.M., Robbins, T.W., 2011a. Prefrontal and Monoaminergic Contributions to Stop-Signal Task Performance in Rats. J. Neurosci. 31, 9254 –9263. doi:10.1523/JNEUROSCI.1543-11.2011

Bari, A., Mar, A.C., Theobald, D.E., Elands, S.A., Oganya, K.C.N.A., Eagle, D.M., Robbins, T.W., 2011b. Prefrontal and monoaminergic contributions to stop-signal task performance in rats. J. Neurosci. Off. J. Soc. Neurosci. 31, 9254–9263. doi:10.1523/JNEUROSCI.1543-11.2011

Barnikol, T.T., Pawelczyk, N.B.A., Barnikol, U.B., Kuhn, J., Lenartz, D., Sturm, V., Tass, P.A., Freund, H.-J., 2010. Changes in apraxia after deep brain stimulation of the nucleus basalis Meynert in a patient with Parkinson dementia syndrome. Mov. Disord. Off. J. Mov. Disord. Soc. 25, 1519–1520. doi:10.1002/mds.23141

Baxter, M.G., Bucci, D.J., Gorman, L.K., Wiley, R.G., Gallagher, M., 1995. Selective immunotoxic lesions of basal forebrain cholinergic cells: effects on learning and memory in rats. Behav. Neurosci. 109, 714–722.

Baxter, M.G., Gallagher, M., 1996. Intact Spatial Learning in Both Young and Aged Rats Following Selective Removal of Hippocampal Cholinergic Input. Behav. Neurosci. 110, 460–467.

Bekker, E.M., Overtoom, C.C., Kenemans, J.L., Kooij, J.J., De Noord, I., Buitelaar, J.K., Verbaten, M.N., 2005. Stopping and changing in adults with ADHD. Psychol. Med. 35, 807–816.

Benabid, A.L., Pollak, P., Gross, C., Hoffmann, D., Benazzouz, A., Gao, D.M., Laurent, A., Gentil, M., Perret, J., 1994. Acute and long-term effects of subthalamic nucleus stimulation in Parkinson's disease. Stereotact. Funct. Neurosurg. 62, 76–84.

Benazzouz, A., Gross, C., Féger, J., Boraud, T., Bioulac, B., 1993. Reversal of rigidity and improvement in motor performance by subthalamic high-frequency stimulation in MPTP-treated monkeys. Eur. J. Neurosci. 5, 382–389.

Beuk, J., Beninger, R.J., Paré, M., 2014. Investigating a race model account of executive control in rats with the countermanding paradigm. Neuroscience. doi:10.1016/j.neuroscience.2014.01.014

Beurrier, C., Bezard, E., Bioulac, B., Gross, C., 1997. Subthalamic stimulation elicits hemiballismus in normal monkey. Neuroreport 8, 1625–1629.

Bissett, P.G., Logan, G.D., 2012. Post-stop-signal adjustments: Inhibition improves subsequent inhibition. J. Exp. Psychol. Learn. Mem. Cogn. doi:10.1037/a0026778

Boucher, L., Palmeri, T.J., Logan, G.D., Schall, J.D., 2007a. Inhibitory control in mind and brain: an interactive race model of countermanding saccades. Psychol. Rev. 114, 376–397. doi:10.1037/0033-295X.114.2.376

Boucher, L., Stuphorn, V., Logan, G.D., Schall, J.D., Palmeri, T.J., 2007b. Stopping eye and hand movements: are the processes independent? Percept. Psychophys. 69, 785–801.

Bourke, W.T., 1954. The effects of frontal lobe damage upon habit reversal in the white rat. J. Comp. Physiol. Psychol. 47, 277–282.

Bromberg-Martin, E.S., Matsumoto, M., Nakahara, H., Hikosaka, O., 2010. Multiple Timescales of Memory in Lateral Habenula and Dopamine Neurons. Neuron 67, 499–510. doi:16/j.neuron.2010.06.031

Broos, N., Schmaal, L., Wiskerke, J., Kostelijk, L., Lam, T., Stoop, N., Weierink, L., Ham, J., de Geus, E.J.C., Schoffelmeer, A.N.M., van den Brink, W., Veltman, D.J., de Vries, T.J., Pattij, T., Goudriaan, A.E., 2012. The relationship between impulsive choice and impulsive action: a cross-species translational study. PloS One 7, e36781. doi:10.1371/journal.pone.0036781

Brown, J.W., Hanes, D.P., Schall, J.D., Stuphorn, V., 2008. Relation of frontal eye field activity to saccade initiation during a countermanding task. Exp. Brain Res. Exp. Hirnforsch. Expérimentation Cérébrale 190, 135–151. doi:10.1007/s00221-008-1455-0

Bryden, D.W., Burton, A.C., Kashtelyan, V., Barnett, B.R., Roesch, M.R., 2012. Response inhibition signals and miscoding of direction in dorsomedial striatum. Front. Integr. Neurosci. 6, 69. doi:10.3389/fnint.2012.00069

Burke, K.A., Takahashi, Y.K., Correll, J., Leon Brown, P., Schoenbaum, G., 2009. Orbitofrontal inactivation impairs reversal of Pavlovian learning by

interfering with “disinhibition”of responding for previously unrewarded cues. Eur. J. Neurosci. 30, 1941–1946.

Burk, J.A., Sarter, M., 2001. Dissociation between the attentional functions mediated via basal forebrain cholinergic and GABAergic neurons. Neuroscience 105, 899–909.

Burwell, R.D., Gallagher, M., 1993. A longitudinal study of reaction time performance in long-evans rats. Neurobiol. Aging 14, 57–64. doi:16/0197-4580(93)90023-5

Caetano, M.S., Horst, N.K., Harenberg, L., Liu, B., Arnsten, A.F.T., Laubach, M., 2012. Lost in Transition: Aging-Related Changes in Executive Control by the Medial Prefrontal Cortex. J. Neurosci. 32, 3765–3777. doi:10.1523/JNEUROSCI.6011-11.2012

Cardin, J.A., Carlén, M., Meletis, K., Knoblich, U., Zhang, F., Deisseroth, K., Tsai, L.-H., Moore, C.I., 2009. Driving fast-spiking cells induces gamma rhythm and controls sensory responses. Nature 459, 663–667. doi:10.1038/nature08002

Carpenter, R.H.S., 1981. Oculomotor Procrastination, in: Eye Movements: Cognition and Visual Perception. pp. 237–246.

Chapman, C.A., Lacaille, J.-C., 1999. Cholinergic Induction of Theta-Frequency Oscillations in Hippocampal Inhibitory Interneurons and Pacing of Pyramidal Cell Firing. J Neurosci 19, 8637–8645.

Chen, X., Scangos, K.W., Stuphorn, V., 2010. Supplementary motor area exerts proactive and reactive control of arm movements. J. Neurosci. Off. J. Soc. Neurosci. 30, 14657–14675. doi:10.1523/JNEUROSCI.2669-10.2010

Coxon, J.P., Impe, A.V., Wenderoth, N., Swinnen, S.P., 2012. Aging and Inhibitory Control of Action: Cortico-Subthalamic Connection Strength Predicts Stopping Performance. J. Neurosci. 32, 8401–8412. doi:10.1523/JNEUROSCI.6360-11.2012

Coyle, J., Price, D., DeLong, M., 1983. Alzheimer's disease: a disorder of cortical cholinergic innervation. Science 219, 1184 –1190. doi:10.1126/science.6338589

Dalley, J.W., Theobald, D.E., Bouger, P., Chudasama, Y., Cardinal, R.N., Robbins, T.W., 2004. Cortical Cholinergic Function and Deficits in Visual Attentional Performance in Rats Following 192 IgG–Saporin-induced Lesions of the Medial Prefrontal Cortex. Cereb. Cortex 14, 922.

De Zeeuw, P., Aarnoudse-Moens, C., Bijlhout, J., König, C., Post Uiterweer, A., Papanikolau, A., Hoogenraad, C., Imandt, L., de Been, D., Sergeant, J.A., Oosterlaan, J., 2008. Inhibitory performance, response speed, intraindividual variability, and response accuracy in ADHD. J. Am. Acad. Child Adolesc. Psychiatry 47, 808–816. doi:10.1097/CHI.0b013e318172eee9

Dornan, W.A., McCampbell, A.R., Tinkler, G.P., Hickman, L.J., Bannon, A.W., Decker, M.W., Gunther, K.L., 1996. Comparison of site-specific injections into the basal forebrain on water maze and radial arm maze performance in

the male rat after immunolesioning with 192 IgG saporin. Behav. Brain Res. 82, 93–101.

Drachman, D.A., Leavitt, J., 1974. Human memory and the cholinergic system. A relationship to aging? Arch. Neurol. 30, 113–121.

Duann, J.-R., Ide, J.S., Luo, X., Li, C.R., 2009. Functional connectivity delineates distinct roles of the inferior frontal cortex and presupplementary motor area in stop signal inhibition. J. Neurosci. Off. J. Soc. Neurosci. 29, 10171–10179. doi:10.1523/JNEUROSCI.1300-09.2009

Dufort, R.H., Guttman, N., Kimble, G.A., 1954. One-trial discrimination reversal in the white rat. J. Comp. Physiol. Psychol. 47, 248–249.

Dunnett, S.B., Everitt, B.J., Robbins, T.W., 1991. The basal forebrain-cortical cholinergic system: interpreting the functional consequences of excitotoxic lesions. Trends Neurosci. 14, 494–501.

Dunnett, S.B., Rogers, D.C., Jones, G.H., 1989. Effects of Nucleus Basalis Magnocellularis Lesions in Rats on Delayed Matching and Non-Matching to Position Tasks. Eur. J. Neurosci. 1, 395–406.

D\üzel, S., M\ünte, T.F., Lindenberger, U., Bunzeck, N., Sch\ütze, H., Heinze, H.J., D\üzel, E., 2010. Basal forebrain integrity and cognitive memory profile in healthy aging. Brain Res. 1308, 124–136.

Eagle, D.M., Bari, A., Robbins, T.W., 2008a. The neuropsychopharmacology of action inhibition: cross-species translation of the stop-signal and go/no-go tasks. Psychopharmacology (Berl.) 199, 439–456. doi:10.1007/s00213-008-1127-6

Eagle, D.M., Baunez, C., Hutcheson, D.M., Lehmann, O., Shah, A.P., Robbins, T.W., 2008b. Stop-signal reaction-time task performance: role of prefrontal cortex and subthalamic nucleus. Cereb. Cortex N. Y. N 1991 18, 178–188. doi:10.1093/cercor/bhm044

Eagle, D.M., Robbins, T.W., 2003a. Inhibitory control in rats performing a stop-signal reaction-time task: effects of lesions of the medial striatum and d-amphetamine. Behav. Neurosci. 117, 1302–1317. doi:10.1037/0735-7044.117.6.1302

Eagle, D.M., Robbins, T.W., 2003b. Lesions of the medial prefrontal cortex or nucleus accumbens core do not impair inhibitory control in rats performing a stop-signal reaction time task. Behav. Brain Res. 146, 131–144.

Emeric, E.E., Brown, J.W., Boucher, L., Carpenter, R.H.S., Hanes, D.P., Harris, R., Logan, G.D., Mashru, R.N., Paré, M., Pouget, P., Stuphorn, V., Taylor, T.L., Schall, J.D., 2007. Influence of history on saccade countermanding performance in humans and macaque monkeys. Vision Res. 47, 35–49. doi:10.1016/j.visres.2006.08.032

Everling, S., Paré, M., Dorris, M.C., Munoz, D.P., 1998. Comparison of the discharge characteristics of brain stem omnipause neurons and superior colliculus fixation neurons in monkey: implications for control of fixation and saccade behavior. J. Neurophysiol. 79, 511–528.

Fletcher, B.R., Baxter, M.G., Guzowski, J.F., Shapiro, M.L., Rapp, P.R., 2007. Selective Cholinergic Depletion of the Hippocampus Spares Both

Behaviorally Induced Arc Transcription and Spatial Learning and Memory. Hippocampus 17.

Fournier, G.N., Materi, L.M., Semba, K., Rasmusson, D.D., 2004. Cortical acetylcholine release and electroencephalogram activation evoked by ionotropic glutamate receptor agonists in the rat basal forebrain. Neuroscience 123, 785–792.

Francis, P.T., Palmer, A.M., Snape, M., Wilcock, G.K., 1999. The cholinergic hypothesis of Alzheimer's disease: a review of progress. J. Neurol. Neurosurg. Psychiatry 66, 137–147.

Freund, H.-J., Kuhn, J., Lenartz, D., Mai, J.K., Schnell, T., Klosterkoetter, J., Sturm, V., 2009. Cognitive functions in a patient with Parkinson-dementia syndrome undergoing deep brain stimulation. Arch. Neurol. 66, 781–785. doi:10.1001/archneurol.2009.102

Freund, T.F., Antal, M., 1988. GABA-containing neurons in the septum control inhibitory interneurons in the hippocampus. Nature 336, 170–173.

Freund, T.F., Gulyás, A.I., 1991. GABAergic interneurons containing calbindin D28K or somatostatin are major targets of GABAergic basal forebrain afferents in the rat neocortex. J. Comp. Neurol. 314, 187–199.

Frick, K.M., Kim, J.J., Baxter, M.G., 2004. Effects of complete immunotoxin lesions of the cholinergic basal forebrain on fear conditioning and spatial learning. Hippocampus 14, 244–254. doi:10.1002/hipo.10169

Fu, Y., Tucciarone, J.M., Espinosa, J.S., Sheng, N., Darcy, D.P., Nicoll, R.A., Huang, Z.J., Stryker, M.P., 2014. A cortical circuit for gain control by behavioral state. Cell 156, 1139–1152. doi:10.1016/j.cell.2014.01.050

Gallagher, M., Burwell, R., Burchinal, M., 1993. Severity of spatial learning impairment in aging: development of a learning index for performance in the Morris water maze. Behav. Neurosci. 107, 618–626.

Gallagher, M., Colombo, P.J., 1995. Ageing: the cholinergic hypothesis of cognitive decline. Curr. Opin. Neurobiol. 5, 161–168. doi:doi: DOI: 10.1016/0959-4388(95)80022-0

Gallagher, M., Rapp, P.R., 1997. The use of animal models to study the effects of aging on cognition. Annu. Rev. Psychol. 48.

Gallagher, M., Stocker, A., Koh, M.T., 2011. Mindspan: Lessons from Rat Models of Neurocognitive Aging. ILAR J. Natl. Res. Counc. Inst. Lab. Anim. Resour. 52, 32–40.

Gamboz, N., Borella, E., Brandimonte, M.A., 2009. The role of switching, inhibition and working memory in older adults' performance in the Wisconsin Card Sorting Test. Neuropsychol. Dev. Cogn. B Aging Neuropsychol. Cogn. 16, 260–284. doi:10.1080/13825580802573045

Gauggel, S., Rieger, M., Feghoff, T.-A., 2004. Inhibition of ongoing responses in patients with Parkinson's disease. J. Neurol. Neurosurg. Psychiatry 75, 539–544.

Gervasoni, D., Lin, S.-C., Ribeiro, S., Soares, E.S., Pantoja, J., Nicolelis, M.A.., 2004. Global Forebrain Dynamics Predict Rat Behavioral States and Their Transitions. J. Neurosci. 24, 11137–11147.

Goard, M., Dan, Y., 2009. Basal forebrain activation enhances cortical coding of natural scenes. Nat. Neurosci. 12, 1444–1449. doi:10.1038/nn.2402

Goudriaan, A.E., Oosterlaan, J., de Beurs, E., van den Brink, W., 2005. Decision making in pathological gambling: a comparison between pathological gamblers, alcohol dependents, persons with Tourette syndrome, and normal controls. Brain Res. Cogn. Brain Res. 23, 137–151. doi:10.1016/j.cogbrainres.2005.01.017

Grant, J.E., Chamberlain, S.R., Schreiber, L.R.N., Odlaug, B.L., Kim, S.W., 2011. Selective decision-making deficits in at-risk gamblers. Psychiatry Res. 189, 115–120. doi:10.1016/j.psychres.2011.05.034

Gritti, I., Mainville, L., Mancia, M., Jones, B.E., 1997. GABAergic and other noncholinergic basal forebrain neurons, together with cholinergic neurons, project to the mesocortex and isocortex in the rat. J. Comp. Neurol. 383, 163–177.

Grottick, A.J., Haman, M., Wyler, R., Higgins, G.A., 2003. Reversal of a vigilance decrement in the aged rat by subtype-selective nicotinic ligands. Neuropsychopharmacol. Off. Publ. Am. Coll. Neuropsychopharmacol. 28, 880–887. doi:10.1038/sj.npp.1300102

Gulyás, A.I., Seress, L., Tóth, K., Acsády, L., Antal, M., Freund, T.F., 1991. Septal GABAergic neurons innervate inhibitory interneurons in the hippocampus

of the macaque monkey. Neuroscience 41, 381–390. doi:doi: DOI: 10.1016/0306-4522(91)90334-K

Gutiérrez, H., Gutiérrez, R., Silva-Gandarias, R., Estrada, J., Miranda, M.I., Bermúdez-Rattoni, F., 1999. Differential effects of 192IgG-saporin and NMDA-induced lesions into the basal forebrain on cholinergic activity and taste aversion memory formation. Brain Res. 834, 136–141.

Haaland, K.Y., Vranes, L.F., Goodwin, J.S., Garry, P.J., 1987. Wisconsin Card Sort Test Performance in a Healthy Elderly Population. J. Gerontol. 42, 345–346. doi:10.1093/geronj/42.3.345

Hanes, D.P., Patterson, W.F., Schall, J.D., 1998. Role of frontal eye fields in countermanding saccades: visual, movement, and fixation activity. J. Neurophysiol. 79, 817–834.

Hanes, D.P., Schall, J.D., 1996. Neural control of voluntary movement initiation. Science 274, 427.

Hardenacke, K., Kuhn, J., Lenartz, D., Maarouf, M., Mai, J.K., Bartsch, C., Freund, H.J., Sturm, V., 2013. Stimulate or degenerate: deep brain stimulation of the nucleus basalis Meynert in Alzheimer dementia. World Neurosurg. 80, S27.e35–43. doi:10.1016/j.wneu.2012.12.005

Hasher, L., Stoltzfus, E.R., Zacks, R.T., Rypma, B., 1991. Age and inhibition. J. Exp. Psychol. Learn. Mem. Cogn. 17, 163–169. doi:10.1037/0278-7393.17.1.163

Hassani, O.K., Lee, M.G., Henny, P., Jones, B.E., 2009. Discharge profiles of identified GABAergic in comparison to cholinergic and putative

glutamatergic basal forebrain neurons across the sleep-wake cycle. J. Neurosci. Off. J. Soc. Neurosci. 29, 11828–11840. doi:10.1523/JNEUROSCI.1259-09.2009

Haynes, W.I.A., Haber, S.N., 2013. The organization of prefrontal-subthalamic inputs in primates provides an anatomical substrate for both functional specificity and integration: implications for Basal Ganglia models and deep brain stimulation. J. Neurosci. Off. J. Soc. Neurosci. 33, 4804–4814. doi:10.1523/JNEUROSCI.4674-12.2013

Henny, P., Jones, B.E., 2008. Projections from basal forebrain to prefrontal cortex comprise cholinergic, GABAergic and glutamatergic inputs to pyramidal cells or interneurons. Eur. J. Neurosci. 27, 654–670.

Hepler, D.J., Wenk, G.L., Cribbs, B.L., Olton, D.S., Coyle, J.T., 1985. Memory impairments following basal forebrain lesions. Brain Res. 346, 8–14.

Hepler, D., Olton, D., Wenk, G., Coyle, J., 1985. Lesions in nucleus basalis magnocellularis and medial septal area of rats produce qualitatively similar memory impairments. J Neurosci 5, 866–873.

Hepler, D., Wenk, G., Olton, D., Coyle, J., 1985. Lesions in nucleus basalis magnocellularis and medial septal area of rats produce similar memory impairments in appetitive and non-appetitive behavioral tasks. Ann. N. Y. Acad. Sci. 444, 518–519.

Herremans, A.H., Hijzen, T.H., Olivier, B., Slangen, J.L., 1995. Cholinergic drug effects on a delayed conditional discrimination task in the rat. Behav. Neurosci. 109, 426–435.

Hughes, M.E., Fulham, W.R., Johnston, P.J., Michie, P.T., 2012. Stop-signal response inhibition in schizophrenia: behavioural, event-related potential and functional neuroimaging data. Biol. Psychol. 89, 220–231. doi:10.1016/j.biopsycho.2011.10.013

Hu, S., Chao, H.H.-A., Zhang, S., Ide, J.S., Li, C.-S.R., 2013. Changes in cerebral morphometry and amplitude of low-frequency fluctuations of BOLD signals during healthy aging: correlation with inhibitory control. Brain Struct. Funct. doi:10.1007/s00429-013-0548-0

Huston, A.E., Aggleton, J.P., 1987. The effects of cholinergic drugs upon recognition memory in rats. Q. J. Exp. Psychol. B 39, 297–314.

Ide, J.S., Li, C.R., 2011. A cerebellar thalamic cortical circuit for error-related cognitive control. NeuroImage 54, 455–464. doi:10.1016/j.neuroimage.2010.07.042

Ide, J.S., Shenoy, P., Yu, A.J., Li, C.R., 2013. Bayesian prediction and evaluation in the anterior cingulate cortex. J. Neurosci. Off. J. Soc. Neurosci. 33, 2039–2047. doi:10.1523/JNEUROSCI.2201-12.2013

Isoda, M., Hikosaka, O., 2007. Switching from automatic to controlled action by monkey medial frontal cortex. Nat. Neurosci. 10, 240–248. doi:10.1038/nn1830

Johannes, S., Wieringa, B.M., Mantey, M., Nager, W., Rada, D., Müller-Vahl, K.R., Emrich, H.M., Dengler, R., Münte, T.F., Dietrich, D., 2001. Altered inhibition of motor responses in Tourette Syndrome and Obsessive-Compulsive Disorder. Acta Neurol. Scand. 104, 36–43.

Kail, R., Salthouse, T.A., 1994. Processing speed as a mental capacity. Acta Psychol. (Amst.) 86, 199–225.

Kamke, M.R., Brown, M., Irvine, D.R.., 2005. Basal forebrain cholinergic input is not essential for lesion-induced plasticity in mature auditory cortex. Neuron 48, 675–686.

Köppen, J.R., Winter, S.S., Stuebing, S.L., Cheatwood, J.L., Wallace, D.G., 2013. Infusion of GAT1-saporin into the medial septum/vertical limb of the diagonal band disrupts self-movement cue processing and spares mnemonic function. Brain Struct. Funct. 218, 1099–1114. doi:10.1007/s00429-012-0449-7

Kramer, A.F., Humphrey, D.G., Larish, J.F., Logan, G.D., Strayer, D.L., 1994. Aging and inhibition: beyond a unitary view of inhibitory processing in attention. Psychol. Aging 9, 491–512.

Kumar, R., Lozano, A.M., Kim, Y.J., Hutchison, W.D., Sime, E., Halket, E., Lang, A.E., 1998. Double-blind evaluation of subthalamic nucleus deep brain stimulation in advanced Parkinson's disease. Neurology 51, 850–855.

Lappin, J.S., Eriksen, C.W., 1966. Use of a delayed signal to stop a visual reaction-time response. J. Exp. Psychol. 72, 805–811. doi:10.1037/h0021266

Lee, S.-H., Dan, Y., 2012. Neuromodulation of Brain States. Neuron 76, 209–222. doi:10.1016/j.neuron.2012.09.012

Leventhal, D.K., Gage, G.J., Schmidt, R., Pettibone, J.R., Case, A.C., Berke, J.D., 2012. Basal ganglia beta oscillations accompany cue utilization. Neuron 73, 523–536. doi:10.1016/j.neuron.2011.11.032

Li, C.R., Huang, C., Constable, R.T., Sinha, R., 2006a. Imaging response inhibition in a stop-signal task: neural correlates independent of signal monitoring and post-response processing. J. Neurosci. Off. J. Soc. Neurosci. 26, 186–192. doi:10.1523/JNEUROSCI.3741-05.2006

Li, C.R., Huang, C., Yan, P., Paliwal, P., Constable, R.T., Sinha, R., 2008. Neural correlates of post-error slowing during a stop signal task: a functional magnetic resonance imaging study. J. Cogn. Neurosci. 20, 1021–1029. doi:10.1162/jocn.2008.20071

Li, C.R., Milivojevic, V., Kemp, K., Hong, K., Sinha, R., 2006b. Performance monitoring and stop signal inhibition in abstinent patients with cocaine dependence. Drug Alcohol Depend. 85, 205–212. doi:10.1016/j.drugalcdep.2006.04.008

Li, C.-S.R., Yan, P., Chao, H.H.-A., Sinha, R., Paliwal, P., Constable, R.T., Zhang, S., Lee, T.-W., 2008. Error-specific medial cortical and subcortical activity during the stop signal task: a functional magnetic resonance imaging study. Neuroscience 155, 1142–1151. doi:10.1016/j.neuroscience.2008.06.062

Lin, S.-C., Gervasoni, D., Nicolelis, M.A.L., 2006. Fast Modulation of Prefrontal Cortex Activity by Basal Forebrain Noncholinergic Neuronal Ensembles. J Neurophysiol 96, 3209–3219.

Lin, S.-C., Nicolelis, M.A.L., 2008. Neuronal Ensemble Bursting in the Basal Forebrain Encodes Salience Irrespective of Valence. Neuron 59, 138–149. doi:10.1016/j.neuron.2008.04.031

Lipszyc, J., Schachar, R., 2010. Inhibitory control and psychopathology: a meta-analysis of studies using the stop signal task. J. Int. Neuropsychol. Soc. JINS 16, 1064–1076. doi:10.1017/S1355617710000895

Logan, G.D., Cowan, W.B., 1984. On the ability to inhibit thought and action: A theory of an act of control. Psychol. Rev. 91, 295–327. doi:10.1037/0033-295X.91.3.295

Logan, G.D., Cowan, W.B., Davis, K.A., 1984. On the ability to inhibit simple and choice reaction time responses: a model and a method. J. Exp. Psychol. Hum. Percept. Perform. 10, 276–291.

Logan, G.D., Cowan, W.B., Davis, K.A., 1984. On the ability to inhibit simple and choice reaction time responses: a model and a method. J. Exp. Psychol. 10, 276–291.

Logan, G.D., Irwin, D.E., 2000. Don't look! Don't touch! Inhibitory control of eye and hand movements. Psychon. Bull. Rev. 7, 107–112.

Logan, G.D., Schachar, R.J., Tannock, R., 1997. Impulsivity and Inhibitory Control. Psychol. Sci. 8, 60–64. doi:10.1111/j.1467-9280.1997.tb00545.x

Macmillan, M., 1992. Inhibition and the control of behavior. From Gall to Freud via Phineas Gage and the frontal lobes. Brain Cogn. 19, 72–104.

Maddux, J.-M., Holland, P.C., 2011. Effects of dorsal or ventral medial prefrontal cortical lesions on five-choice serial reaction time performance in rats. Behav. Brain Res. 221, 63–74. doi:10.1016/j.bbr.2011.02.031

Manns, I.D., 2002. Rhythmically Discharging Basal Forebrain Units Comprise Cholinergic, GABAergic, and Putative Glutamatergic Cells. J. Neurophysiol. 89, 1057–1066. doi:10.1152/jn.00938.2002

Manns, I.D., Mainville, L., Jones, B.E., 2001. Evidence for glutamate, in addition to acetylcholine and GABA, neurotransmitter synthesis in basal forebrain neurons projecting to the entorhinal cortex. Neuroscience 107, 249–263.

Markowska, A.L., Wenk, G.L., Olton, D.S., 1990. Nucleus basalis magnocellularis and memory: differential effects of two neurotoxins. Behav. Neural Biol. 54, 13–26.

Mayse, J.D., Nelson, G.M., Park, P., Gallagher, M., Lin, S.-C., 2014. Proactive and reactive inhibitory control in rats. Front. Neurosci. 8, 104. doi:10.3389/fnins.2014.00104

McAlonan, G.M., Cheung, V., Chua, S.E., Oosterlaan, J., Hung, S., Tang, C., Lee, C., Kwong, S., Ho, T., Cheung, C., Suckling, J., Leung, P.W.L., 2009. Age-related grey matter volume correlates of response inhibition and shifting in attention-deficit hyperactivity disorder. Br. J. Psychiatry J. Ment. Sci. 194, 123–129. doi:10.1192/bjp.bp.108.051359

McGaughy, J., Dalley, J.W., Morrison, C.H., Everitt, B.J., Robbins, T.W., 2002. Selective Behavioral and Neurochemical Effects of Cholinergic Lesions Produced by Intrabasalis Infusions of 192 IgG-Saporin on Attentional Performance in a Five-Choice Serial Reaction Time Task. J Neurosci 22, 1905–1913.

McGaughy, J., Kaiser, T., Sarter, M., 1996. Behavioral vigilance following infusions of 192 IgG-saporin into the basal forebrain: selectivity of the behavioral impairment and relation to cortical AChE-positive fiber density. Behav. Neurosci. 110, 247–265.

Mirabella, G., Iaconelli, S., Romanelli, P., Modugno, N., Lena, F., Manfredi, M., Cantore, G., 2011. Deep Brain Stimulation of Subthalamic Nuclei Affects Arm Response Inhibition In Parkinson's Patients. Cereb. Cortex N. Y. N 1991. doi:10.1093/cercor/bhr187

Muggleton, N.G., Chen, C.-Y., Tzeng, O.J.L., Hung, D.L., Juan, C.-H., 2010. Inhibitory control and the frontal eye fields. J. Cogn. Neurosci. 22, 2804–2812. doi:10.1162/jocn.2010.21416

Muir, J.L., Bussey, T.J., Everitt, B.J., Robbins, T.W., 1996. Dissociable effects of AMPA-induced lesions of the vertical limb diagonal band of Broca on performance of the 5-choice serial reaction time task and on acquisition of a conditional visual discrimination. Behav. Brain Res. 82, 31–44.

Muir, J., Page, K., Sirinathsinghji, D., Robbins, T.W., Everitt, B.J., 1993. Excitotoxic lesions of basal forebrain cholinergic neurons: effects on learning, memory, and attention. Behav Brain Res 57, 123–131.

Nelder, J.A., Mead, R., 1965. A Simplex Method for Function Minimization. Comput. J. 7, 308–313. doi:10.1093/comjnl/7.4.308

Nelson, M.J., Boucher, L., Logan, G.D., Palmeri, T.J., Schall, J.D., 2010. Nonindependent and nonstationary response times in stopping and

stepping saccade tasks. Atten. Percept. Psychophys. 72, 1913–1929. doi:10.3758/APP.72.7.1913

Nguyen, D.P., Lin, S.-C., 2014. A frontal cortex event-related potential driven by the basal forebrain. eLife 3, e02148.

North, A.J., 1950. Improvement in successive discrimination reversals. J. Comp. Physiol. Psychol. 43, 442–460. doi:10.1037/h0061372

Odlaug, B.L., Chamberlain, S.R., Kim, S.W., Schreiber, L.R.N., Grant, J.E., 2011. A neurocognitive comparison of cognitive flexibility and response inhibition in gamblers with varying degrees of clinical severity. Psychol. Med. 41, 2111–2119. doi:10.1017/S0033291711000316

Olton, D., Markowska, A., Voytko, M.L., Givens, B., Gorman, L., Wenk, G., 1991. Basal forebrain cholinergic system: a functional analysis. Adv. Exp. Med. Biol. 295, 353–372.

Olton, D.S., Wenk, G.L., Church, R.M., Meck, W.H., 1988. Attention and the frontal cortex as examined by simultaneous temporal processing. Neuropsychologia 26, 307–318.

Pang, K.C.H., Jiao, X., Sinha, S., Beck, K.D., Servatius, R.J., 2011. Damage of GABAergic neurons in the medial septum impairs spatial working memory and extinction of active avoidance: effects on proactive interference. Hippocampus 21, 835–846. doi:10.1002/hipo.20799

Parasuraman, R., Nestor, P., Greenwood, P., 1989. Sustained-attention capacity in young and older adults. Psychol. Aging 4, 339–345.

Paré, M., Hanes, D.P., 2003. Controlled movement processing: superior colliculus activity associated with countermanded saccades. J. Neurosci. Off. J. Soc. Neurosci. 23, 6480–6489.

Pouget, P., Logan, G.D., Palmeri, T.J., Boucher, L., Paré, M., Schall, J.D., 2011. Neural Basis of Adaptive Response Time Adjustment during Saccade Countermanding. J. Neurosci. 31, 12604 –12612. doi:10.1523/JNEUROSCI.1868-11.2011

Rapp, P.R., 1990. Visual discrimination and reversal learning in the aged monkey (Macaca mulatta). Behav. Neurosci. 104, 876–884.

Ray, N.J., Brittain, J.-S., Holland, P., Joundi, R.A., Stein, J.F., Aziz, T.Z., Jenkinson, N., 2012. The role of the subthalamic nucleus in response inhibition: evidence from local field potential recordings in the human subthalamic nucleus. NeuroImage 60, 271–278. doi:10.1016/j.neuroimage.2011.12.035

Richardson, R.T., DeLong, M.R., 1990. Context-dependent responses of primate nucleus basalis neurons in a go/no-go task. J. Neurosci. Off. J. Soc. Neurosci. 10, 2528–2540.

Rieger, M., Gauggel, S., 1999. Inhibitory after-effects in the stop signal paradigm. Br. J. Psychol. 90, 509–518. doi:10.1348/000712699161585

Rieger, M., Gauggel, S., Burmeister, K., 2003. Inhibition of ongoing responses following frontal, nonfrontal, and basal ganglia lesions. Neuropsychology 17, 272–282.

Robbins, T.W., Everitt, B.J., Ryan, C.N., Marston, H.M., Jones, G.H., Page, K.J., 1989. Comparative effects of quisqualic and ibotenic acid-induced lesions of the substantia innominata and globus pallidus on the acquisition of a conditional visual discrimination: differential effects on cholinergic mechanisms. Neuroscience 28, 337–352.

Roberts, A.C., Robbins, T.W., Everitt, B.J., Muir, J.L., 1992. A specific form of cognitive rigidity following excitotoxic lesions of the basal forebrain in marmosets. Neuroscience 47, 251–264.

Robinson, E.S.J., Eagle, D.M., Economidou, D., Theobald, D.E.H., Mar, A.C., Murphy, E.R., Robbins, T.W., Dalley, J.W., 2009. Behavioural characterisation of high impulsivity on the 5-choice serial reaction time task: specific deficits in “waiting” versus “stopping.” Behav. Brain Res. 196, 310–316. doi:10.1016/j.bbr.2008.09.021

Roland, J.J., Janke, K.L., Servatius, R.J., Pang, K.C.H., 2014. GABAergic neurons in the medial septum-diagonal band of Broca (MSDB) are important for acquisition of the classically conditioned eyeblink response. Brain Struct. Funct. 219, 1231–1237. doi:10.1007/s00429-013-0560-4

Roland, J.J., Stewart, A.L., Janke, K.L., Gielow, M.R., Kostek, J.A., Savage, L.M., Servatius, R.J., Pang, K.C.H., 2014. Medial septum-diagonal band of Broca (MSDB) GABAergic regulation of hippocampal acetylcholine efflux is dependent on cognitive demands. J. Neurosci. Off. J. Soc. Neurosci. 34, 506–514. doi:10.1523/JNEUROSCI.2352-13.2014

Rush, B.K., Barch, D.M., Braver, T.S., 2006. Accounting for cognitive aging: context processing, inhibition or processing speed? Neuropsychol. Dev. Cogn. B Aging Neuropsychol. Cogn. 13, 588–610. doi:10.1080/13825580600680703

Salthouse, T.A., 1996. The processing-speed theory of adult age differences in cognition. Psychol. Rev. 103, 403–428.

Salthouse, T.A., 2000. Aging and measures of processing speed. Biol. Psychol. 54, 35–54. doi:16/S0301-0511(00)00052-1

Salthouse, T.A., Babcock, R.L., Shaw, R.J., 1991. Effects of adult age on structural and operational capacities in working memory. Psychol. Aging 6, 118–127.

Sara, S.J., Bouret, S., 2012. Orienting and Reorienting: The Locus Coeruleus Mediates Cognition through Arousal. Neuron 76, 130–141. doi:10.1016/j.neuron.2012.09.011

Sarter, M., Bruno, J.P., 1999. Cortical cholinergic inputs mediating arousal, attentional processing and dreaming: differential afferent regulation of the basal forebrain by telencephalic and brainstem afferents. Neuroscience 95, 933–952.

Schall, J.D., Godlove, D.C., 2012. Current advances and pressing problems in studies of stopping. Curr. Opin. Neurobiol. 22, 1012–1021. doi:10.1016/j.conb.2012.06.002

Schmidt, R., Leventhal, D.K., Mallet, N., Chen, F., Berke, J.D., 2013. Canceling actions involves a race between basal ganglia pathways. Nat. Neurosci. 16, 1118–1124. doi:10.1038/nn.3456

Schoenbaum, G., Nugent, S.L., Saddoris, M.P., Setlow, B., 2002a. Orbitofrontal lesions in rats impair reversal but not acquisition of go, no-go odor discriminations. Neuroreport 13, 885–890.

Schoenbaum, G., Nugent, S., Saddoris, M.P., Gallagher, M., 2002b. Teaching old rats new tricks: age-related impairments in olfactory reversal learning. Neurobiol. Aging 23, 555–564.

Smith, R., 1992. Inhibition: history and meaning in the sciences of mind and brain. University of California Press, Berkeley.

Sparks, D.L., 1978. Functional properties of neurons in the monkey superior colliculus: coupling of neuronal activity and saccade onset. Brain Res. 156, 1–16.

Squire, L.R., 1992. Memory and the hippocampus: A synthesis from findings with rats, monkeys, and humans. Psychol. Rev. 99, 195–231. doi:doi:10.1037/0033-295X.99.2.195

Staub, B., Doignon-Camus, N., Bacon, E., Bonnefond, A., 2014a. Age-related differences in the recruitment of proactive and reactive control in a situation of sustained attention. Biol. Psychol. 103C, 38–47. doi:10.1016/j.biopsycho.2014.08.007

Staub, B., Doignon-Camus, N., Bacon, É., Bonnefond, A., 2014b. The effects of aging on sustained attention ability: an ERP study. Psychol. Aging 29, 684–695. doi:10.1037/a0037067

Staub, B., Doignon-Camus, N., Bacon, E., Bonnefond, A., 2014c. Investigating sustained attention ability in the elderly by using two different approaches:

inhibiting ongoing behavior versus responding on rare occasions. Acta Psychol. (Amst.) 146, 51–57. doi:10.1016/j.actpsy.2013.12.003

Stuphorn, V., 2014. Neural mechanisms of response inhibition. Curr. Opin. Behav. Sci. doi:10.1016/j.cobeha.2014.10.009

Swann, N.C., Cai, W., Conner, C.R., Pieters, T.A., Claffey, M.P., George, J.S., Aron, A.R., Tandon, N., 2012. Roles for the pre-supplementary motor area and the right inferior frontal gyrus in stopping action: electrophysiological responses and functional and structural connectivity. NeuroImage 59, 2860–2870. doi:10.1016/j.neuroimage.2011.09.049

Swann, N.C., Tandon, N., Pieters, T.A., Aron, A.R., 2013. Intracranial electroencephalography reveals different temporal profiles for dorsal- and ventro-lateral prefrontal cortex in preparing to stop action. Cereb. Cortex N. Y. N 1991 23, 2479–2488. doi:10.1093/cercor/bhs245

Swann, N., Tandon, N., Canolty, R., Ellmore, T.M., McEvoy, L.K., Dreyer, S., DiSano, M., Aron, A.R., 2009. Intracranial EEG reveals a time-and frequency-specific role for the right inferior frontal gyrus and primary motor cortex in stopping initiated responses. J. Neurosci. 29, 12675.

Szatkowska, I., Szymańska, O., Bojarski, P., Grabowska, A., 2007. Cognitive inhibition in patients with medial orbitofrontal damage. Exp. Brain Res. 181, 109–115. doi:10.1007/s00221-007-0906-3

Tsubokawa, T., Katayama, Y., Yamamoto, T., 1995. Control of persistent hemiballismus by chronic thalamic stimulation. Report of two cases. J. Neurosurg. 82, 501–505. doi:10.3171/jns.1995.82.3.0501

Turchi, J., Holley, L.A., Sarter, M., 1996. Effects of benzodiazepine receptor inverse agonists and nicotine on behavioral vigilance in senescent rats. J. Gerontol. A. Biol. Sci. Med. Sci. 51, B225–231.

Van den Wildenberg, W.P.M., van Boxtel, G.J.M., van der Molen, M.W., Bosch, D.A., Speelman, J.D., Brunia, C.H.M., 2006. Stimulation of the subthalamic region facilitates the selection and inhibition of motor responses in Parkinson's disease. J. Cogn. Neurosci. 18, 626–636. doi:10.1162/jocn.2006.18.4.626

Verbruggen, F., Logan, G.D., 2009a. Proactive adjustments of response strategies in the stop-signal paradigm. J. Exp. Psychol. Hum. Percept. Perform. 35, 835–854. doi:10.1037/a0012726

Verbruggen, F., Logan, G.D., 2009b. Models of response inhibition in the stop-signal and stop-change paradigms. Neurosci. Biobehav. Rev. 33, 647–661. doi:10.1016/j.neubiorev.2008.08.014

Verbruggen, F., Logan, G.D., 2009c. Proactive adjustments of response strategies in the stop-signal paradigm. J. Exp. Psychol. Hum. Percept. Perform. 35, 835–854. doi:10.1037/a0012726

Volle, E., de Lacy Costello, A., Coates, L.M., McGuire, C., Towgood, K., Gilbert, S., Kinkingnehun, S., McNeil, J.E., Greenwood, R., Papps, B., van den Broeck, M., Burgess, P.W., 2011. Dissociation between Verbal Response Initiation and Suppression after Prefrontal Lesions. Cereb. Cortex N. Y. N 1991. doi:10.1093/cercor/bhr322

Voytko, M.L., Olton, D.S., Richardson, R.T., Gorman, L.K., Tobin, J.R., Price, D.L., 1994. Basal forebrain lesions in monkeys disrupt attention but not learning and memory. J. Neurosci. Off. J. Soc. Neurosci. 14, 167–186.

Wang, M., Gamo, N.J., Yang, Y., Jin, L.E., Wang, X.-J., Laubach, M., Mazer, J.A., Lee, D., Arnsten, A.F.T., 2011. Neuronal basis of age-related working memory decline. Nature 476, 210–213. doi:10.1038/nature10243

Wenk, G.L., Markowska, A.L., Olton, D.S., 1989. Basal forebrain lesions and memory: alterations in neurotensin, not acetylcholine, may cause amnesia. Behav. Neurosci. 103, 765–769.

White, C.N., Congdon, E., Mumford, J.A., Karlsgodt, K.H., Sabb, F.W., Freimer, N.B., London, E.D., Cannon, T.D., Bilder, R.M., Poldrack, R.A., 2014. Decomposing decision components in the stop-signal task: a model-based approach to individual differences in inhibitory control. J. Cogn. Neurosci. 26, 1601–1614. doi:10.1162/jocn_a_00567

Whitehouse, P., Price, D., Struble, R., Clark, A., Coyle, J., Delon, M., 1982. Alzheimer's disease and senile dementia: loss of neurons in the basal forebrain. Science 215, 1237 –1239. doi:10.1126/science.7058341

Wiest, M.C., Bentley, N., Nicolelis, M.A.L., 2005. Heterogeneous integration of bilateral whisker signals by neurons in primary somatosensory cortex of awake rats. J. Neurophysiol. 93, 2966–2973. doi:10.1152/jn.00556.2004

Worbe, Y., Savulich, G., Voon, V., Fernandez-Egea, E., Robbins, T.W., 2014. Serotonin Depletion Induces "Waiting Impulsivity" on the Human Four-Choice Serial Reaction Time Task: Cross-Species Translational

Significance. Neuropsychopharmacol. Off. Publ. Am. Coll. Neuropsychopharmacol. doi:10.1038/npp.2013.351

Yang, C., McKenna, J.T., Zant, J.C., Winston, S., Basheer, R., Brown, R.E., 2014. Cholinergic neurons excite cortically projecting basal forebrain GABAergic neurons. J. Neurosci. Off. J. Soc. Neurosci. 34, 2832–2844. doi:10.1523/JNEUROSCI.3235-13.2014

Zandbelt, B.B., Vink, M., 2010. On the Role of the Striatum in Response Inhibition. PLoS ONE 5, e13848. doi:10.1371/journal.pone.0013848

Curriculum Vitae

Jeffrey D. Mayse, B.S., M.A., Ph.D

PERSONAL INFORMATION

Name: Jeffrey Daniel Mayse
Position: Post-Doctoral Fellow
Address: Department of Neuroscience
Brown University
185 Meeting Street
Phone: 817-637-0909 (m)
Email: Jeffrey_mayse@brown.edu

EDUCATION

Institution	Degree	Year
Area		
Johns Hopkins University	Ph.D	2014
Psychology		
Johns Hopkins University	M.A.	2012
Psychology		
Texas A&M University	B.S.	2009
Psychology		

ACADEMIC, RESEARCH, AND PROFESSIONAL APPOINTMENTS

2015- Post-Doctoral Fellow
Laboratories of Dr. Gilad Barnea & Dr. Chris Moore
Department of Neuroscience
Brown University

2009-2015 Doctoral Student
Laboratory of Dr. Michela Gallagher
Department of Psychological and Brain Sciences
Johns Hopkins University

2010-2015 Volunteer Scientist
Laboratory of Dr. Shih-Chieh Lin
Neural Circuits and Cognition Unit,
Laboratory of Behavioral Neuroscience
National Institute on Aging, National Institutes of Health

Bayview, MD, 21224

2007-2009 Research Assistant
Laboratory of Dr. Barry Setlow
Department of Psychology
Texas A&M University
4235 TAMU
College Station, TX, 77843

2007-2009 Research Assistant
Laboratory of Dr. Jennifer Bizon
Department of Psychology
Texas A&M University
4235 TAMU
College Station, TX, 77843

PUBLICATIONS (* denotes corresponding author)

1. **Mayse, J.D.,** Nelson, G.M., Avila, I., Gallagher, M., *Lin, S.-C. (2014). Basal forebrain neuronal inhibition enables rapid behavioral stopping. *Under Review, Nature Neuroscience*

2. **Mayse, J.D.,** Nelson, G.M., Park, P., Gallagher, M., *Lin, S.-C. (2014). Proactive and Reactive Inhibitory Control in Rats. Frontiers in Neuroscience, Decision Neuroscience 8(104) [Abs].

3. LaSarge C.L., Bañuelos C., **Mayse J.D., ***Bizon J.L. (2009). Blockade of GABA(B) Receptors Completely Reverses Age-Related Learning Impairment. Neuroscience 164(3):941-7 [Abs].

4. Simon N.W., Gilbert R.J., **Mayse J.D.,** Bizon J.L., *Setlow B. (2009). Balancing Risk and Reward: A Rat Model of Risky Decision Making. Neuropsychopharmacology 34(10):2208-17 [Abs].

GRANTS AND FUNDING

2014 Johns Hopkins University Department of Psychological and Brain Sciences Collaborative Research Award ($1000)

2013-2015 National Institute on Aging, F31 AG045039-01A1
The Neural Basis of Response Inhibition
Principal Investigator

2009-2011 National Institute on Aging, T32 AG027668
Albert, M. (P.I.)
Research Training in Age Related Cognitive Disorders
Trainee

TECHNICAL EXPERTISE & SKILLS

Animal Techniques (rats): *In vivo* recording of single-unit and local field potential data from awake, behaving animals. Stereotaxic surgery techniques, including cannulation and implantation of chronic recording electrode. Experience with a wide variety of behavioral paradigms, from Morris Water Maze to many decision-making paradigms (e.g., delay/temporal/risk discounting, Go/No-Go, Stop Signal, etc.).

Data Analysis & Acquisition Techniques: Extensive training and experience with analysis of behavioral and physiological data including single-unit and local field potentials with a focus on understanding the contribution of neural circuits and ensembles to cognition.

Laboratory Techniques: Extensive training and experience with histological techniques, including immunohistochemical staining and stereological analyses.

INVITED LECTURES AND TALKS

1. **Mayse, J.D.** (2014). Neural Correlates of Response Inhibition in Basal Forebrain Bursting Neurons. Invited Lecture, Department of Neuroscience, Brown University, Providence, RI.
2. **Mayse, J.D.** (2014). Basal Forebrain Neurons Track Trial Outcome in the Stop Signal Task. Lecture, Department of Psychological and Brain Sciences, Johns Hopkins University, Baltimore, MD.
3. **Mayse, J.D.** (2013). A Neural Correlate of Stop Signal Reaction Time in the Basal Forebrain. Lecture, Stuphorn Lab, Mind/Brain Institute, Johns Hopkins University, Baltimore, MD.
4. **Mayse, J.D.** (2013). A Neural Correlate of Stop Signal Reaction Time in the Basal Forebrain. Lecture, Department of Psychological and Brain Sciences, Johns Hopkins University, Baltimore, MD.
5. **Mayse, J.D.** (2012). Response Inhibition Signals in Basal Forebrain Neurons. Lecture, Department of Psychological and Brain Sciences, Johns Hopkins University, Baltimore, MD.
6. **Mayse, J.D.** (2012). Fine Temporal Analysis of Decision-Making in Rodents. Lecture, Rapp Lab, Laboratory of Experimental Gerontology, NIA, NIH, Baltimore, MD, 21224

7. **Mayse, J.D.** (2011). Selective Impairment of Rapid Behavioral Discrimination in Aged F344xBN F1 Rats. Lecture, Department of Psychological and Brain Sciences, Johns Hopkins University, Baltimore, MD.
8. **Mayse, J.D.** (2011). Impaired Outcome Processing in Aged F344xBN F1 Rats. Lecture, Rapp Lab, Laboratory of Experimental Gerontology, NIA, NIH, Baltimore, MD, 21224
9. **Mayse, J.D.** (2011). Impaired Outcome Processing in Aged F344xBN F1 Rats. Lecture, Department of Psychological and Brain Sciences, Johns Hopkins University, Baltimore, MD

POSTER PRESENTATIONS

1. Park, P., **Mayse, J.D.**, Perez, E.J., Gallagher, M., Rapp, P.R., and Lin, S.-C. (2014). Inhibitory Control is Impaired in Aged Rats Independent of Memory Decline. Poster, Society for Neuroscience Conference
2. **Mayse, J.D.**, Gallagher, M., and Lin, S.-C. (2014). Neural Correlates of Proactive Control in the Basal Forebrain. Poster, Society for Neuroscience Conference
3. **Mayse, J.D.,** Nelson, G., Avila, I., Gallagher, M., & Lin, S.-C. (2013). Better Late than Never - the Role of Basal Forebrain Inhibition in Successful and Failed Stopping in the Stop Signal Task. Poster, Society for Neuroscience Conference
4. **Mayse, J.D.,** Nelson, G., Avila, I., Gallagher, M., & Lin, S.-C. (2013). Better Late than Never - the Role of Basal Forebrain Inhibition in Successful and Failed Stopping in the Stop Signal Task. Poster, National Institute on Aging Intramural Research Program Annual Research Symposium
5. **Mayse, J.D.,** Nelson, G., Avila, I., Gallagher, M., & Lin, S.-C. (2012). A Neural Correlate of Stop-Signal Reaction Time in the Basal Forebrain. Poster, Society for Neuroscience Conference.
6. **Mayse, J.D.,** Nelson, G., Avila, I., Gallagher, M., & Lin, S.-C. (2012). A Neural Correlate of Stop-Signal Reaction Time in the Basal Forebrain. Poster, National Institute on Aging Intramural Research Program Annual Research Symposium
7. **Mayse, J.D.**, Gallagher, M., & Lin, S.-C. (2011). Selective Impairment of Outcome Processing in Aged F344xBN F1 Rats. Poster, National Institute on Aging Intramural Research Program Annual Research Symposium.
8. **Mayse, J.D.**, Gallagher, M., & Lin, S.-C. (2011). Selective Impairment of Rapid Behavioral Discrimination in Aged F344xBN F1 Rats. Poster, Society for Neuroscience Conference.

MEMBERSHIP IN PROFESSIONAL ORGANIZATIONS

2009-present	Society for Neuroscience, Member
2011	Pavlovian Society, Member

TEACHING EXPERIENCE

2011-2012 **Johns Hopkins University**
Advanced Rsrch. Design (Grad.), TA (Dr. Amy Shelton)

2010-2011 **Johns Hopkins University**
Laboratory for Analysis of Psychological Data, Co-taught
Laboratory for Analysis of Psychological Data, Co-taught
Neuroscience of Economic Decisions, Designed & Taught

2009-2010 **Johns Hopkins University**
Neurobiology of Decision Making, TA (Dr. Veit Stuphorn)

PROFESSIONAL AWARDS AND HONORS

2012 Recipient, Walter L. Clark Teaching & Service Award
Johns Hopkins University
Department of Psychological & Brain Sciences

2009 2nd Place (Overall)
1st Annual Texas A&M Department of Neuroscience Symposium Poster Session

2009 1st Place (Session), 2nd Place (Taxonomy)
Biochemical Engineering/Medicine/Health Sciences Taxonomy
Texas A&M University Student Research Week Poster Session

2009 Member, Texas A&M Brain Bowl Team
2nd Place
Texas Regional Brain Bowl

2009	Undergraduate Research Scholar Texas A&M University
2009	Recipient, Undergraduate Research Scholar Travel Grant Texas A&M University Honors Office
2008	Member, Texas A&M Brain Bowl Team 1st Place Texas Regional Brain Bowl
2008	Undergraduate Research Scholar Texas A&M University

SERVICE

1. Departmental Representative, Graduate Representative Organization (2009-2011)
2. Participated in Brain Awareness Week local outreach (2012)

REFERENCES

Michela Gallagher, PhD (Thesis Advisor)
Krieger-Eisenhower Professor of Psychology and Neuroscience
Department of Psychological and Brain Sciences
Johns Hopkins University
3400 N. Charles Street – Ames Hall
Baltimore, Maryland, 21218-2686, USA

Phone: (410) 516-0167
Email: michela@jhu.edu
Fax: (410) 516-4478

Shih-Chieh Lin, M.D., PhD (Collaborator)
Senior Investigator
Neural Circuits and Cognition Unit
Laboratory of Behavioral Neuroscience
National Institute on Aging, National Institutes of Health
Biomedical Research Center
251 Bayview Boulevard, Suite 100, 09C220
Baltimore, Maryland, 21224, USA

Phone: (410) 558-8509
Email: Shih-Chieh.Lin@nih.gov
Fax: (410) 558-8328

Peter Holland, PhD
Krieger-Eisenhower Professor of Psychology
Department of Psychological and Brain Sciences
2400 N. Charles Street – 222 Ames Hall
Baltimore, Maryland, 21218-2686, USA

Phone: (410) 516-6396
Email: pch@jhu.edu
Fax: (410) 516-4478